1190

TRANSPORTATION RESEARCH RECORD

Artificial Ground Freezing and Soil Stabilization

TRANSPORTATION RESEARCH BOARD
NATIONAL RESEARCH COUNCIL
WASHINGTON, D.C. 1988

Transportation Research Record 1190
Price: $13.00
Editor: Naomi Kassabian

modes
1 highway transportation
2 public transit
3 rail transportation

subject areas
24 pavement design and performance
33 construction
34 general materials
62 soil foundations
63 soil and rock mechanics

Transportation Research Board publications are available by ordering directly from TRB. They may also be obtained on a regular basis through organizational or individual affiliation with TRB; affiliates or library subscribers are eligible for substantial discounts. For further information, write to the Transportation Research Board, National Research Council, 2101 Constitution Avenue, N.W., Washington, D.C. 20418.
Printed in the United States of America

Library of Congress Cataloging-in-Publication Data
National Research Council. Transportation Research Board.

Artificial ground freezing and soil stabilization.

p. cm.—(Transportation research record, ISSN 0361-1981 ; 1190)
Papers presented at the 67th Annual Meeting of the Transportation Research Board, held Jan. 1988 in Washington, D.C.
ISBN 0-309-04758-7
1. Roads—Subgrades. 2. Soil stabilization. 3. Frozen ground. I. National Research Council (U.S.). Transportation Research Board. Meeting (67th : 1988 : Washington, D.C.) II. Series.
TE7.H5 no. 1190 [TE210.4] 380.5 s—dc20
[625.7'35] 89-12867
CIP

Transportation Research Record 1190

Contents

Behavior of Cement-Treated Soils in Flexure

LUTFI RAAD

Response and fracture of cement-treated layers in flexure are significantly influenced by their load-deformation characteristics in tension and compression and their tensile strength. The purpose of this paper is to use the flexure beam test to investigate the flexural behavior of a cement-treated silty clay and a cement-treated sand mix. Specifically, material properties such as tensile and compressive moduli, flexural moduli, tensile strength, flexural strength, and tensile strain at failure are determined for different compaction variables, cement contents, and curing ages. The observed difference in tensile and compressive moduli (i.e., bimodular properties) is explained using proposed mechanistic models, and the practical significance of bimodular behavior is illustrated.

Cement-treated subbases and bases in pavement structures are subjected to flexural stresses and strains under applied traffic loads. Response prediction and fracture behavior of these layers are significantly influenced by tensile strength and tensile and compressive stress-strain properties (*1, 2*). Although these properties can be determined by direct tension and compression testing, the flexural test is believed to simulate better the mode of stress to which a road base is subjected by wheel loading. The flexural modulus and flexural strength are determined in this case by using simple beam-theory assumptions (*3–5*). Strength and modulus values determined, however, do not account for possible nonlinear stress-strain behavior and different stress-strain properties in tension and compression.

The purpose of this paper is to illustrate the use of the flexure test to predict the load-deformation behavior of stabilized soils in tension and compression. Flexural beam tests are conducted on a cement-treated silty clay and a cement-treated sand mix compacted at different densities and moisture contents. Material properties such as tensile and compressive moduli, flexural moduli, tensile strength, flexural strength, and tensile strain at failure are determined for different compaction variables, curing age, and cement content. The difference of stress-strain properties in tension and compression (i.e., bimodular properties) is explained by using proposed mechanistic models, and the practical significance of bimodular behavior in response prediction and fracture of stabilized layers is illustrated.

American University of Beirut, 850 Third Avenue, New York, N.Y. 10022. Current affiliation: Department of Civil Engineering, University of Alaska, 306 Tanana Drive, Fairbanks, Alaska 99775.

EXPERIMENTAL INVESTIGATION

Flexural beam tests were conducted on compacted specimens of a cement-treated silty clay and a cement-treated sand mix. The properties of the silty clay and the sand mix are summarized in Table 1. Test group, level of treatment, curing age, and compaction data are summarized in Tables 2 and 3. Beam specimens 21 × 6 × 6 in. were prepared by using a drop hammer compactor (10 lb, 18-in. drop height). Each specimen was compacted in seven layers, and the number of blows per layer was determined for four energy levels that varied from 100 to 26 percent modified AASHTO compaction energy. The compaction curve associated with a given energy was defined by using a five-point representation in terms of dry density and compaction moisture content. After compaction, the specimens were wrapped in polyethylene sheets and cured in a humid room at 73°F. At the end of the curing period, specimens were air dried in the laboratory for 1 week, after which 1-in.-long SR-4 strain gauges were glued to the top and bottom of the beam specimens in the middle third portion. The load was applied through a loading head at a constant rate of displacement equal to 0.0120 in./min. Vertical deflections at the center of the beam specimens were measured by using a 0.00010-in. dial gauge. The applied load, strains, and vertical deflections were monitored continuously during testing. A schematic representation of the testing apparatus is shown in Figure 1.

RESULTS

The stress-strain behavior was determined with simple beam theory for a given applied load but with the assumption that the tensile and compressive moduli for the same load were different. In this case, the compressive stress σ_c and tensile stress σ_t at the top and bottom of the beam are given by

$$\sigma_c = \frac{3M}{bh^2}\frac{(\varepsilon_c + \varepsilon_t)}{\varepsilon_c} \quad (1)$$

$$\sigma_t = \frac{3M}{bh^2}\frac{(\varepsilon_c + \varepsilon_t)}{\varepsilon_t} \quad (2)$$

TABLE 1 GRADATION, SPECIFIC GRAVITY, AND INDEX PROPERTIES OF SOILS

	Silty Clay	Sand Mix
No. 4–No. 10 (%)	2	–
No. 10–No. 40 (%)	3	12
No. 40–No. 200 (%)	10	73
Percent less than No. 200	85	15
Percent less than 2μ	20	2
Specific gravity	2.71	2.67
Liquid limit	27	NP
Plasticity index	13	NP
AASHTO classification	A-6	A-2-4
Unified classification	CL	SM

NOTE: Sand mix is composed of a mixture of medium uniform sand and silty clay in a 5:1 ratio by weight.

where

ε_c = measured compressive top strain,
ε_t = measured tensile bottom strain,
M = moment at central section of beam,
b = width of beam, and
h = depth of beam.

The corresponding compressive modulus E_c and tensile modulus E_t for the same applied load could be determined as follows:

$$E_c = \frac{3M}{bd^2}\frac{(\varepsilon_c + \varepsilon_t)}{\varepsilon_c^2} \quad (3)$$

$$E_t = \frac{3M}{bd^2}\frac{(\varepsilon_c + \varepsilon_t)}{\varepsilon_t^2} \quad (4)$$

and the bimodular ratio (E_c/E_t) is expressed as

$$E_c/E_t = (\varepsilon_t/\varepsilon_c)^2 \quad (5)$$

Flexural moduli values $\overline{E}_f$ and E_f based on moment curvature equations and deflection at the center of the beam, respectively, were also determined by using the following relations:

$$\overline{E}_f = \frac{PL}{3I}\left(\frac{h}{\varepsilon_c + \varepsilon_t}\right) \quad (6)$$

$$E_f = \frac{23}{648}\left(\frac{PL^3}{dI}\right) \quad (7)$$

where

P = applied load at third points,
L = length of beam,
I = moment of inertia of beam cross section, and
d = deflection at center of beam.

Values of $\overline{E}_f$ and E_f have been used by many investigators (*3, 6, 7*) to characterize stabilized materials in flexure. These values, however, are determined by using simple beam-theory assumptions without accounting for the bimodular behavior of the material.

Flexural beam test results of cement-treated silty clay and cement-treated sand mix are presented below. All modulus values, unless otherwise specified, are determined by using the initial tangent to the load-deflection, load-tensile strain, and load-compressive strain relations.

TABLE 2 COMPACTION DATA FOR CEMENT-TREATED SILTY CLAY

Test Group	Cement Content (%)	Curing Age (days)	Compaction Energy (blows/layer)[a]	Compaction Moisture Content (%)	Maximum Dry Density (lb/ft³)	Optimum Moisture Content (%)
C_1	11	42	240	Variable	132.0	10.44
C_2	11	42	170	Variable	130.9	11.12
C_3	11	42	107	Variable	129.5	11.49
C_4	11	42	64	Variable	125.9	12.15
C_5	3,5,7,9,11	42	240	9.96	—	—
C_6	11	1,7,14,42	240	11.66	129.3	—

[a]Seven layers.

TABLE 3 COMPACTION DATA FOR CEMENT-TREATED SAND MIX

Test Group	Cement Content (%)	Curing Age (days)	Compaction Energy (blows/layer)[a]	Compaction Moisture Content (%)	Maximum Dry Density (lb/ft³)	Optimum Moisture Content (%)
S_1	9	42	240	Variable	127.6	9.20
S_2	9	42	170	Variable	122.6	10.65
S_3	9	42	107	Variable	122.0	10.90
S_4	9	42	64	Variable	118.8	11.72
S_5	3,5,7,9,11	42	240	9.25	—	—
S_6	9	1,7,14,42	240	9.31	120.4	—

[a]Seven layers.

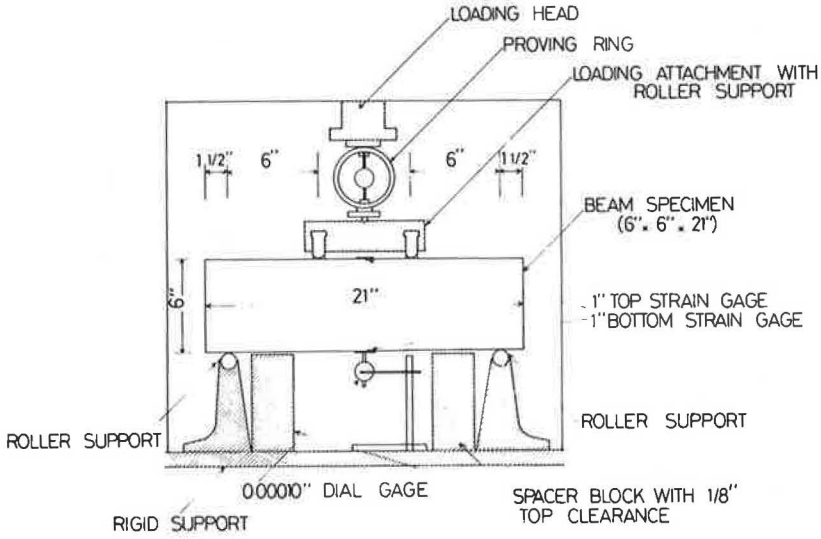

FIGURE 1 Flexural beam test apparatus.

These values are for test groups C_1–C_6 and S_1–S_6 with compaction variables summarized in Tables 2 and 3.

1. The stress-strain relationships for the cement-treated silty clay (Figure 2) and the cement-treated sand mix (Figure 3) determined by using Equations 1 and 2 are nonlinear and exhibit different behavior in compression and in tension in that the compressive modulus is larger than the tensile modulus for a given applied stress.

2. The variation of tensile strength, tensile strain at failure, and tensile, compressive, and flexural moduli with compaction moisture content by using modified AASHTO compaction energy is shown in Figures 4 and 5. The moduli in tension and compression are different, and the bimod-

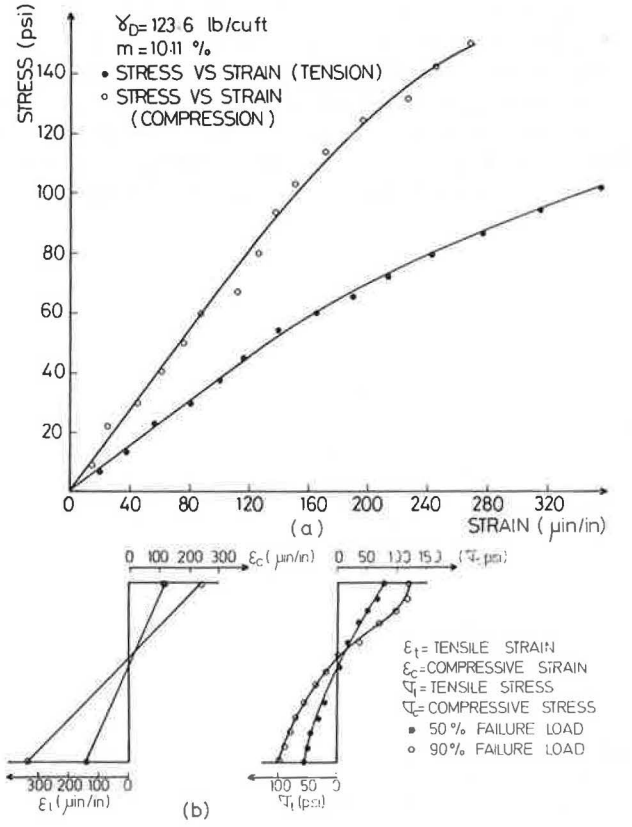

FIGURE 2 Stress-strain behavior of cement-treated silty clay in tension and compression.

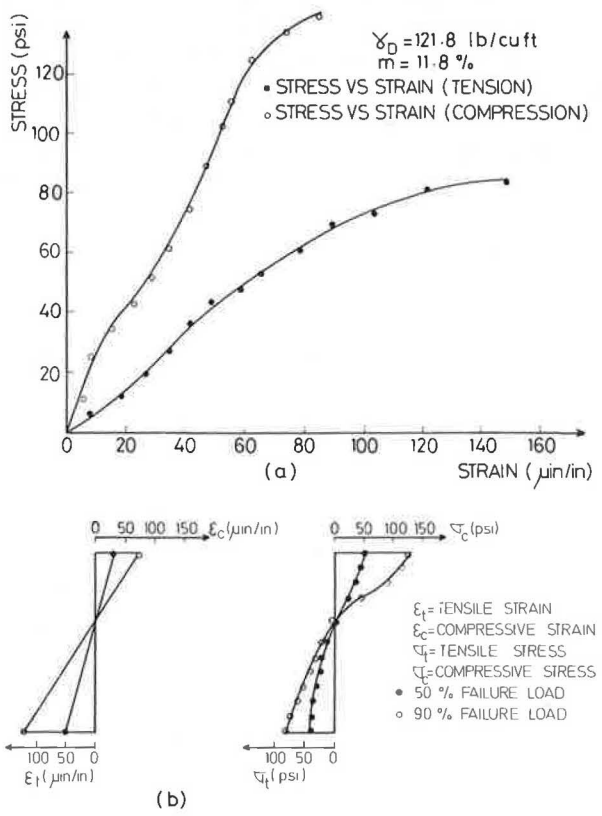

FIGURE 3 Stress-strain behavior of cement-treated sand mix in tension and compression.

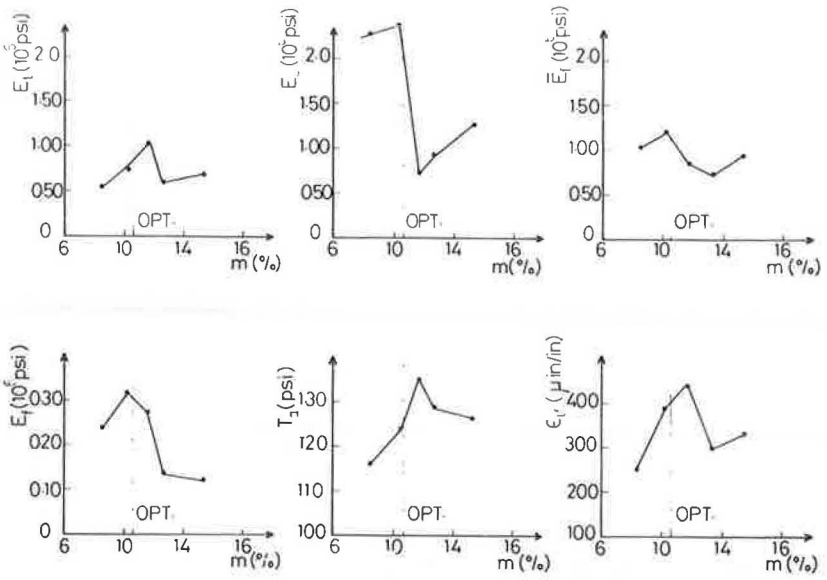

FIGURE 4 Influence of compaction variable on properties of cement-treated silty clay in flexure.

ular ratio (i.e., ratio of compressive modulus, E_c, to tensile modulus, E_t) could be less than or greater than unity depending on compaction moisture content. The modulus in flexure E_f based on deflection measurements at the center of the beam is smaller than the flexural modulus $\bar{E}_f$ associated with moment curvature relations.

3. The influence of increasing dry density γ_D for a given moisture content on the tensile and compressive properties of the cement-treated silty clay and the cement-treated sand mix is shown in Figures 6–9. The tensile modulus, E_t; compressive modulus, E_c; tensile strength, T_a; and tensile strain at failure, ε_{tf}, are normalized by their respective values, E_{to}, E_{co}, T_{ao}, ε_{tfo}, corresponding to maximum dry density γ_{DO} and optimum moisture content using modified AASHTO compaction energy. Results are compared for compaction dry of optimum (opt − 2%), at optimum (opt), and wet of optimum (opt + 2%). Increasing the dry density could yield larger or smaller values of tensile properties than those associated with compaction at maximum dry density and optimum moisture content. In the case of cement-treated silty clay, compaction wet of optimum results in larger values of tensile properties (E_t, T_a, ε_{tf}) than those obtained at optimum or dry of optimum (Figures 6 and 7), whereas lower values of E_t, T_a, and ε_{tf} are observed in the case of the cement-treated sand mix (Figures 8 and 9). The cement-treated silty clay exhibits more shrinkage than

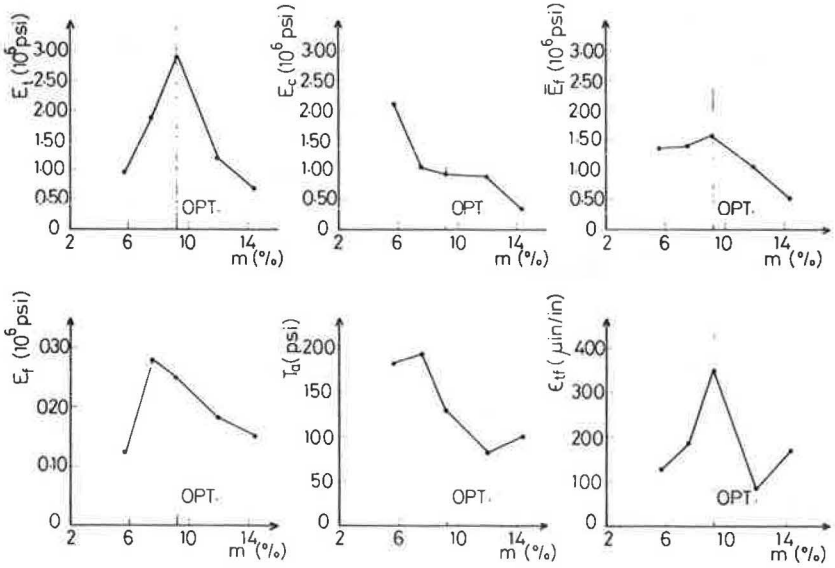

FIGURE 5 Influence of compaction variables on properties of cement-treated sand mix in flexure.

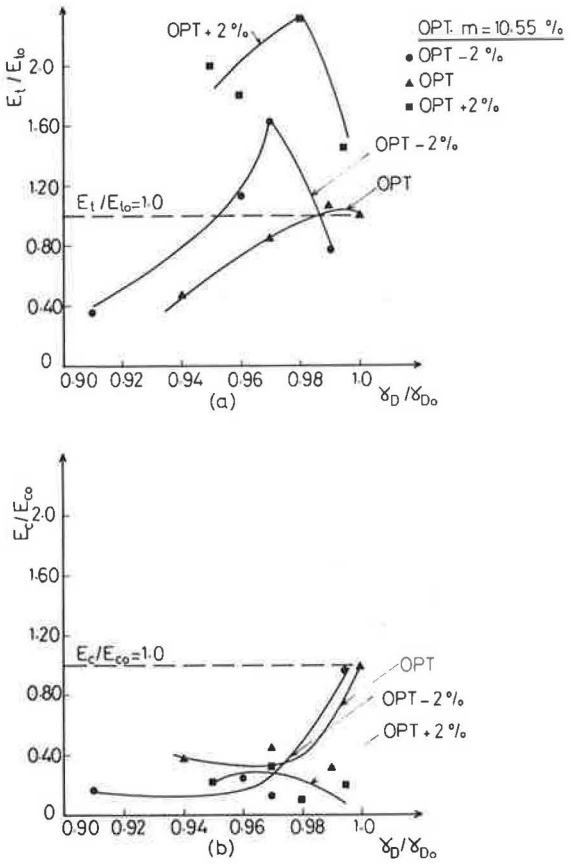

FIGURE 6 Variation of E_c and E_t with γ_D for cement-treated silty clay.

the cement-treated sand mix, which could be reflected as small microcracks in the matrix of the stabilized soil. Compaction wet of optimum in this case could lead to better moisture distribution and cement hydration with the net effect of improving tensile properties.

4. Flexural moduli E_f and $\bar{E}_f$ are generally used to characterize stabilized soils in flexure (*3, 7*). E_f is obtained from central beam deflections, whereas $\bar{E}_f$ is determined by using average top and bottom strains in the flexure test. In both cases, simple beam theory is used without consideration of potential differences in the tensile and compressive stress-strain properties of the stabilized material. Comparisons of tensile modulus E_t with E_f and $\bar{E}_f$ are given in Figure 10. Results indicate that E_t varies in the range of $0.60\bar{E}_f$ and $1.30\bar{E}_f$ with an average close to E_f but is much greater than E_f and ranges between $2.6E_f$ and $11.5E_f$. The lower values of E_f are associated with relatively larger central deflections that are probably caused by stress concentrations at the roller supports across both ends of the tested specimen, shear deformations, bimodular material behavior, and an effectively larger specimen in flexure as compared with the zone at which tensile strains are measured. A limited number of observations indicated that deflections at roller supports could reach 27 percent of the total measured central deflection. Correcting E_f for shear deformation effects (*3*) and stress concentrations at roller supports resulted on the average in values that were about 46 percent higher. Even after the corrections had been made, values of E_f were still much lower than those for E_t. It follows that the use of E_f in the design and analysis of stabilized layers should be treated with discretion. On the other hand, $\bar{E}_f$ could be used as an average value for tensile modulus E_t or in conjunction with improved analytical procedures as summarized elsewhere (*2*).

5. Correlation between the flexural strength T_f and the tensile strength T_a for all flexure test data indicates that T_f is in the range of T_a and $1.6T_a$ with a best fit representation of $T_f = 1.15T_a$. The flexural strength, T_f, varies from 70 to 220 psi for the cement-treated silty clay and from 30 to 320 psi for the cement-treated sand mix.

6. The tensile strain on the underside of cement-treated layers has been proposed by many investigators (*6*) as an alternative criterion to the tensile stress for design purposes. However, most available data for tensile strains are determined from flexural tests as the ratio of flexural stress to flexural modulus, E_f, and not as a direct measurement of strains on the underside of beam specimens. Results of this study indicate that measured tensile strain values at failure, ε_{tf}, vary from 200 to 600 μin./in. for the cement-treated silty clay and from 70 to 300 μin./in. for the cement-treated sand mix. An attempt to correlate ε_{tf} with corresponding values of T_f reflected a considerable scatter in the data (i.e., a relatively small coefficient of determina-

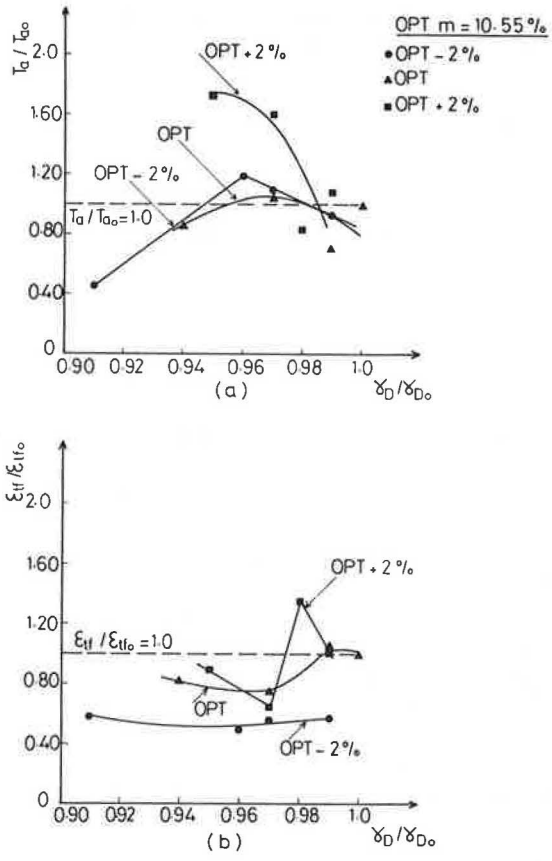

FIGURE 7 Variation of T_a and ε_{tf} with γ_D for cement-treated silty clay.

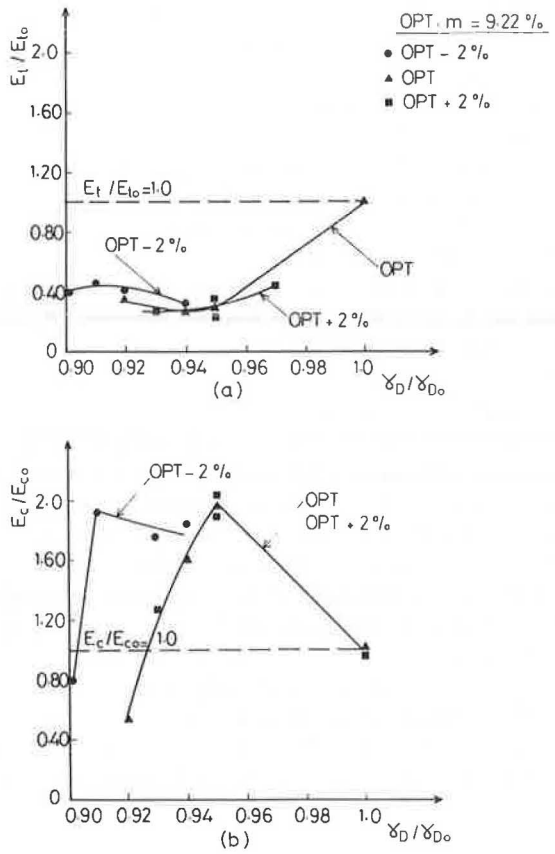

FIGURE 8 Variation of E_c and E_t with γ_D for cement-treated sand mix.

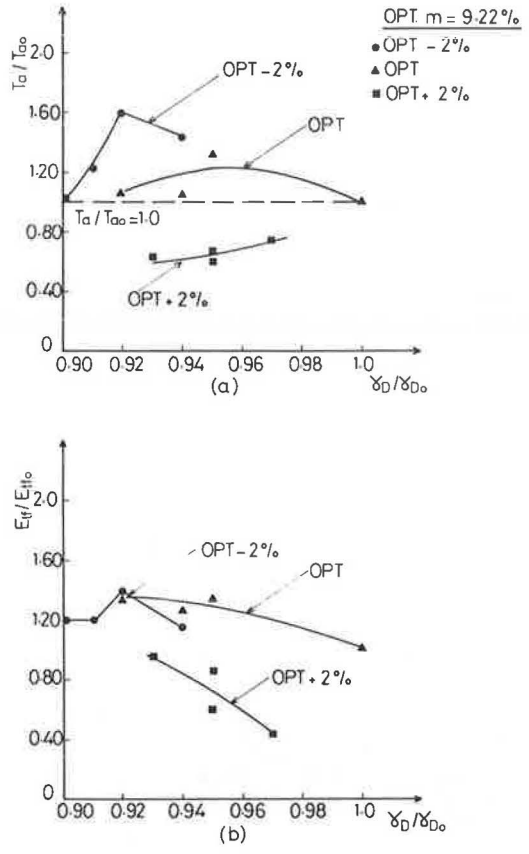

FIGURE 9 Variation of T_a and ε_{tf} with γ_D for cement-treated sand mix.

tion, R^2) The following relations, however, demonstrate the trend of variation.

For the cement-treated silty clay,

$$\varepsilon_{tf} = 423 - 0.61T_f \qquad (R^2 = 0.58) \tag{8}$$

and for the cement-treated sand mix,

$$\varepsilon_{tf} = 405 - 0.96T_f \qquad (R^2 = 0.26) \tag{9}$$

where ε_{tf} is expressed in microinches per inch and T_f is in pounds per square inch.

7. The influence of compaction variables, stress level, curing age, and cement content on bimodular ratio E_c/E_t is shown in Figures 11–15. Figures 11 and 12 are contour plots of E_c/E_t for the cement-treated silty clay and the cement-treated sand mix in terms of compaction moisture content and dry density. In the case of the cement-treated silty clay, an increase in compaction moisture content for a given dry density will result in a decrease in E_c/E_t followed by an increase for moisture content values wet of optimum (Figure 11). An opposite trend is observed for the cement-treated sand mix, in which E_c/E_t increases with compaction moisture content followed by a decrease for compaction wet of optimum (Figure 12). The variation of E_c/E_t with applied stress level (i.e., ratio of applied load to rupture load) is shown in Figure 13. Results indicate that the bimodular ratio is stress dependent and tends to increase in general for stress levels greater than 80 percent. The influence of curing age and cement content using test groups C_5,S_5 and C_6,S_6, respectively, is presented in Figures 14 and 15. Results of the limited number of tests

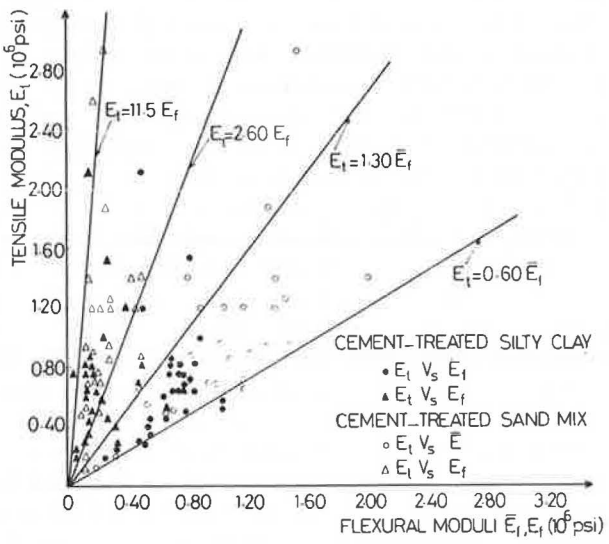

FIGURE 10 Correlation of tensile modulus and flexural moduli.

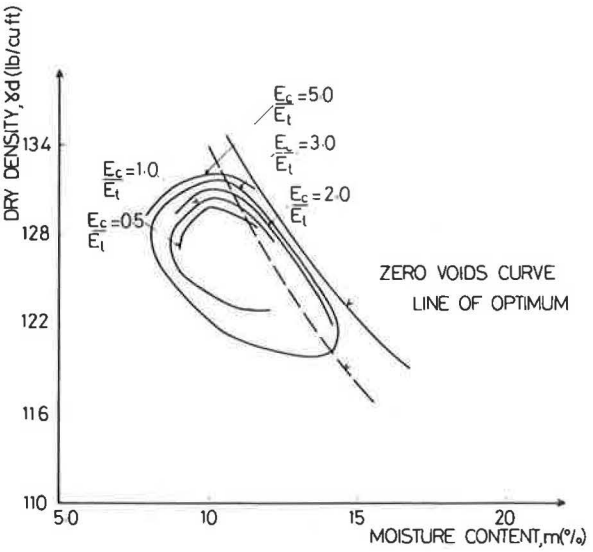

FIGURE 11 Influence of compaction variables on bimodular ratio for cement-treated silty clay.

performed reflect in general a decreasing tendency of bimodular ratio with increasing cement content and curing age. Correlations of compressive modulus, E_c; tensile modulus, E_t; and bimodular ratio, E_c/E_t, with flexural strength, T_f, are shown below. Although E_c and E_t tend to increase with increasing T_f, E_c/E_t would decrease in general. Moreover, lower values of E_c and E_t and higher values of E_c/E_t are obtained for a given T_f in the case of the cement-treated silty clay in comparison with the cement-treated sand mix.

For the cement-treated silty clay,

$$E_c = 66.9 + 5.39T_f \qquad (R^2 = 0.44) \tag{10}$$

$$E_t = -35.9 + 5.07T_f \qquad (R^2 = 0.63) \tag{11}$$

$$E_c/E_t = 5.43 - 0.02T_f \qquad (R^2 = 0.23) \tag{12}$$

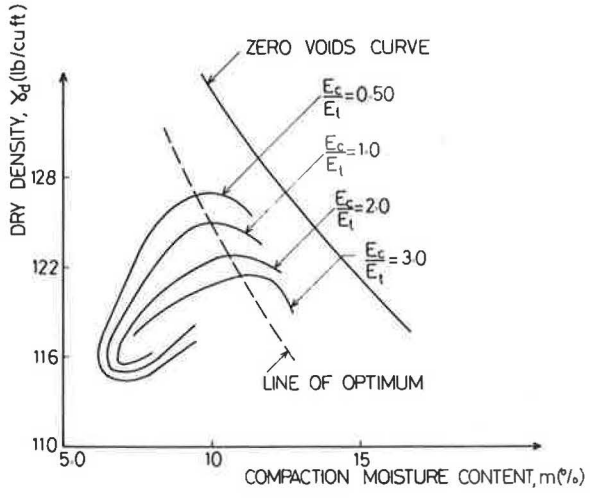

FIGURE 12 Influence of compaction variables on bimodular ratio for cement-treated sand mix.

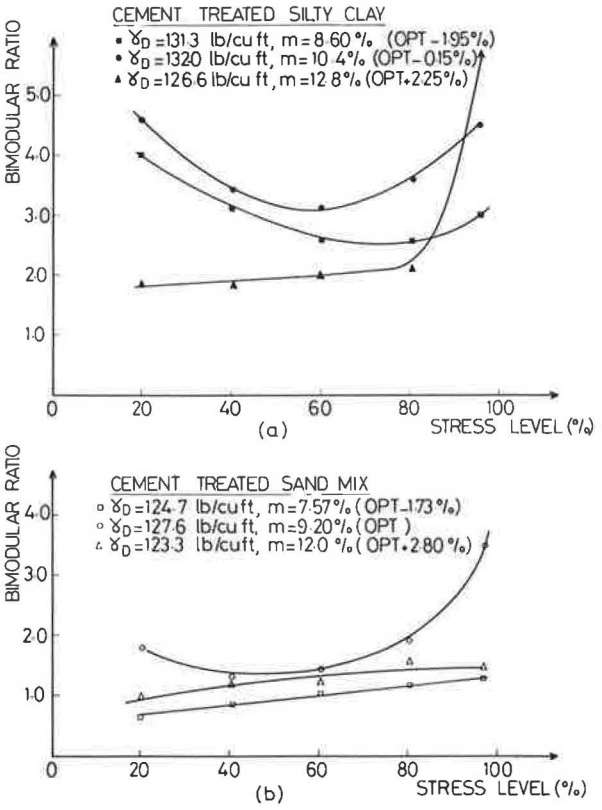

FIGURE 13 Influence of stress level on bimodular ratio.

and for the cement-treated sand mix,

$$E_c = 320 + 7.84T_f \qquad (R^2 = 0.43) \tag{13}$$

$$E_t = -108 + 9.94T_f \qquad (R^2 = 0.68) \tag{14}$$

$$E_c/E_t = 3.31 - 0.01T_f \qquad (R^2 = 0.24) \tag{15}$$

where E_c and E_t are expressed in kips per square inch and T_f is in pounds per square inch.

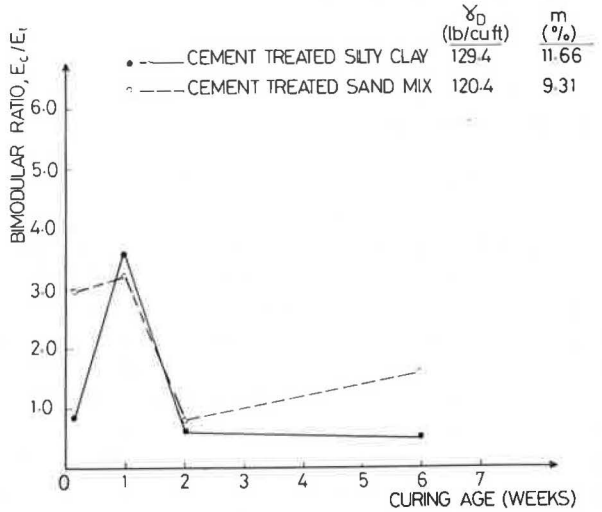

FIGURE 14 Influence of curing age on bimodular ratio.

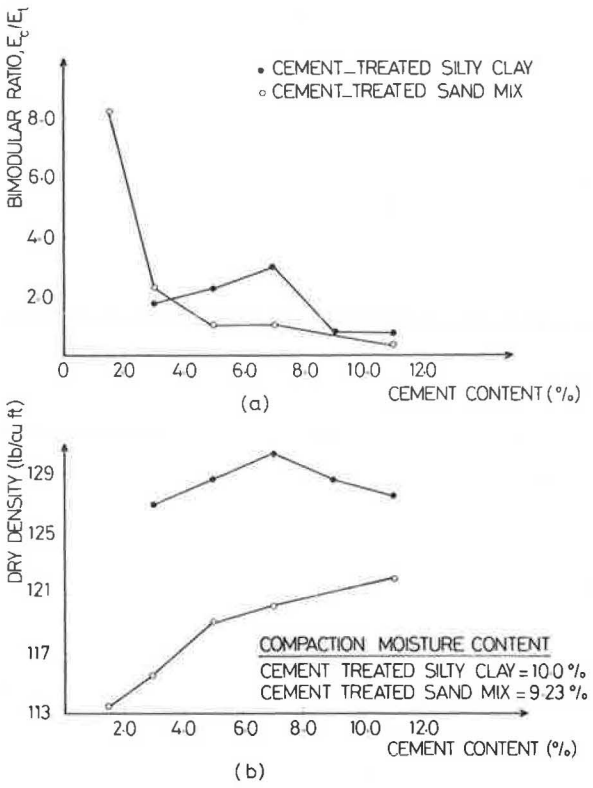

FIGURE 15 Influence of cement content on bimodular ratio.

MECHANISMS OF BIMODULAR BEHAVIOR

Flexural beam test results indicate that for the cement-treated silty clay the bimodular ratio is in the range of 0.5 to 5, whereas for the cement-treated sand mix it ranges from 0.5 to 3. Similar behavior is observed for cement-treated materials under direct tension and compression testing, in which bimodular ratio values ranging from 1 to 10 have been reported (*8, 9*). The probable mechanisms of bimodular behavior could be described as one or more of those discussed in the following sections.

Resistance to Shear under Normal Tensile and Compressive Stresses

It is assumed that under normal tensile and compressive stresses, the stabilized soil will exhibit a greater resistance to shear deformation along a given plane if the applied normal stress on that plane is compressive than if the same applied stress is tensile. Schematically this is shown using a Mohr circle representation for a uniaxial tensile and compressive stress application (Figure 16). On a given plane, the normal stress is compressive under uniaxial compression, whereas it is tensile under uniaxial tension. The magnitude of the shear stress acting on the same plane is equal in both cases, indicating a greater shear deformation potential under uniaxial tension than under uniaxial compression. This would result in a greater modulus in compression than in tension for the same applied uniaxial stress.

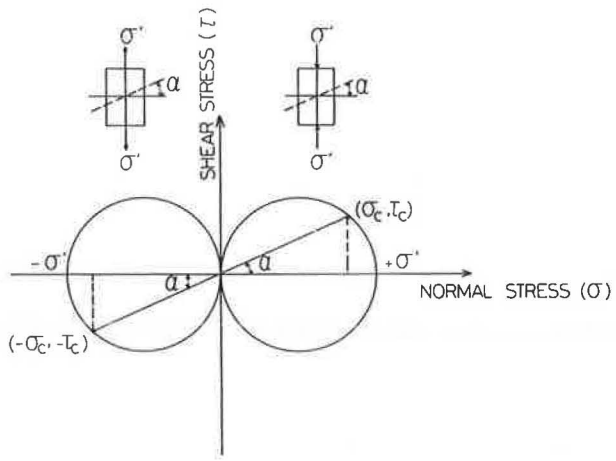

FIGURE 16 Stress state on a given plane in specimens under direct tension and compression.

Fracture Propagation of Flaws and Microcracks

Fracture mechanics principles are used to demonstrate the effect of cracking on the stress-strain behavior. For a given specimen with a thin microcrack of length $2a$, as shown in Figure 17, the propagation of the crack under a given tensile stress associated with applied displacement (Δ) or

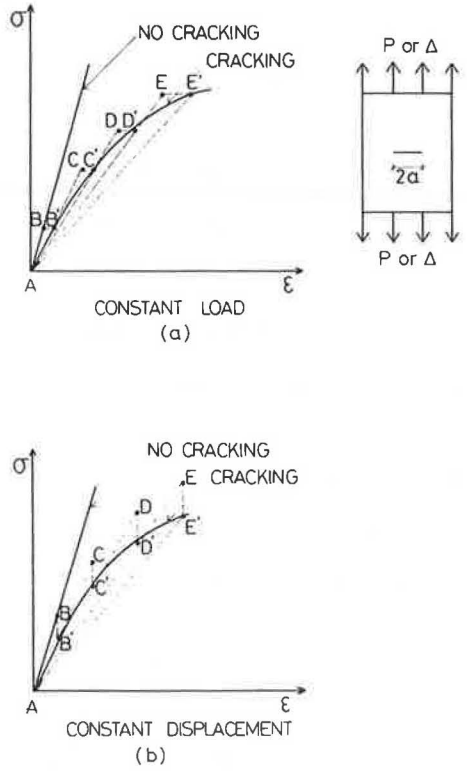

FIGURE 17 Effect of cracking on stress-strain behavior.

tensile load (P) would result in a release of stored elastic energy at a constant stress (Figure 17a) or at a constant strain (Figure 17b), thereby yielding the stress-strain representation (A,B',C',D').

Local Stiffness Variation Within the Material

The material in this case is discretized into elements (i,j,k) as shown in Figure 18. Assuming that each element has a designated stiffness E_{ijk}, the measured modulus E under uniaxial tension will be given by

$$E = 1/C \tag{16}$$

where

$$C = \frac{ml}{n}\left(\frac{1}{\sum_{i=1}^{l}\sum_{j=1}^{m} E_{ijl} + \ldots + \sum_{i=1}^{l}\sum_{j=1}^{m} E_{ijn}}\right) \tag{17}$$

such that

l = number of elements in the i-direction,
m = number of elements in the j-direction, and
n = number of elements in the k-direction.

A loss of element stiffness under uniaxial tensile stress could be induced by an existing microcrack or by crack propagation at the tip of a flaw or a discontinuity. As a result, C will increase and the measured modulus E will decrease. Because stabilized materials are weaker in tension than in compression (*8, 10*), it is more likely that loss of element stiffness will occur if the applied stress is tensile than if it is compressive. The measured compressive modulus is therefore expected to be larger than the measured tensile modulus for the same applied uniaxial stress. With this discretized model it could also be inferred that the probability of encountering an element with low stiffness increases with increasing specimen volume V as shown in Figure 18. The effect of size on measured stiffness will be more significant under tensile stresses than under compressive stresses. Mathematical treatment by other investigators (*11*) yielded similar results concerning the effect of specimen size on the probability of failure of brittle solids.

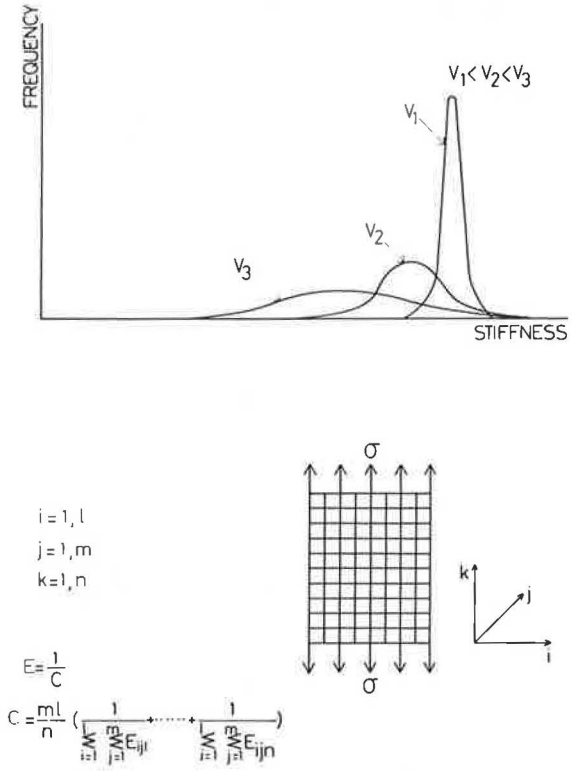

FIGURE 18 Discrete model and probable effect of specimen size on stiffness.

SIGNIFICANCE OF BIMODULAR BEHAVIOR

A two-layer pavement system consisting of a cement-treated base over a subgrade was analyzed to study the influence of bimodular properties on response and fracture behavior under repeated traffic loads. An iterative technique utilizing the finite-element method and a fatigue failure model for the cement-treated layer was employed. Plane strain conditions were assumed. Details of the analytical procedure have been presented elsewhere (*12*). A finite-element representation of the pavement system is shown in Figure 19.

Results of the analysis indicate that structural response is significantly influenced by the bimodular properties of the cement-treated base (Figure 20). A reduction in tensile modulus, for example, from a value equal to its compressive modulus (i.e., bimodular ratio of 1) to a value equal to one-tenth the compressive modulus (i.e., bimodular ratio of 10) results in an increase in subgrade vertical stress, σ_v, and surface deflection, d. However, the most significant influence seems to be associated with the tensile stress σ_t

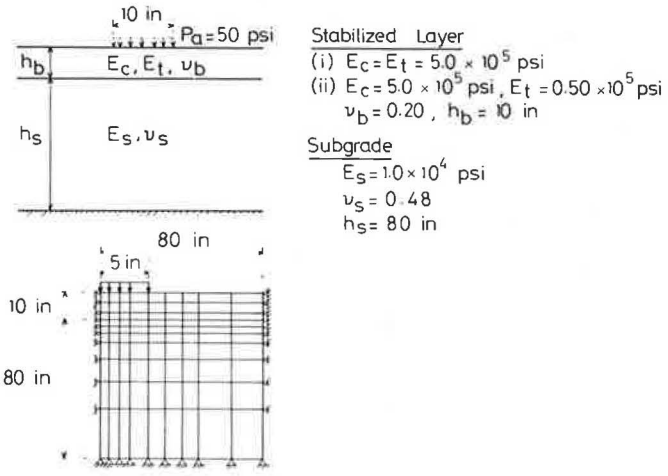

FIGURE 19 Finite-element representation of pavement section.

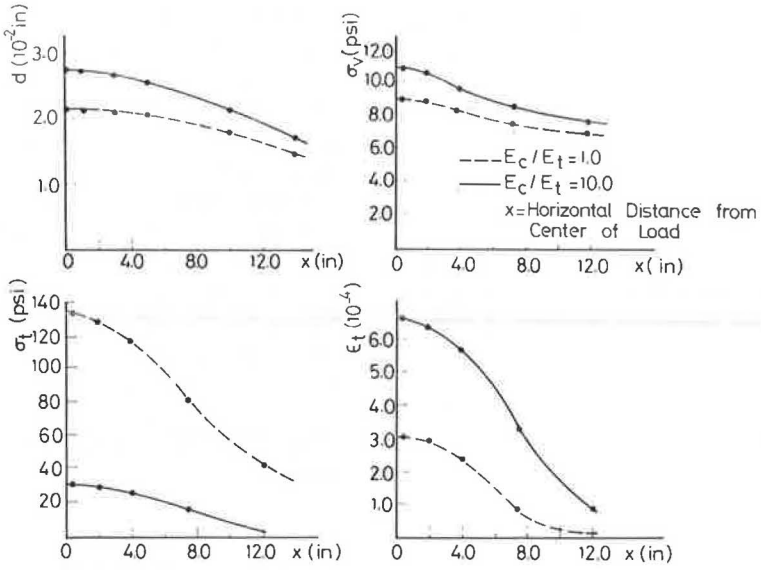

FIGURE 20 Response of stabilized layer under applied load.

and the tensile strain ε_t on the underside of the base. The maximum tensile stress is reduced about 5 times, whereas the maximum tensile strain becomes twice as much.

The influence of the bimodular ratio on fatigue crack initiation and propagation for a given number of load repetitions (106 repetitions in this case) is shown in Figure 21. For a given thickness of base, flexural strength, and compressive modulus, a decrease in bimodular ratio seems to increase the resistance of the stabilized layer to fatigue crack initiation and propagation. Moreover, a smaller increment of load is required to propagate the crack from the underside of the base to its surface for the case of $E_c/E_t = 10$ as compared with the case of $E_c/E_t = 1$, indicating a higher rate of crack propagation.

Similar analyses were also conducted to investigate the fatigue behavior of the stabilized base when the cement-treated silty clay was used as compared with use of the cement-treated sand mix. The two-layer representation of the pavement section is shown in Figure 19. The applied load needed for crack initiation and propagation was estimated for different values of flexural strength and tensile and compressive moduli as determined from Equations 10–15. Results are presented in Figure 22. Increasing the flexural strength would increase the load required for fatigue crack initiation on the underside of the base and propagation to its surface. The increase in flexural strength in

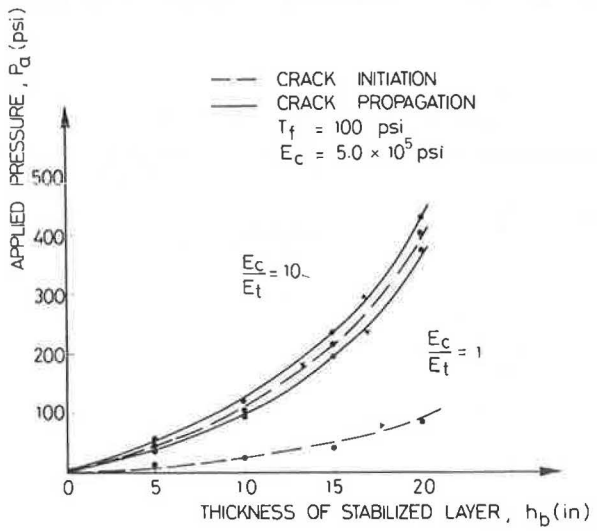

FIGURE 21 Influence of bimodular properties on fatigue crack initiation and propagation after 10^6 repetitions.

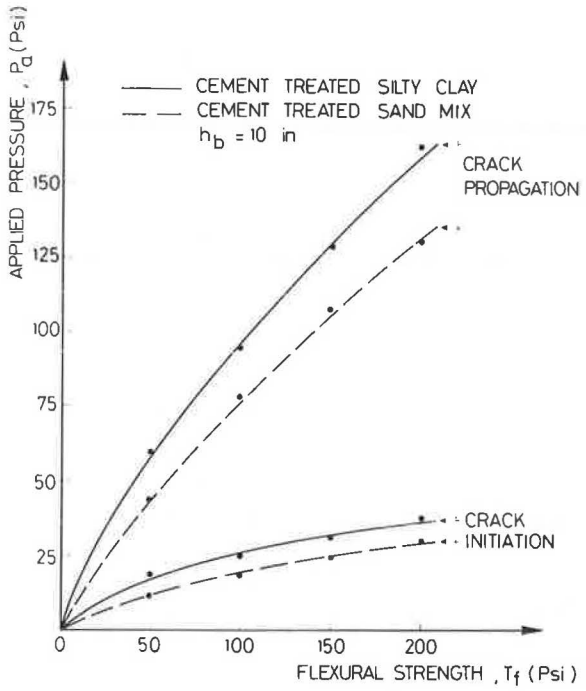

FIGURE 22 Fatigue behavior after 10^6 repetitions: 10-in. base of cement-treated silty clay versus cement-treated sand mix.

this case seems to outweigh the reduction in fatigue load capacity associated with the resulting higher compressive modulus and lower bimodular ratio, with the net effect of enhancing the fatigue resistance of the base. Moreover, for a given flexural strength, the cement-treated silty clay seems to exhibit more resistance to fatigue loading when used as a base in comparison with the cement-treated sand mix.

These results agree with similar conclusions presented by Williams (*13*). They are, however, tentative. Additional research is needed to compare tensile and compressive properties of stabilized soils using static and repeated load tests. Of particular interest is the influence of fatigue on bimodular behavior. Fatigue data for a cement-treated clayey gravel presented by Pretorius (*14*, p. 67) show an increase in bimodular ratio from an initial value of 1.2 to about 4 during flexure fatigue testing.

SUMMARY AND CONCLUSIONS

Flexure tests have been used to study the flexural behavior of a cement-treated silty clay and a cement-treated sand mix. The influence of compaction variables, cement content, and curing age on stress-strain characteristics in tension and compression, flexural strength, tensile strength, tensile strain at failure, and flexural moduli have been investigated.

The flexural modulus $\overline{E}_f$ determined from moment curvature relations has been found to attain an average value essentially equal to the tensile modulus E_t, whereas the flexural modulus E_f obtained using simple beam theory and central beam deflection is much smaller than E_t. Although $\overline{E}_f$ could be used as an average estimate for tensile modulus E_t and in conjunction with improved analytical procedures as summarized elsewhere (*2*), the use of E_f in design and analysis of stabilized layers should be treated with discretion.

Computation of flexural strength T_f using simple beam theory assumptions yields values that are essentially equal to 1.15 times the actual tensile strength T_a associated with tensile failure on the underside of the beam. The tensile strain at failure, ε_{tcf}, varies from 200 to 600 μin./in. for the cement-treated silty clay and from 70 to 300 μin./in. for the cement-treated sand mix. An increase in flexural strength T_f results in a reduction of failure tensile strain ε_{tf}.

Stress-strain predictions using top and bottom strain measurements in beam specimens indicate different load-deformation properties in tension and compression. Values of compressive modulus E_c, tensile modulus E_t, tensile strength T_a, and tensile strain at failure ε_{tf} could be higher or lower than the corresponding values at optimum moisture content and maximum AASHTO dry density, depending on type of stabilized soil, compaction moisture content, and dry density. The bimodular ratio E_c/E_t ranges between 0.5 and 5 for the cement-treated silty clay and from 0.5 to 3 for the cement-treated sand mix. Although E_c and E_t tend to increase with increasing T_f, E_c/E_t would decrease in general. The observed differences in compressive and tensile moduli have been explained using a number of mechanistic models.

Results of the analysis indicate that the bimodular properties have a significant effect on the traffic-induced stresses and strains on the underside of the stabilized base and on its fracture behavior in terms of fatigue crack initiation and propagation. The proper assessment of these properties is therefore desirable for developing a better understanding of the behavior of stabilized layers under applied traffic loads.

ACKNOWLEDGMENTS

This work was supported by a grant from the University Research Board of the American University of Beirut. Laboratory assistance by H. Minassian, S. Saboudjian, B. Zeid, and M. Itani is gratefully acknowledged.

REFERENCES

1. L. Raad, C. L. Monismith, and J. K. Mitchell. Crack Propagation in Soil-Cement Bases Subjected to Repeated Wheel Loads. In *Transportation Research Record 690,* TRB, National Research Council, Washington, D.C., 1978, pp. 1–5.
2. L. Raad. Behavior of Stabilized Layers Under Repeated Loads. In *Transportation Research Record 1022,* TRB, National Research Council, Washington, D.C., 1985, pp. 72–79.
3. E. J. Felt and M. S. Abrams. Strength and Elastic Properties of Compacted Soil-Cement Mixtures. In *Special Technical Publication 206,* American Society for Testing and Materials, Philadelphia, Pa., Sept. 1956, pp. 153–173.
4. J. S. Gregg. The Significance of Compressive, Tensile, and Flexural Strength Tests in the Design of Cement-Stabilized Pavement Foundations. In *Proceedings, Fourth Regional Conference for Africa on Soil Mechanics and Foundation Engineering,* Capetown, South Africa, Dec. 1967, pp. 185–190.
5. J. L. M. Scott. *Flexural Stress-Strain Characteristics of Saskatchewan Soil-Cements.* Technical Report 23. Saskatchewan Department of Highways and Transportation, Regina, Saskatchewan, Canada, Dec. 1974.
6. E. Otte, P. F. Savage, and C. L. Monismith. Structural Design of Cement-Treated Layers. *Journal of the Transportation Engineering Division,* ASCE, Vol. 108, No. TE4, July 1982, pp. 428–446.
7. L. P. Sudath and M. R. Thompson. *Load-Deflection Behavior of Lime Stabilized Layers.* Technical Report M-118. Construction Engineering Research Laboratory, Urbana-Champaign, Ill., Jan. 1975.
8. L. Raad, C. L. Monismith, and J. K. Mitchell. Tensile Strength Determinations of Cement-Treated Materials. In *Transportation Research Record 641,* TRB, National Research Council, Washington, D.C., 1977, pp. 48–51.
9. H.E. Bofinger. *The Measurement of the Tensile Properties of Soil-Cement.* Report LR365. U.K. Transport and Road Research Laboratory, Crowthorne, Berkshire, England, 1970.
10. A. A. Griffith. Theory of Rupture. In *Proceedings of First International Congress for Applied Mechanics,* Delft, Netherlands, 1924, pp. 55–63.
11. H. L. Oh and I. Finnie. On the Location of Fracture in Brittle Solids. I: Due to Static Loading. *International Journal of Fracture Mechanics,* Vol. 6, 1970, pp. 287–300.

12. L. Raad, C. L. Monismith, and J. K. Mitchell. Crack Propagation in Soil-Cement Bases Subjected to Repeated Wheel Loads. In *Transportation Research Record 690,* TRB, National Research Council, Washington, D.C., 1978, pp. 1–5.
13. R. I. T. Williams. Properties of Cement-Stabilized Materials. *Journal of the Institution of Highway Engineers,* Feb. 1972, pp. 5–19.
14. P.C. Pretorius. Design Considerations for Pavements Containing Soil-Cement Bases. Ph.D. dissertation. University of California, Berkeley, 1970.

Publication of this paper sponsored by Committee on Soil-Portland Cement Stabilization.

Effect of Lime on Highly Plastic Clay with Special Emphasis on Aging

D. A. SWEENEY, D. K. H. WONG, AND D. G. FREDLUND

A laboratory study was undertaken to evaluate the effect of aging on the properties of Regina clay treated with 2 and 4 percent quick lime. Aging is generally referred to as the time interval between the addition of lime and water to the soil and the compaction of the mixture. Regina clay, a highly expansive clay, was selected for this study because it forms a common subgrade material in Saskatchewan. As a result of this study, it was found that aging had a pronounced effect on the properties of the treated soil. The properties also depended on the percentage of lime. The results indicate that both density and strength decreased as a result of an increased aging period for the treated samples prepared using constant compactive effort. However, the reduction in strength could be eliminated or could even result in an increase if the treated specimens with low percentages (e.g., 2 percent) were subjected to an increased compactive effort. Nevertheless, the results show that increasing the compactive effort could not eliminate the reduced strength for samples treated with higher percentages of lime (e.g., 4 percent) and increased aging (e.g., 24 hr). Increased compaction may well lead to a lower strength as a consequence of overcompaction. Aging appears to have had no significant effect on swell for treated samples prepared by both constant and increased compactive efforts, and little effect as well on the plasticity index.

Lime has been used for more than 20 years on Saskatchewan highways to improve the engineering properties of subgrade soils. However, use of lime in Saskatchewan is relatively limited because of the costs involved and some unsatisfactory experiences in the past. Lime has been used on a few full-scale experimental test sections throughout the province and on some small projects. Consequently, little information is available concerning the performance of lime-treated soils in Saskatchewan. In particular, there is limited information available on the long-term performance of lime-treated highway pavement.

PURPOSE AND SCOPE

In an attempt to develop a fuller understanding of the behavior of lime-treated clays native to Saskatchewan, the Saskatchewan Highways and Transportation Department is committed to sponsoring a 3-year lime research program at the University of Saskatchewan; the program began in 1986. The main purposes of the research program are twofold: (a) to investigate the behavior of the lime-treated clay native to Saskatchewan under the influences of various design and environmental factors, and (b) to develop appropriate methods for predicting the long-term strength and durability of the lime-treated native clay, a highly plastic material referred to as Regina clay.

The following research program has been established in order to accomplish the foregoing purposes. The program consists of (a) a literature search and synthesis of data, (b) a laboratory testing program, (c) an evaluation of the field design mix and construction procedure, and (d) the study of a full-scale field test section.

The purpose of the literature search and synthesis of data was to critically examine the past literature pertinent to lime-treated soils. The literature review was used to help establish a relevant laboratory testing program to investigate the behavior of the lime-treated native clays under the influence of various design and environmental variables. An attempt was made to establish appropriate testing procedures for predicting the strength and durability of the lime-treated clays on a long-term basis. Upon completion of the laboratory program, design and construction procedures specific to Saskatchewan climate conditions will be proposed. The proposed procedures will then be evaluated by studying a field test section through a long-term monitoring program.

The laboratory investigation began in the spring of 1986. It consisted of a short-term and long-term property evaluation of a lime-treated native clay. In the short-term property evaluation the effects of variables such as lime percentage, initial water content, aging period, and compactive effort on lime-treated clays were studied. The long-term property evaluation emphasizes the influences of the environmental variables on lime-treated clays. The variables studied included curing, wetting and drying, and freezing and thawing. This paper contains the results of the short-term property evaluation; the research findings of the long-term property evaluation will be presented in a separate paper.

BACKGROUND

Considerable research has been conducted during the past few decades on the behavior of lime-treated soils. The literature review indicated that efforts have concentrated mainly on evaluating variables such as soil type, lime type, lime content, and curing. However, the influence of aging

Department of Civil Engineering, University of Saskatchewan, Saskatoon, Saskatchewan S7N 0W0, Canada.

has not been thoroughly examined (*1*). Aging is generally referred to as the elapsed time between the addition of lime and water to the soil and the compaction of the mixture. This term has also been referred to as "rotting" and "mellowing."

It appears that researchers have not believed that aging critically affects the properties of lime-treated soils. McDowell (*2*) and Dumbleton (*3*) pointed out that aging was helpful in breaking down clay clods, which provided a better mix uniformity and workability. However, Taylor and Arman (*4*) reported that most of the failures associated with lime-treated bases in Louisiana were due to improper mixing and delayed compaction after the initial mixing of the soil and lime.

Mitchell and Hooper (*5*) performed an investigation to study the effect of aging on an expansive clay treated with 4 percent dolomitic hydrated lime. It was found that aging was detrimental in terms of density, unconfined compressive strength, and swell characteristics for samples prepared using a constant compactive effort. It was reported, however, that the detrimental effects related to aging could be eliminated if extra compactive effort was provided to compact the aged samples to the same densities as the unaged samples.

Other properties affected by aging are permeability and suction. Fossberg (*6*) reported that the addition of lime decreases permeability and increases soil suction. Klym (*7*) used a longer aging period than Fossberg and showed that the addition of lime resulted in an increase in permeability and a decrease in suction.

The effect of aging on the durability of lime-treated soils has not been thoroughly investigated, possibly because of an earlier understanding that aging only provides better mix uniformity and workability. O'Flaherty and Andrews (*8*) performed a series of freezing and thawing tests, and concluded that aging has a deleterious effect on the durability of lime-treated soils.

Aging not only influences the physical properties of the soil but also plays an important role in the field construction procedure. This is particularly true for highly plastic clays native to Saskatchewan. It therefore appeared desirable to initiate a thorough laboratory study to better define the effects of aging and compaction. The initial phase of the study, which evaluated the short-term properties of lime-treated native clays, emphasized the influence of aging and compaction.

MATERIALS

Soil

The soil selected for this study was Regina clay, a material commonly used for highway subgrades in Saskatchewan. Its relevant properties are summarized in Table 1. The soil consists of approximately 80.0 percent clay and 20.0 percent silt. The average liquid limit is 86.0 percent and the average plasticity index is 58.8 percent. The soil is classified as CH in the Unified Soil Classification System.

The average specific gravity of Regina clay is 2.83. The maximum ASTM standard proctor density is 1.42 Mg/m^3 at an optimum water content of 30.0 percent. The maximum modified ASTM density is 1.66 Mg/m^3 at an optimum water content of 21.8 percent.

X-ray analysis indicates that the soil has a mixture of smectite and illite clay minerals. The soil swells excessively when wet and shrinks when drying, forming large shrinkage cracks.

Lime

The lime used in this study was a commercial calcitic quick lime (CaO) having the composition and gradation indicated in Table 1. It was kept in sealed containers until immediately before use to prevent carbonation with the carbon dioxide in the air.

SAMPLE PREPARATION

To prepare the material for the various tests, Regina clay was air dried and pulverized using a Los Angeles abrasion resistance machine. The soil was then sieved, and material passing the 2.00-mm (No. 10) sieve was used for the density, unconfined compression, and swell tests. Material passing the 0.425-mm (No. 40) sieve was used for the plasticity index testing. Before lime was added to the soil samples, distilled water was added to the air-dried soil to achieve the desired initial water content (7 or 15 percent). The samples were placed in a moist room for at least 2 days. The quick lime was then added to the soil samples and dry-mixed for several minutes. Distilled water was added to the soil-lime samples to achieve the desired aging water contents of approximately 25, 30, or 35 percent. After being mixed by hand for several minutes, the samples were mechanically mixed for 3 to 5 min to ensure complete and thorough mixing. The samples were then placed in sealed double plastic bags and allowed to age for 1, 4, or 24 hr. Immediately after aging, the soil-lime samples were tested for density, unconfined compressive strength, percent swell, and plasticity. It should be emphasized that no curing period was permitted; only initial values were measured. The curing portion of the research program is to follow.

A large number of samples was required to complete this portion of the study (approximately 300). In order for each variable to be studied, only one sample for each particular combination of aging water content, lime percentage, aging period, compactive effort, and initial water content was prepared. Thus for the tests of unconfined compressive strength and percent swell, only one sample was prepared for each data point. The density data are a result of three tests, because compaction was required for preparation of the unconfined compressive strength and swell tests. One test per point was also performed for the plasticity index results. No statistical comparisons were made.

TABLE 1 MATERIALS

REGINA CLAY

		CLAY MINERALOGY	
LIQUID LIMIT	86.0%	ILLITE/SMECTITE MIXED LAYER	48.0%
PLASTIC LIMIT	27.2%	ILLITE	9.0%
PLASTICITY INDEX	58.8%	KAOLINITE	10.0%
% CLAY	80.0%	QUARTZ	33.0%
% SILT	20.0%		

OPTIMUM WATER CONTENT AND MAXIMUM DRY DENSITY

STANDARD PROCTOR: 30.3%, 1.415 Mg/m^3

MODIFIED PROCTOR: 21.8%, 1.658 Mg/m^3

CHEMICAL ANALYSIS

SOLUABLE SULFATE	2050 ppm (.205 %)
ORGANIC CARBON	10000 ppm (1.0 %)

LIME ANALYSIS	% BY WEIGHT
CaO plus MgO	96.35%
MgO	01.45%
IMPURITIES	03.65%

GRADATION	% BY WEIGHT PASSING
2.00 mm	100%
0.16 mm	100%

LABORATORY TESTS

Plasticity Index

The plasticity index tests were performed according to ASTM D424-59 (1971). The soil-lime samples that were tested for plasticity were aged at a water content of 30.0 percent.

Density Tests

Standard Compaction

After mixing and allowing the soil-lime samples to age, compaction was performed according to ASTM D698-78. Compaction was achieved with a mechanical dynamic compactor. The soil was compacted in three layers with a 2.49-kg (5.5-lb) rammer and a 305-mm (12-in.) drop. A standard 101-mm (4-in.) proctor mold was used to form the specimens.

Increased Compaction

Figure 1 shows a plot of dry density versus number of blows per layer for various lime percentages and aging periods. Each point represents a lime-treated soil compacted by using a mechanical dynamic compactor with a 2.49-kg rammer and a 305-mm drop. Three compaction layers were used; however, the number of blows per layer varied for each specimen. A maximum dry density of 1.4 Mg/m^3 at a water content of 30.0 percent was desired. This density is equivalent to the maximum dry density of untreated Regina clay according to ASTM D698-78. Figure 1 shows the required number of blows per layer to achieve 1.4 Mg/m^3 for a particular aging period and lime percentage. The increased compactive effort required to achieve the

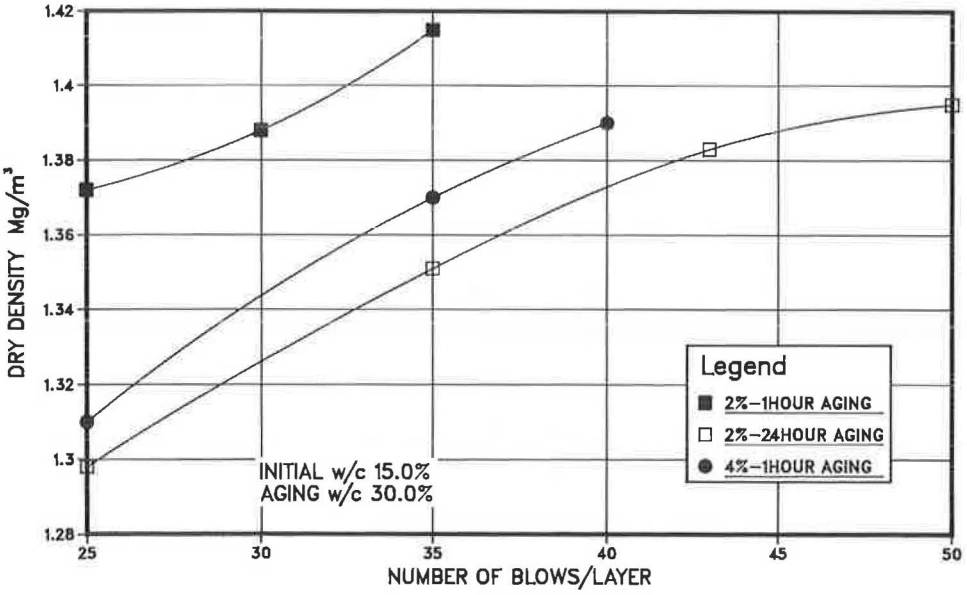

FIGURE 1 Number of blows per layer versus dry density for 2 percent lime-modified clay aged for 1 and 24 hr and 4 percent lime-modified clay aged for 1 hr (initial water content 15 percent and aging water content 30 percent).

constant density was then used to prepare the specimens for the unconfined and the swell tests.

Unconfined Compression

Unconfined compression tests were performed according to ASTM D2166-66 (1979), with a constant strain rate of 1.0 percent and a length-to-diameter ratio of 2.4. To obtain a sample for the unconfined compression test, the soil-lime specimens were compacted in the proctor mold, either to standard proctor density or untreated density (1.4 Mg/m^3). A 50.8-mm (2-in.) diameter Shelby tube was then hydraulically pressed through the compaction specimen. Extruding the sample from the Shelby tube resulted in a specimen 47.2 mm (1.9 in.) in diameter and 117 mm (4.6 in.) long. This sampling technique proved successful, resulting in minimal sample disturbance.

Swell

Swell tests were conducted according to ASTM D4546-85, with a 64-mm (2.5-in.) diameter steel ring and a vertical overburden pressure of 7 kPa (1 psi). The swell test specimens were formed by manually pressing the 64-mm steel ring into the compaction specimen; they were then trimmed. The specimens were allowed to swell in one-dimensional odometers and then loaded back to the original void ratio. The swelling pressures were determined by reloading the specimens to their original void ratio. However, only the percent swell results are reported in this paper.

RESULTS AND DISCUSSION

Effect of Aging on Lime-Treated Samples Using Constant Compactive Effort

The effect of aging on the lime-treated Regina clay was assessed in terms of Atterberg limits, the relationship between water content and density, unconfined compressive strength, and swell characteristics. All compacted samples were prepared using a standard compactive effort.

Atterberg Limits

Figure 2 shows the effect of aging on the plasticity characteristics of lime-treated Regina clay. In general, the results indicate that the plasticity index decreases only slightly with increasing aging period. The difference is so small that no conclusions can be drawn without additional tests. Nevertheless, the effect of aging on plasticity index tends to increase with increasing lime content.

The relationship between lime content and the plasticity characteristics of lime-treated Regina clay aged 24 hr is shown in Figure 3. As can be seen, the addition of lime results in a decrease in the liquid limit and an increase in the plastic limit. The net effect is a significant reduction in plasticity index, a commonly observed consequence of lime addition. In addition, the results show that the largest reduction in plasticity index occurs at the first addition of lime. With the addition of only 2 percent lime, the plasticity index is reduced dramatically from 58.8 to 20 percent. However, the decrease with a further increase in lime content is reduced.

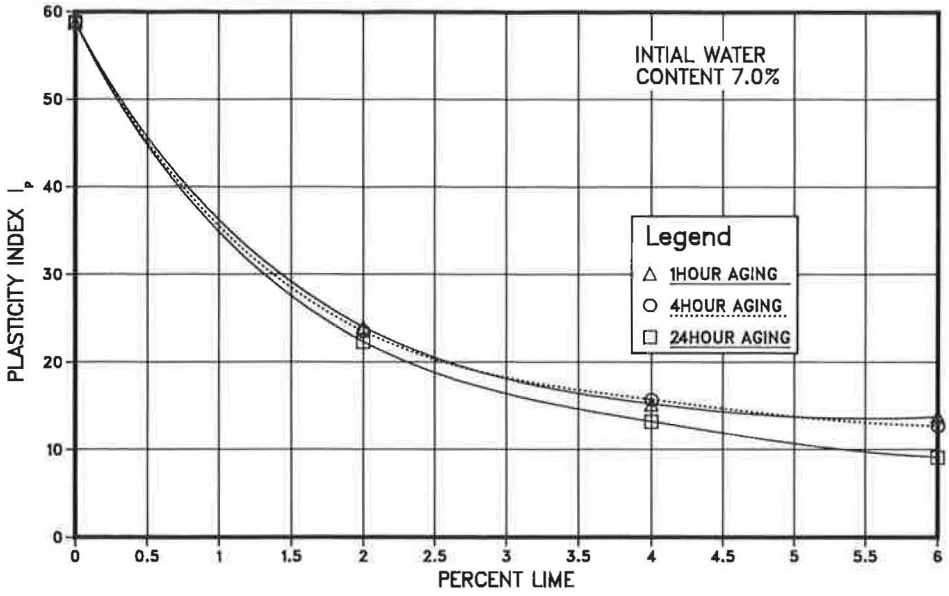

FIGURE 2 Percentage of lime added versus plasticity index for 1-, 4-, and 24-hr aging.

Water Content Versus Density

The standard compaction curves for the untreated clay with 2 and 4 percent lime aged for 1 hr and the clay treated with 2 and 4 percent lime aged for 24 hr are shown in Figure 4. These curves indicate the following trends.

1. The effect of aging on lime-treated Regina clay is to reduce the density. It is generally agreed that the initial stage of the soil-lime reaction, which is referred to as immediate amelioration, begins upon the addition of lime. It is believed that the immediate amelioration, which takes place before compaction, will result in the cementation of particles into a loose structure (*9*). Cementation that has developed at the points of contact between the edges and the faces of adjacent clay particles in the house-of-cards type of structure will cause the soil to offer a greater resistance to compaction. Therefore, for a given compactive effort, a lower density would be expected as the time available for this reaction increases. However, the extent to which aging affects density is related to aging water content. At low aging water content (24 to 26 percent) the difference in density between samples aged for 1 and 24 hr is small irrespective of lime percentage. The difference in density increases with increasing aging water content. This may be attributed to the fact that the lime hydration

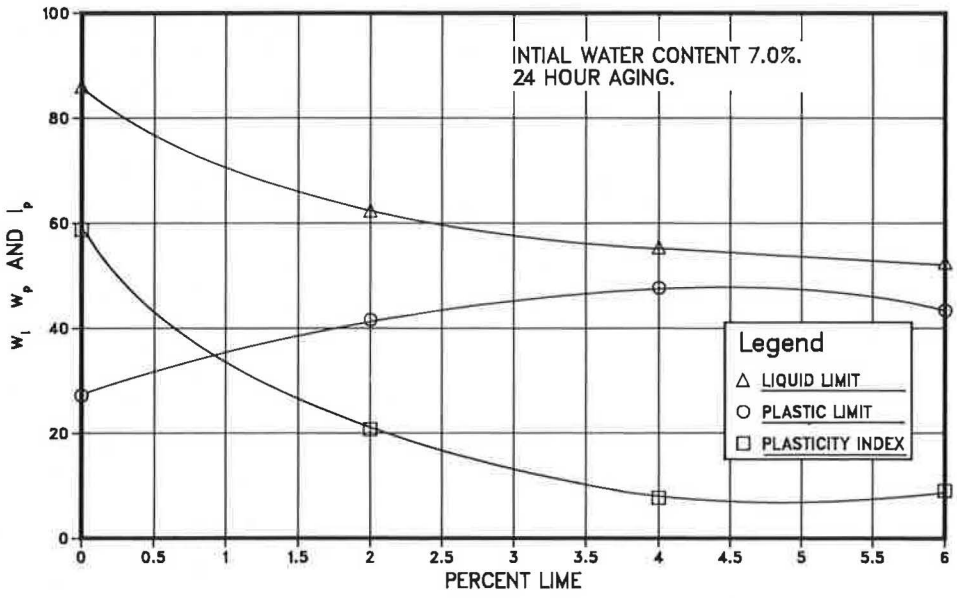

FIGURE 3 Percentage of lime added versus liquid limit, plastic limit, and plasticity index for 24-hr aging with 7 percent initial water content.

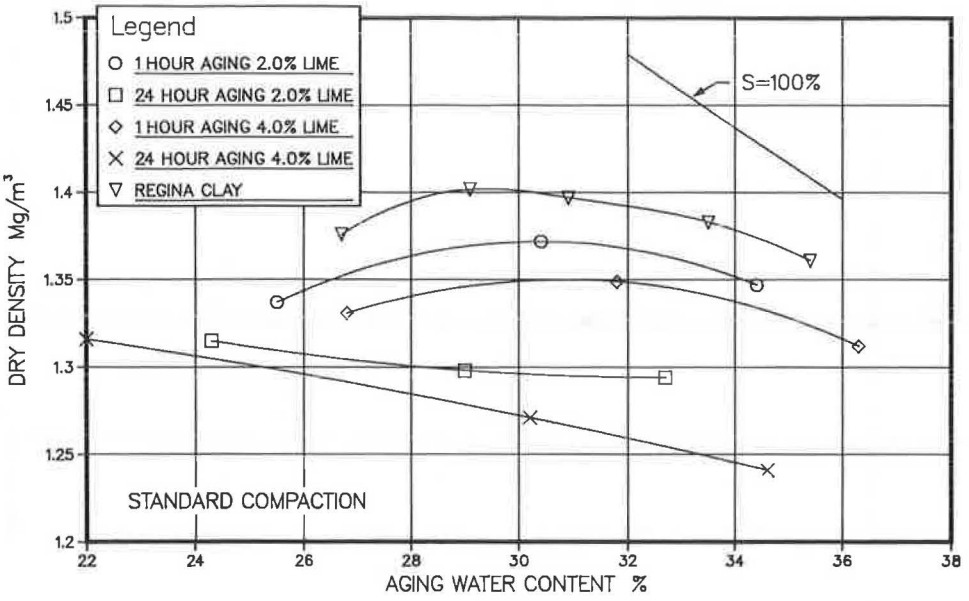

FIGURE 4 Aging water content versus dry density for 2 and 4 percent lime-modified samples aged 1 and 24 hr, with standard compaction and 15 percent initial water content for 2 percent samples and 7 percent initial water content for 4 percent samples.

process cannot occur freely without sufficient water. On the other hand, the effect of aging becomes more pronounced if adequate water is added to the lime to satisfy its initial chemical affinity for water.

2. Aging not only reduces density but also affects the shape of the compaction curve, depending on the duration of the aging period. The results indicate that the effect of short-term aging (e.g., 1 hr) is to produce a lower dry density and higher optimum water content for a given compactive effort. The shape of the compactive curves for soil treated with 2 and 4 percent lime and aged for 1 hr is comparable with that of the untreated soil. As the aging

TABLE 2 SUMMARY OF TEST RESULTS UNDER CONSTANT (STANDARD) COMPACTIVE EFFORT

		COMPRESSIVE STRENGTH (kPa)			PERCENT SWELL %		
LIME %	INITIAL w/c,%	AGING w/c,%	1 HOUR AGING	24 HOUR AGING	AGING w/c,%	1 HOUR AGING	24 HOUR AGING
2	7	23.55	285.3	260.8	23.95	3.62	2.00
2	7	27.85	344.1	264.2	30.65	1.11	1.45
2	7	32.40	374.7	249.7	33.80	0.24	0.84
2	15	24.75	287.3	234.0	25.50	3.70	3.30
2	15	29.70	393.7	353.7	29.80	1.95	2.40
2	15	33.30	269.0	280.5	34.65	0.67	1.11
4	7	23.80	295.3	224.2	24.50	1.64	0.34
4	7	28.15	366.9	228.0	31.25	1.02	0.78
4	7	32.60	333.8	307.9	36.15	0.84	0.40
4	15	25.30	262.0	-	26.80	2.39	-
4	15	30.70	336.0	-	30.30	0.92	-
4	15	34.60	202.6	-	35.20	0.83	-

(-) tests not performed

period increases from 1 to 24 hr, the compaction curves appear to become flatter with no definable optimum water content.

3. The influence of aging on density is more pronounced than that of lime percentages, particularly at higher aging water contents. For example, soil samples treated with 2 percent lime and prepared at 30 percent (aging) water content indicated a reduction in density by as much as 75 kg/m^3 when the aging periods were increased from 1 to 24 hr. The density decreased by only 30 kg/m^3 when lime treatment was increased from 2 to 4 percent for soil specimens prepared at the same water content with a 1-hr aging period. It is known that the addition of lime will reduce the maximum density and increase the optimum water content relative to values for the untreated soil. These effects are similar to the effects of aging under short duration.

Unconfined Compressive Strength

The unconfined compressive strength test results on the lime-treated soil specimens under 1- and 24-hr aging periods are compared and presented in Table 2. The results show that the unconfined compressive strength decreases as the aging period increases. However, it should be noted that one value is contrary to this trend.

A typical plot of aging water content versus unconfined compressive strength of lime-treated specimens aged for 1 and 24 hr is shown in Figure 5. The unconfined compressive strength of the untreated Regina clay is also included in Figure 5 for comparison purposes. As indicated in Figure 4, an increase in aging period leads to lower unconfined compressive strengths for a given compactive effort. Herrin and Mitchell (*10*) indicated that the immediate amelioration will take place rapidly, particularly when the soil-lime mixture is in a loose state. Thus, it would be expected that a significant portion of this reaction would take place if there were a prolonged delay between mixing and compaction. As previously discussed, the reaction before compaction results in the cementation of particles, which, in turn, increases the strength. However, this appreciable increase in strength is likely to be overshadowed by the loss in strength caused by the decrease in density as a result of the delay between mixing and compaction. Subsequent compaction can destroy the bonds between the particles. Therefore, the net effect is a reduction in strength.

The effect of aging on strength is also related to aging water content. Figure 5 shows that the effect of aging on strength becomes more pronounced as the aging water content increases. This trend appears to lend support to the fact that sufficient water must be added to the soil-lime mixture in order to hydrate the lime before the soil-lime reaction can proceed.

Swell Characteristics

The effects of aging water content on the percent swell of the specimens treated with 2 and 4 percent lime and aged for 1 and 24 hr are shown in Figures 6 and 7 along with the swell characteristics of the untreated Regina clay. The results of the swell tests conducted using constant compactive effort are also summarized in Table 2.

The beneficial effect of lime treatment on the reduction in swell is shown in Figures 6 and 7. The reduced swell characteristics may be attributed to the decreased affinity for water of the flocculated calcium-saturated clay, the formation of which is caused by the increased electrolyte content of the pore water and the cation exchange of the clay to the calcium form as a consequence of the addition

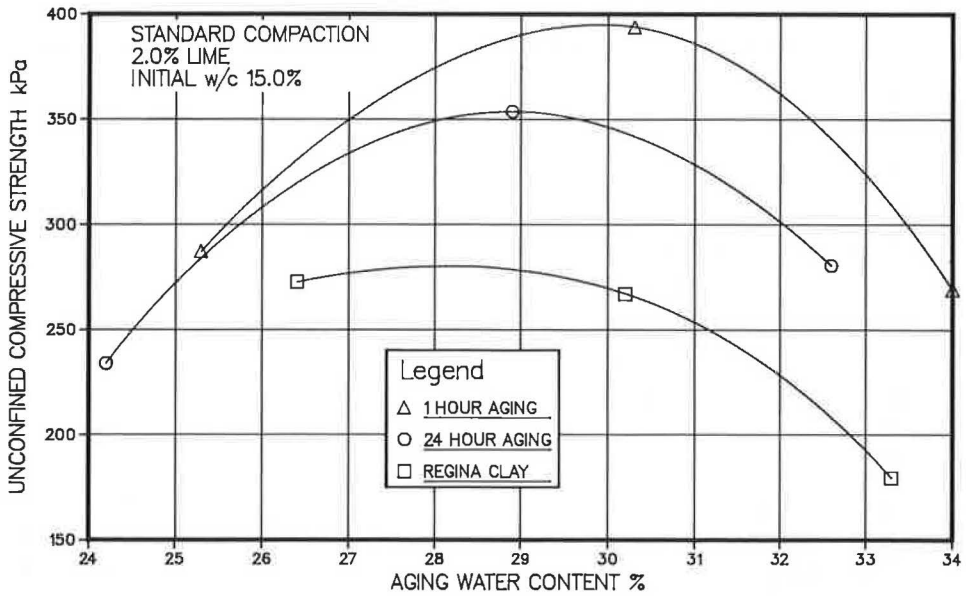

FIGURE 5 Aging water content versus unconfined compressive strength for 2 percent lime samples aged for 1 and 24 hr, with standard compaction and 15 percent initial water content.

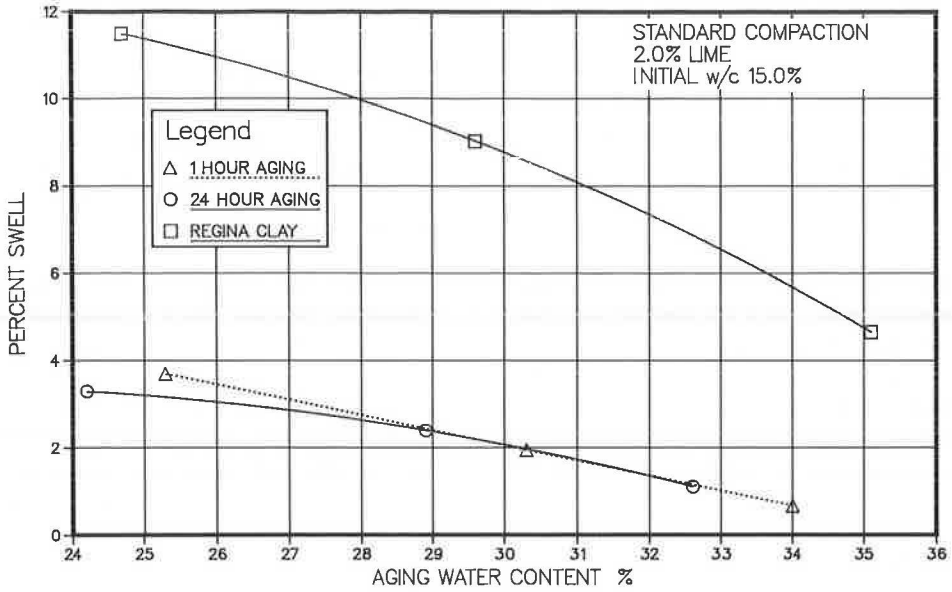

FIGURE 6 Aging water content versus percent swell for 2 percent lime samples aged for 1 and 24 hr, with standard compaction and 15 percent initial water content.

of lime. Figures 6 and 7 show that the reduction in swell percentage is more significant with the addition of smaller percentages of lime.

Figures 6 and 7 indicate that the aging water content at which compaction is carried out has an important influence on swell percentage. At the same compactive effort, the soil fabric becomes increasingly oriented with increasing water content. Soil samples compacted dry of optimum have flocculated structures, whereas samples compacted wet of optimum have a more oriented or dispersed structure. The compacted clay soils with a flocculent structure tend to swell more than those with a dispersed structure. Figures 6 and 7 show that the swell percentage decreases with increasing aging water content regardless of the aging periods. Aging appears to have no significant effect on swell for the soil studied.

Effect of Aging on Lime-Treated Specimens Using Increased Compactive Effort

The influence of aging examined thus far is based on constant compactive effort. In order to compare the effect of

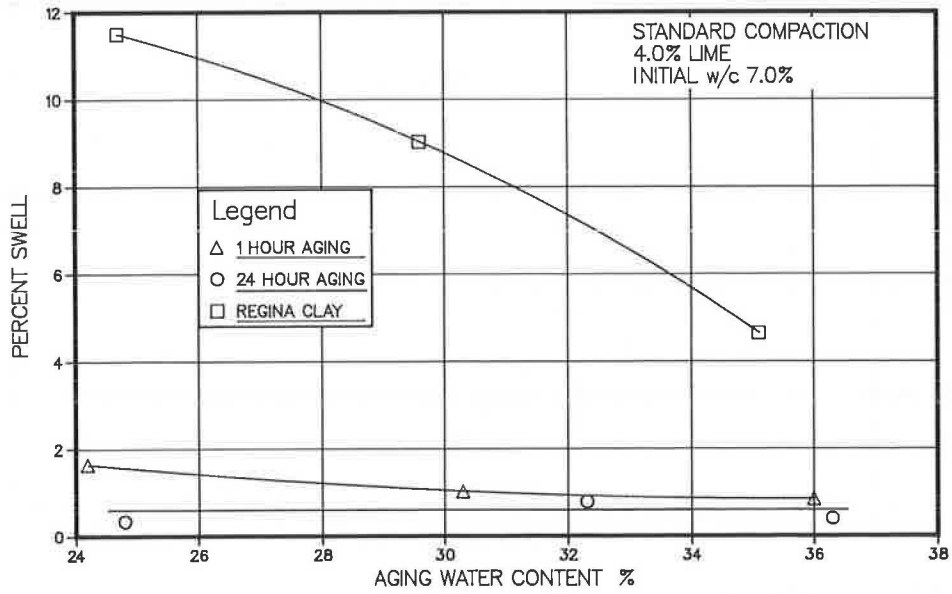

FIGURE 7 Aging water content versus percent swell for 4 percent lime samples aged for 1 and 24 hr, with standard compaction and 15 percent initial water content.

aging on lime-treated specimens at equal densities, specimens were prepared at densities equal to those of the untreated specimens.

Unconfined Compressive Strength

Figure 8 indicates that if specimens were treated with 2 percent lime and compacted to equal densities, the samples aged for 24 hr showed a greater unconfined compressive strength than those aged for 1 hr. However, an increase in compactive effort was required to achieve the required density. The increase in strength may be attributed to the flocculated soil structure.

The results shown in Figure 8 can be compared with those in Figure 5, which shows the influence of aging on strength of lime-treated specimens prepared at constant compactive effort. The decrease in strength with increasing aging period is mainly due to the decrease in density. A similar conclusion was reached in the study conducted by Mitchell and Hooper (*4*).

An increase in compactive effort does not always result in a greater strength in the case of samples treated with higher lime contents and aged for longer periods. There is probably a greater degree of flocculation under these conditions, which offers greater resistance to compaction. However, a greater compactive effort must be provided to attain the desired density. Overcompaction may cause the specimens to become weak and friable, resulting in sampling problems. Some test results were considered to be nonrepresentative because of the poor condition of the specimens after sampling (Table 3).

Swell Characteristics

Figure 9 shows that aging has little or no effect on swell characteristics of lime-treated samples prepared using an increased compactive effort. As previously noted, similar behavior was found at a constant compactive effort (Figure 7). The insignificant effect of aging on swell, as indicated by the two different compactive efforts, would suggest that the main factor responsible for the decreased swell characteristics is due to flocculation and agglomeration of the soil structure and not cementation before compaction. If cementation were a primary factor, it would be expected that the longer aging period would result in greater swell for samples prepared using both constant and increased compactive efforts. As explained by Herzog and Mitchell (*11*), the flocculation and agglomeration are caused by the increased electrolyte content of the pore water and cation exchange of clay to a calcium form following the addition of lime to the soil. As a consequence of this series of reactions, the original clay is changed to a flocculated calcium-saturated clay that has the tendency to reduce swell because of its decreased affinity for water.

CONCLUSIONS

1. An increasing aging period does not significantly affect the plasticity index results. More tests would have to be performed in order to confirm that longer aging periods decrease the plasticity index slightly, especially at higher lime contents.
2. Aging produces a lower density and a reduced strength for specimens prepared using a constant compaction effort.

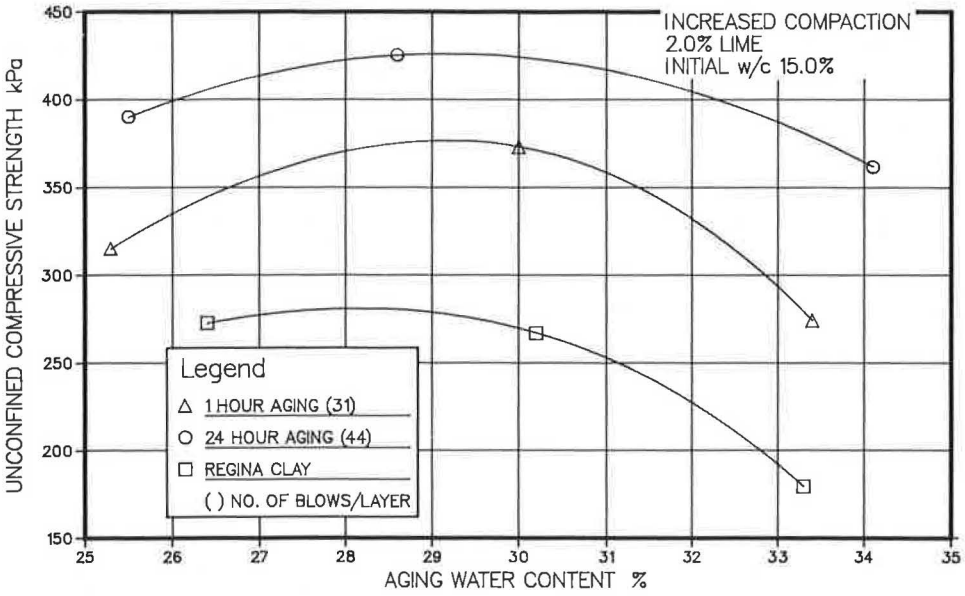

FIGURE 8 Aging water content versus unconfined compressive strength for 2 percent lime samples aged for 1 and 14 hr, with standard compaction and 15 percent initial water content.

TABLE 3 SUMMARY OF TEST RESULTS UNDER INCREASED COMPACTIVE EFFORT

		COMPRESSIVE STRENGTH (kPa)			PERCENT SWELL %		
LIME %	INITIAL w/c,%	AGING w/c,%	1 HOUR AGING	24 HOUR AGING	AGING w/c,%	1 HOUR AGING	24 HOUR AGING
2	7	24.90	369.7	492.5	25.75	2.50	4.60
2	7	29.70	449.4	545.3	30.40	0.98	1.70
2	7	34.15	304.4	247.5	34.05	0.54	0.65
2	15	25.40	315.2	390.1	-	-	-
2	15	29.30	373.0	425.4	29.8	1.60	1.40
2	15	33.75	274.3	361.6	-	-	-
4	7	24.05	365.1	346.6	27.40	1.40	1.00
4	7	29.80	524.5	511.6	31.25	0.28	0.63
4	7	35.60	319.2	*	35.80	0.85	0.11
4	15	25.50	384.6	-	26.10	2.40	-
4	15	30.00	430.0	-	30.50	0.79	-
4	15	34.80	207.1	-	34.60	0.59	-

(-) tests not performed
* specimen too weak to be sampled

The extent to which aging affects the density and strength depends on the aging water content at which the specimens were compacted. The reduction is small at low aging water contents, but it becomes more pronounced at higher aging contents.

3. The reduction in strength as a result of aging can be compensated for or even improved upon by using an increased compactive effort for specimens treated with low percentages of lime. However, an increased compactive effort does not always produce higher strengths when the specimens are treated with higher percentages of lime and aged for longer periods. In other words, increased compaction may cause a reduction in strength.

4. Aging appears to have no significant effect on the

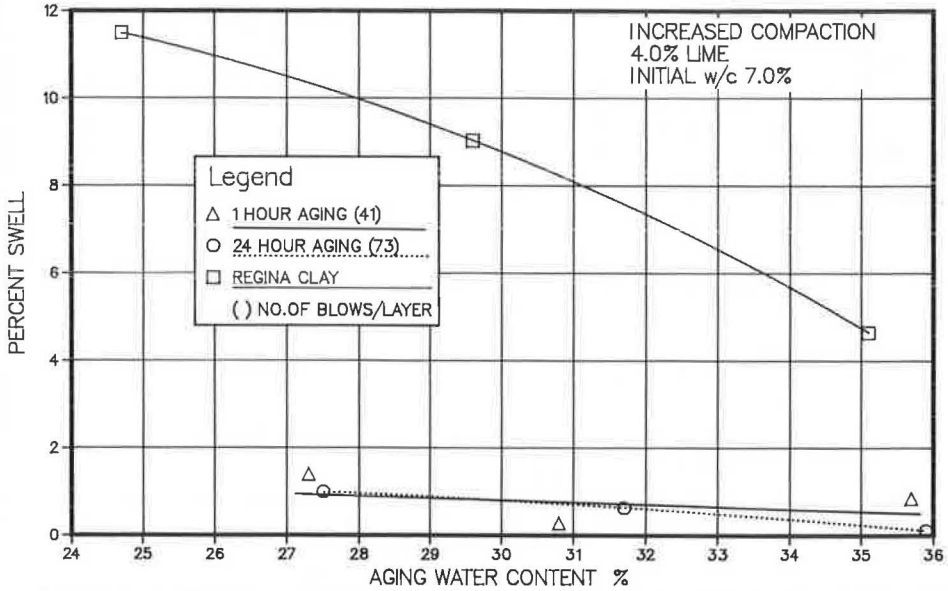

FIGURE 9 Aging water content versus percent swell for 4 percent lime samples, with increased compactive effort and 7 percent initial water content.

swell of treated specimens prepared with constant and increased compaction.

5. The influence of aging on lime-treated Regina clay has been examined in terms of plasticity, the relationship of water content to density, unconfined compressive strength, and swell. These are referred to as short-term effects. This investigation did not take into consideration such variables as curing, wetting and drying, and freezing and thawing, which are known to have a significant influence on the behavior of lime-treated soils in a long-term basis. Therefore, further studies are now being conducted in order to better define the effect of aging in a long-term basis.

ACKNOWLEDGMENTS

The material for this paper was obtained as part of the research program on lime-modified clay sponsored by the Saskatchewan Highways and Transportation Department in cooperation with the Department of Civil Engineering, University of Saskatchewan.

Additional financial assistance was provided by Steel Brothers Canada Ltd., and the authors wish to thank them for their interest in the research program.

REFERENCES

1. D. K. H. Wong. *A Report on the Literature Search and Review Phase of the Lime-Modified Clay Research Program.* Lime-Modified Clay Research Program, Department of Civil Engineering, University of Saskatchewan, Aug. 1986.
2. C. McDowell. Stabilization of Soils with Lime, Lime-Flyash, and other Lime Reactive Materials. *Bulletin 231*, HRB, National Research Council, Washington, D.C., 1959, pp. 60–66.
3. M. J. Dumbleton. *A Comparative Study of the Properties of Clay Soils Stabilized with Hydrated Lime and Portland Cement.* Research Note RN/3434. Road Research Laboratory, Department of Scientific and Industrial Research, Pretoria, South Africa, March 1959.
4. W. H. Taylor and A. Arman. Lime Stabilization Utilizing Pre-Conditioned Soils. *Bulletin 262*, HRB, National Research Council, Washington, D.C., 1960, pp. 1–19.
5. J. K. Mitchell and D. R. Hooper. Influence of Time between Mixing and Compaction on Properties of a Lime Stabilized Expansive Clay. *Bulletin 304*, HRB, National Research Council, Washington, D.C., 1961, pp. 14–31.
6. P. E. Fossberg. Some Fundamental Engineering Properties of a Lime-Stabilized Clay. In *Proceedings of the Sixth International Conference on Soil Mechanics and Foundation Engineering*, Canada, Vol. 1, 1965, pp. 221–225.
7. T. W. Klym. Lime Stabilized Soils Under Freezing and Thawing. Ph.D. thesis. Queen's University, Kingston, Ontario, Canada, 1965, 200 pp.
8. C. O'Flaherty and D. Andrews. Frost Effects in Lime and Cement-Treated Soils. In *Highway Research Record 235*, HRB, National Research Council, Washington, D.C., 1968, pp. 49–60.
9. S. Diamond and E. B. Kinter. Mechanisms of Soil-Lime Stabilization: An Interpretive Review. In *Highway Research Record 92*, HRB, National Research Council, Washington, D.C., 1965, pp. 83–102.
10. M. Herrin and H. Mitchell. Lime-Soil Mixtures. *Bulletin 304*, HRB, National Research Council, Washington, D.C., 1961, pp. 99–138.
11. A. Herzog and J. K. Mitchell. Reactions Accompanying Stabilization of Clay with Cement. In *Highway Research Record 36*, HRB, National Research Council, Washington, D.C., 1963, pp. 146–171.

Publication of this paper sponsored by Committee on Lime and Lime-Fly Ash Stabilization.

Strength Developed from Carbonate Cementation in Silica-Carbonate Base Course Materials

ROBIN E. GRAVES, JAMES L. EADES, AND LARRY L. SMITH

Strength increases resulting from carbonate cementation in compacted sands and cemented coquina highway base course materials of variable quartz-calcite composition were investigated through the use of limerock-bearing-ratio (LBR) testing. Quartz and calcite sands were mixed in various proportions, compacted into LBR molds, soaked for time periods from 2 days up to 60 days, and tested to determine strength increase with time. For comparison, cemented coquina highway base course materials of variable quartz-calcite composition were also compacted, soaked, and tested. In addition, duplicate sets of specimens were tested that had 1 percent $Ca(OH)_2$ (hydrated lime) mixed with the dry materials before compacting and soaking. This was done to provide a source of Ca^{2+} ions for formation of additional calcium carbonate cement. Results of the LBR testing program showed that more strength developed as the calcium carbonate composition of both the quartz-calcite sand mixes and the cemented coquina samples increased. Addition of $Ca(OH)_2$ to the samples enhanced carbonate cementation effects, with large strength increases occurring in high-carbonate materials. Scanning electron microscopic examinations of the tested LBR materials, base course materials cored from in-service highways, and naturally occurring calcite-cemented quartz sandstones and limestones revealed different bonding characteristics between calcite cement-calcite particle and calcite cement-quartz particle systems, which would explain the strength development patterns observed in LBR testing.

Highway base courses in Florida constructed with crushed-limestone materials have been observed to increase in strength with time after construction. The Florida Department of Transportation (FDOT) has conducted studies, both in the laboratory (*1, 2*) and on satellite road projects, investigating the strength increase of high-carbonate-composition (60 to 100 percent) base course materials. The research indicated that the strength increases were due to a slight drying of the base course (*2*) and to dissolution and reprecipitation of fine carbonate particles, which serve as a cementing agent within the base course (*1*).

High-carbonate-composition base course materials have traditionally been preferred for construction of state highways in Florida. However, as the sources of these materials are depleted, new sources must be found to accommodate the transportation needs of the state's rapidly expanding population. Materials obtained from the newer quarries often have a different mineralogical composition because of the great variability of geologic conditions affecting their deposition.

This has been the case with cemented coquina base course materials in Florida (*3*). Currently mined cemented coquina contains abundant quartz sand, often resulting in carbonate compositions below the 50 percent required by FDOT. The quartz occurs in two forms. Some is incorporated into cemented limestone rock, but most exists as unconsolidated quartz sand. Field observations in operating quarries indicated that the quartz sand occurs in layers of variable thickness interbedded within the cemented limestone rock material. The rock and quartz sand become mixed during mining and processing operations, resulting in a final product that often has a high silica composition.

Several instances of deterioration have occurred in county-built roads when low-carbonate materials were used for the base course. Therefore, research is being conducted to determine the effects of high silica composition on the engineering behavior of highway base courses in Florida. This project has focused on the role of quartz particles in the carbonate cementation process and the resulting strength development.

PARTICLE CEMENTATION

Calcium carbonate is a very common cementing agent in natural geological materials because of its high susceptibility to dissolution and precipitation under the range of physical and chemical conditions encountered on and within the earth (*4*). Because highways are constructed on the earth's surface, they are subjected to fluctuating environmental conditions such as temperature and atmospheric pressure. Therefore, behavior of base courses composed of calcium carbonate materials may be influenced by cementation processes operating within them.

The strength behavior of sands and gravels is considered to be purely frictional in nature, and therefore they are termed "cohesionless" materials. Cementation of the particles provides a cohesive component to the system (*5, 6*),

R. E. Graves and J. L. Eades, Department of Geology, 1112 Turlington Hall, University of Florida, Gainesville, Fla. 32611. L. L. Smith, Bureau of Materials and Research, Florida Department of Transportation, 2006 N.E. Waldo Road, Gainesville, Fla. 32601.

thereby increasing the overall strength of the soil mass. Therefore, natural cementation of particles, such as carbonate cementation in limestones, within a highway base course could cause an increase in strength of the material with time as cementation progresses.

STRENGTH-TESTING METHODS

The objective of this research has been to evaluate strength development with time due to carbonate cementation in highway base course materials consisting primarily of quartz and calcite particles. The testing program involved the use of limerock-bearing-ratio (LBR) tests (*7*) on materials of varying quartz-calcite composition in order to determine strength changes as a function of composition and time.

The standard LBR test method involves compacting the material into 6-in. molds at modified AASHTO compactive efforts and soaking the compacted material in water for 48 hr. The material is then removed from the water and penetrated by a loading device with an LBR value calculated as follows:

$$\text{LBR} = \frac{\text{unit load (psi) at 0.1-in. penetration}}{\text{800 (psi) (value for standard limerock)}} \times 100 \quad (1)$$

The test is performed at different water contents and the maximum LBR value is taken. The LBR test is similar to the more commonly used California-bearing-ratio (CBR) test. An approximate correlation has been established between the two methods, with a LBR value of 100 corresponding to a CBR value of 80.

Sand Mixes

Quartz and calcite sands were mixed in various proportions, resulting in percent-quartz-to-percent-calcite compositional ratios of 0/100, 25/75, 40/60, 50/50, 60/40, 75/25, and 100/0. The various mixes were compacted into LBR molds at maximum modified proctor densities and continuously soaked in water at room temperature (70° ± 2°) for time intervals of 2, 7, 14, 30, and 60 days before testing.

In Figure 1, LBR values for 7-, 14-, 30-, and 60-day soaking periods for sand mixes are shown relative to the standard 2-day-soak LBR values for the various mix compositions. LBR values for the extended soaking periods are plotted as percent increase over the 2-day reference LBR for each compositional mix. Figure 1 shows the differences in strength development as composition varies. Low-carbonate sands (0 and 25 percent) show no strength increase up to 60 days' soaking, whereas higher-carbonate sands (40 to 100 percent) showed strength increases, with more strength developing as carbonate content increases. Maximum increase was obtained after 14 days' soaking, with no additional strength developing for 30- and 60-day soaking periods. This may be related to the small amount

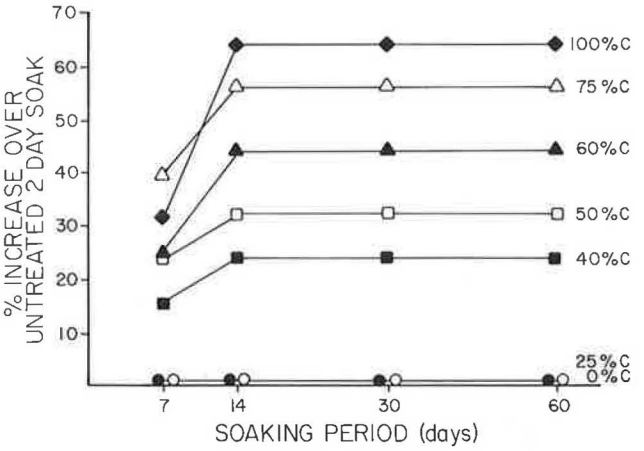

FIGURE 1 Strength development in quartz-calcite sand mixes.

(<2 percent) of fine-grained material (< No. 200 sieve) in the carbonate sand. Dissolution is likely to be more efficient for small carbonate particles than for coarser particles because of the higher surface area available in fine-grained materials. It is possible that the fine carbonate particles have been "used up" in the cementation process after 14 days and that the coarser particles are not providing cementing material as efficiently. However, it is suspected that over longer periods of time, cementing material would be provided by coarser carbonate particles but at a slower rate because there is less available surface area for dissolution and a smaller amount of water held by large particle contacts.

Cemented Coquina

Cemented coquina base course materials were also compacted, soaked, and tested to be compared with sand-mix data. Compositional variation was more limited in these materials, with quartz-to-calcite ratios of 45/55, 55/45, and 65/35 used for testing. Soaking periods were 2, 7, 14, and 30 days; the 60-day soaking periods were omitted because of a limited amount of sample material. LBR data for soaked and tested cemented coquina materials also indicate differential strength development as composition varies.

Figure 2 shows percent increase in strength of each composition for soaking periods of 7, 14, and 30 days compared with the standard 2-day-soak LBR value. More strength developed in the cemented coquina materials as carbonate content increased, as was the case for the quartz-calcite sand mixes. However, differences in the pattern of strength development can be seen when the two materials are compared. Cemented coquina materials continued to increase in strength up to 30 days' soaking, whereas quartz-calcite sand mix strength did not increase after soaking 14 days. This is thought to be due to slightly more carbonate fines (< No. 200 sieve) occurring in the cemented coquina materials than in the sand mixes.

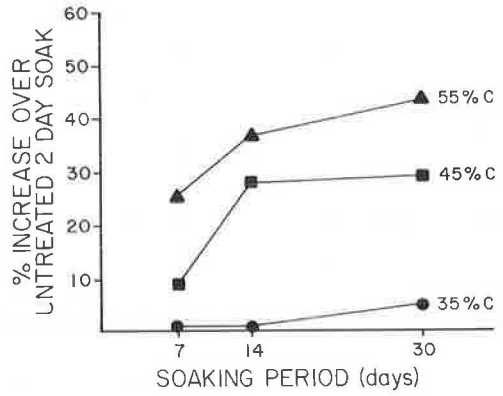

FIGURE 2 Strength development in cemented coquina materials.

$Ca(OH)_2$ Treatment

Another portion of the LBR testing program involved the addition of 1 percent $Ca(OH)_2$ (hydrated lime) to the dry materials before compaction for each sample composition and soaking period. This was done in an attempt to enhance carbonate cementation and therefore strength development. Carbonation of additional Ca^{2+} ions furnished by the $Ca(OH)_2$ should provide an additional source of calcite cement, thereby enhancing cementation effects. In Figure 3, LBR values after 2-, 7-, 14-, 30-, and 60-day soaking periods for sand mixes treated with 1 percent $Ca(OH)_2$ before compaction are compared relative to the standard 2-day soak for untreated sand mixes. The effects are shown of an additional source of carbonate cement on strength increase with time and compositional variation of the mixes. It may be seen that $Ca(OH)_2$ treatment significantly enhanced strength development and variational patterns observed in LBR data for the untreated sand mixes. Very large increases (>450 percent) in strength occurred for high-carbonate sands, with strength developed continuously up to 60 days. Less strength was developed in the sand mixes as carbonate contents decreased. Quartz sands developed no additional strength after 30 days' soaking and only a slight increase (30 percent) after 60 days' soaking.

Treatment of cemented coquina materials with $Ca(OH)_2$ also resulted in enhanced cementation effects as shown in Figure 4. Strength increases for each composition after soaking periods of 2, 7, 14, and 30 days relative to the standard untreated 2-day-soak LBR values have been plotted. More strength was developed when cemented coquina materials were treated with $Ca(OH)_2$; the trend of more strength developing with increasing carbonate composition persisted in these experiments.

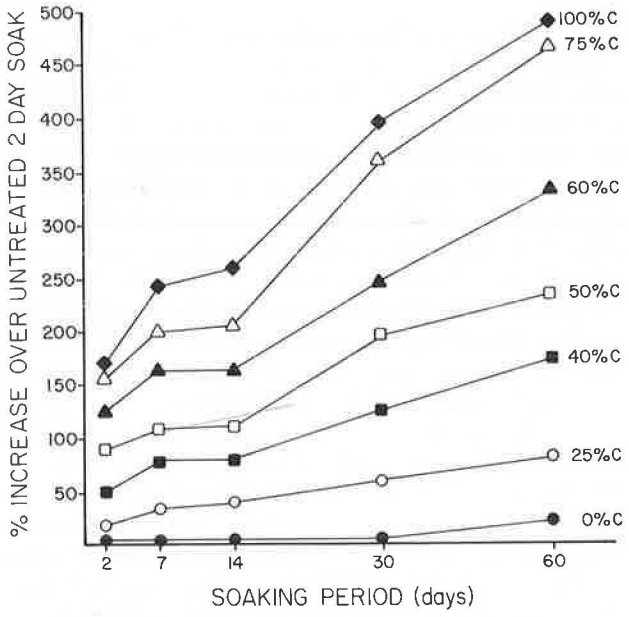

FIGURE 3 Strength development in quartz-calcite sand mixes treated with 1 percent $Ca(OH)_2$.

SEM EXAMINATIONS

Scanning electron microscope (SEM) examinations were conducted on tested LBR materials to aid in explanation of strength testing data by observing cementation characteristics. In addition, cemented coquina base course materials cored from in-service highways and some naturally occurring calcite-cemented quartz sandstones and limestones were also examined with the SEM to further investigate cementation characteristics.

LBR Materials

Samples of the LBR materials were removed from the molds after soaking and testing, dried, and prepared for SEM examination. The micrographs presented are images of broken surfaces of the cemented materials. Figures 5 and 6 show the different characteristics between carbonate cementation of quartz and calcite particles in the sand mixes. In Figure 5, the carbonate cement (C_c) has not bonded to the quartz particles (Q), as shown by the clean

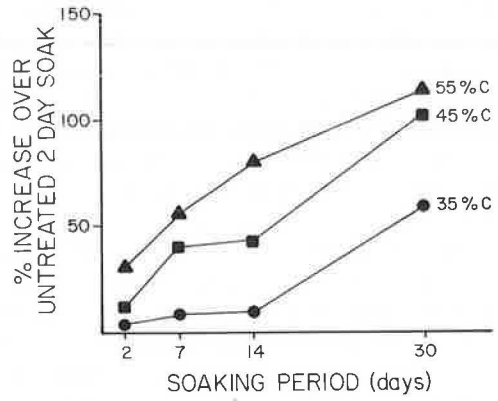

FIGURE 4 Strength development in cemented coquina materials treated with 1 percent $Ca(OH)_2$.

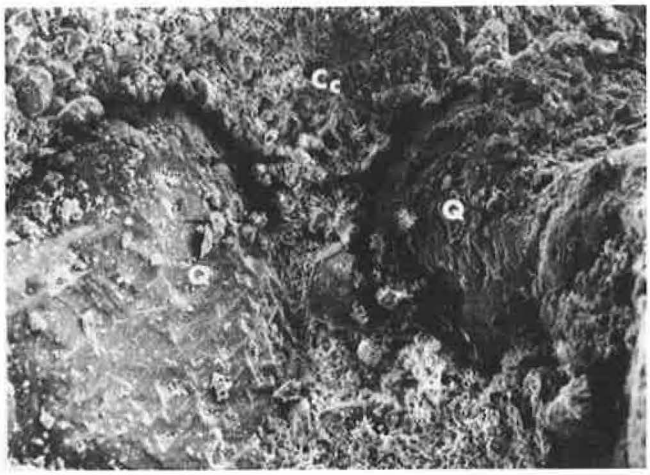

FIGURE 5 Sand mix, 75 percent carbonates, 1 percent $Ca(OH)_2$, 14-day soak (×308).

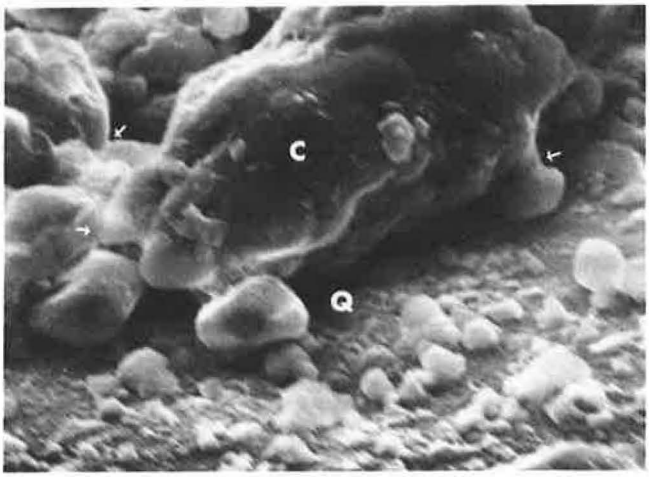

FIGURE 7 Sand mix, 25 percent carbonates, 7-day soak (×1,800).

quartz particle surfaces and the large void separating the particles and the cement. In contrast, Figure 6 shows a calcite particle (C_p) that seems to be well bonded to the carbonate cement (C_c). Carbonate cementing material has adhered to the particle surface during fracture, and the cement is in good contact around the calcite particle edges, unlike the cement in Figure 5, which is separated from the quartz particles by a large void.

Higher-magnification micrographs of cement-particle contact for quartz and calcite are shown in Figures 7 and 8. The carbonate cement (C) and quartz particle (Q) are separated by a void in Figure 7. Note the arrows indicating where small carbonate particles have been cemented together. Figure 8 shows carbonate cement (C_c) bonded to a large carbonate particle (C_p).

Similar cementation characteristics were observed in examination of cemented coquina LBR materials after soaking and testing. In Figure 9, calcite particles (C) are

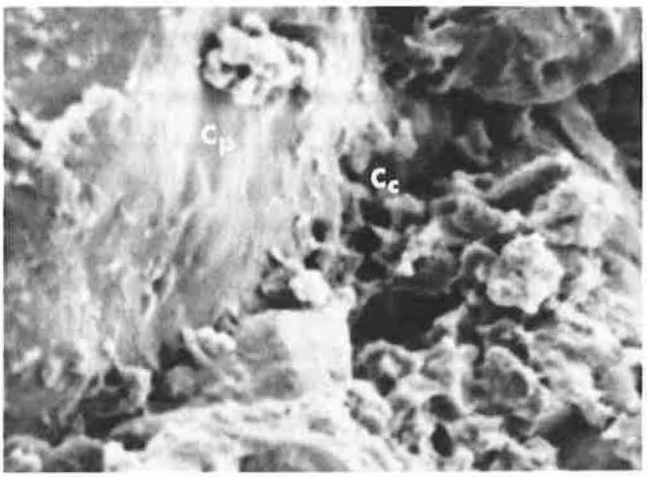

FIGURE 8 Sand mix, 100 percent carbonates, 1 percent $Ca(OH)_2$, 30-day soak (×2,400).

FIGURE 6 Sand mix, 100 percent carbonates, 1 percent $Ca(OH)_2$, 14-day soak (×143).

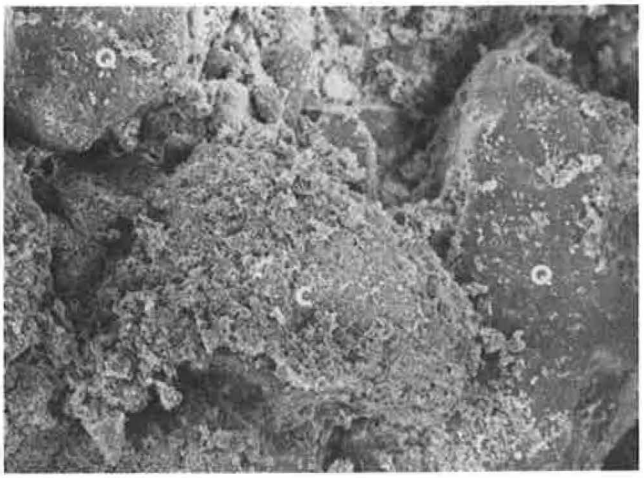

FIGURE 9 Cemented coquina, 45 percent carbonates, 1 percent $Ca(OH)_2$, 30-day soak (×113).

FIGURE 10 Cored cemented coquina highway base course, 59 percent carbonates (×218).

well cemented, whereas quartz particles (Q) exhibit clean particle surfaces, free of carbonate cement.

Highway Cores

Cemented coquina base course materials of variable carbonate composition (35 to 60 percent) were cored from highways in service from 3 to 5 years. These materials were examined with the SEM to provide field evidence of cementation for comparison with observations from laboratory experiments.

Cementation characteristics observed in these materials were very similar to those from soaked LBR materials. Figure 10 shows carbonate particles that have been well cemented in a 50 percent carbonate highway core sample. In Figure 11, carbonate particles (C) have been well cemented, whereas quartz particles (Q) exhibit clean particle surfaces. Small amounts of cement can be seen filling some pore spaces around the quartz particles, but close examination reveals voids at cement-particle contact.

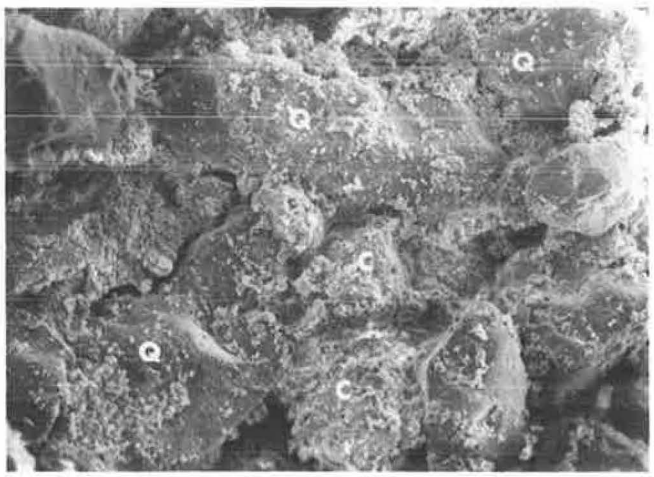

FIGURE 11 Cored cemented coquina highway base course, 37 percent carbonates (×75).

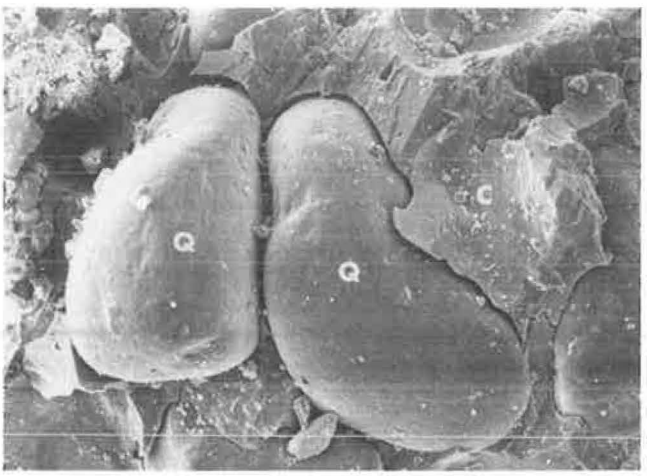

FIGURE 12 Calcite-cemented quartz sandstone, Badlands, South Dakota (×113).

Sandstones and Limestones

Naturally occurring calcite-cemented quartz sandstones from the Badlands of South Dakota and limestones from the Anastasia formation in Florida were examined to observe cement-particle contact of some materials in more advanced stages of cementation. The South Dakota sandstones are unique in that the calcite cement has grown as large scalenohedral crystals, incorporating quartz particles into the crystal structure as it developed. Figure 12 is a micrograph of a fractured surface of the material showing the quartz particles (Q) in a calcite cement matrix (C). The cement has pulled away, leaving clean quartz particle surfaces, and large voids exist at cement-particle contact.

In contrast to the lack of carbonate cement-quartz particle bonding observed in the sandstone, Figure 13 shows a carbonate particle (C_p) surrounded by carbonate cement (C_c) in the Florida limestone. Note that the fracture has occurred through the carbonate particle rather than around it, as was the case for the quartz particles in Figure 12. The cement appears to be bonded to the carbonate par-

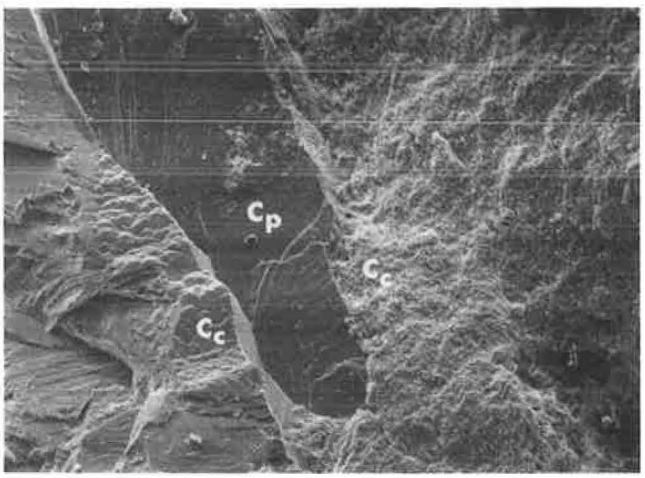

FIGURE 13 Cemented coquina, Anastasia formation, Florida (×94).

ticle, as shown by the lack of any voids at the cement-particle contact.

DISCUSSION

The high susceptibility of calcium carbonate to dissolution and reprecipitation under normal physical and chemical conditions operating at the earth's surface was demonstrated in the LBR testing program by the strength increases occurring in the laboratory samples after extended soaking in water. Because the samples remained at constant temperature (70° ± 2°) during soaking, the cementation process operating within the samples is thought to be controlled by variations in atmospheric pressure. This would cause changes in the CO_2 content of the pore water, which is the main controlling factor over carbonate dissolution and precipitation (*8, 9*). Field evidence of the ability of calcium carbonate to form cementing material under surface conditions was obtained from microscopic examinations of in-service cemented coquina highway base course materials.

Differential strength gains as a function of mineralogical composition in the tested LBR materials, along with microscopic observations of the different bonding characteristics of carbonate cement to calcite and quartz particles, support the idea of "compatible" and "incompatible" cements as put forth by Dapples (*10*) and others (*11–13*). Carbonate cementation of carbonate particles (compatible system) exhibited much better cement-particle bonding than carbonate cementation of quartz particles (incompatible system). This was revealed in the LBR testing program by the higher strength increases for high-carbonate samples as compared with high-silica samples.

Microscopic examinations supported LBR testing data by revealing the different cement bonding characteristics as a function of cement particle composition. Carbonate cement appears to nucleate directly onto calcite particle surfaces, creating a strong cement-particle bond compared with the carbonate cement-quartz particle system, in which the cement seems to precipitate from solution into pore spaces without nucleation and bonding to the quartz particle surfaces. Examination of the fractured surfaces of the various materials demonstrated this well; quartz particles exhibited clean surfaces, free of adhering cement, and voids existed between cement and particles at cement-particle contact. This was in contrast to carbonate cementation of calcite particles, which appear to be well bonded to the cement as shown by cement-covered particle surfaces and absence of voids at cement-particle contact.

Treatment of both quartz-calcite sand mixes and cemented coquina materials with 1 percent $Ca(OH)_2$ before compacting and soaking the samples proved to be very effective in providing an additional source of calcium carbonate cementing material, which resulted in larger and more rapid strength increases than in untreated materials. These experiments also enhanced the effects of cement-particle composition, with more strength developing as carbonate composition of the samples increased. As discussed previously, the $Ca(OH)_2$ provides an additional source of Ca^{2+} ions, which form carbonate cementing material through carbonation in the pore water during soaking. Calcium hydroxide has a solution pH of 12.4 at 25°C (*14*), which would increase the CO_3^{2-} species of dissolved carbonate in the pore water of the sand mixes (*15*). The Ca^{2+} ions and CO_3^{2-} combine and precipitate as calcium carbonate cement, thus increasing the strength of the soaked materials.

The large strength increases obtained from $Ca(OH)_2$ treatment of high-carbonate samples suggest that this procedure may be useful for strength improvement of high-carbonate foundation materials and as a testing method for determination of self-cementation potential of foundation materials. A suggested method of test would be as follows:

1. Mix 1 percent $Ca(OH)_2$ with dry materials before compaction into LBR (or CBR) molds at optimum water content.
2. Soak the compacted sample in water for 2 to 7 days.
3. Test the sample and compare with the standard 2-day-soak LBR (or CBR) value for the untreated materials to determine a percent increase in strength.

The strength developed in the treated sample should be indicative of the strength that would be developed in untreated materials soaked for 30 to 60 days. However, one problem with the test is that the soaking interval required for the treated samples may vary among different materials because of differences in particle size and distribution. This may affect the amount of strength developed because of differences in compacted density between various materials.

The results of the research project indicate that the strength of cemented coquina base course materials will be affected by their mineralogical composition. High-carbonate cemented coquina materials should cement much better than high-silica cemented coquina materials, providing a stronger and more stable base course from increased cohesion provided by strong bonding of precipitated carbonate cement to carbonate particles. High-silica cemented coquina materials would be less stable because of several factors. Lack of bonding between carbonate cement and quartz particles would result in decreased strength and stability derived from carbonate cement precipitating in the base course. In addition, less carbonate cementing material would be produced in the high-silica materials because the base course serves as its own source of cement; that is, fewer carbonate particles would be available for dissolution to provide precipitated carbonate cement. Silica cement would not be expected to precipitate in these materials because quartz particles are very stable under the earth's surface conditions (*15*), thus prohibiting a source of dissolved silica for precipitation.

Because large amounts of quartz sand are present in the high-silica materials, larger carbonate aggregate particles may effectively "float" in the sandy material. This would reduce material stability by decreasing the number of large aggregate contacts. In addition, the large areas of quartz grains are not likely to cement together because of the lack

of carbonate cement-quartz particle bonding and reduced supply of carbonate cement, as discussed earlier. High-carbonate cemented coquina materials have less quartz sand, resulting in more large aggregate contacts. Quartz grains "floating" in the matrix of carbonate materials would tend to be bound by the carbonate materials, thereby preventing their movement.

CONCLUSIONS

1. Laboratory soaking of compacted quartz-calcite sand mixes and cemented coquina base course materials continuously in plain water resulted in strength increases with time except for samples with high silica composition.
2. Higher strengths were developed in proportion to increasing carbonate composition for both quartz-calcite sand mixes and cemented coquina base course materials.
3. Treatment of quartz-calcite sand mixes and cemented coquina base course materials with the addition of 1 percent $Ca(OH)_2$ before compacting and soaking proved to be an effective method of enhancing cementation effects on strength development by furnishing a more soluble source of Ca^{2+} ions, which form carbonate cement through carbonation of Ca^{2+} ions.
4. Treatment of high-carbonate materials with 1 percent $Ca(OH)_2$ greatly increased their strength after extended soaking periods (30 to 60 days), whereas treatment of high-silica materials resulted in little or no strength increase. This suggests that $Ca(OH)_2$ treatment might be effectively used to improve strength of high-carbonate composition materials and as a testing method to determine the self-cementation potential of quartz-carbonate soils.
5. SEM examinations of soaked quartz-calcite sand mixes and cemented coquina base course materials, with and without $Ca(OH)_2$ treatment, showed that the observed strength gain variations were due to the different cement-particle bonding properties of carbonate cement-calcite particle and carbonate cement-quartz particle systems. Strength increases were more pronounced in high-carbonate materials because of good bonding of carbonate cement to calcite particles. In contrast, high-silica materials developed little or no strength because of a lack of bonding between carbonate cement and quartz particles.
6. Field evidence of cementation characteristics observed in laboratory samples was obtained from microscopic examinations of naturally occurring calcite-cemented sandstones and cemented coquina base course materials cored from in-service highways. These materials provided good field correlation of laboratory results, with similar cement-particle bonding characteristics being observed.

ACKNOWLEDGMENT

The studies presented here were part of a project sponsored through a research grant from the Florida Department of Transportation. The support and cooperation of the FDOT Bureau of Materials and Research are gratefully acknowledged.

REFERENCES

1. J. D. Gartland. *Florida Limerock Cementation Investigation.* Final Report. Department of Geology, University of Florida, Gainesville, 1979.
2. W. H. Zimpher. *Florida Limerock Investigation: Strength Gain Study of High and Low Carbonate Base Materials.* Final Report. Department of Civil Engineering, University of Florida, Gainesville, 1981.
3. *Standard Specifications for Road and Bridge Construction.* Florida Department of Transportation, Tallahassee, 1982.
4. P. K. Weyl. The Solution Kinetics of Calcite. *Journal of Geology,* Vol. 66, 1958, pp. 163–176.
5. A. E. Z. Wissa and C. C. Ladd. *Shear Strength Generation in Stabilized Soils.* Research Report R65-17, Soils Publication 173. Department of Civil Engineering, Massachusetts Institute of Technology, Cambridge, June 1965.
6. S. K. Saxena and R. M. Lastrico. Static Properties of Lightly Cemented Sand. *Journal of the Geotechnical Engineering Division,* ASCE, Vol. 104, No. GT12, Dec. 1978, pp. 1449–1464.
7. *Florida Method of Test for Limerock Bearing Ratio, Designation: FM 5–515.* Florida Department of Transportation, Tallahassee.
8. J. P. Miller. A Portion of the System Calcium Carbonate-Carbon Dioxide-Water with Geological Implications. *American Journal of Science,* Vol. 250, 1952, pp. 161–203.
9. D. C. Thorstenson, F. T. Mackenzie, and B. L. Ristvet. Experimental Vadose and Phreatic Cementation of Skeletal Carbonate Sand. *Journal of Sedimentary Petrology,* Vol. 42, 1972, pp. 162–167.
10. E. C. Dapples. Diagenesis of Sandstones. In *Diagenesis in Sediments and Sedimentary Rocks* (G. Larsen and G.V. Chilingar, eds.), Elsevier, Amsterdam, 1979.
11. G. W. Devore. Surface Chemistry as a Chemical Control on Mineral Association. *Journal of Geology,* Vol. 64, 1956, pp. 31–55.
12. R. G. C. Bathurst. *Carbonate Sediments and Their Diagenesis,* 2nd ed. Elsevier, Amsterdam, 1975.
13. R. E. Graves. *Strength Developed from Carbonate Cementation in Silica/Carbonate Systems.* Final Report. Department of Geology, University of Florida, 1987.
14. R. S. Boynton. *Chemistry and Technology of Lime and Limestone,* 2nd ed. Wiley, New York, 1980.
15. H. Blatt, G. Middleton, and R. Murray. *Origin of Sedimentary Rocks.* Prentice-Hall, Englewood Cliffs, N.J., 1980.

Publication of this paper sponsored by Committee on Lime and Lime-Fly Ash Stabilization.

Comparison of Quicklime and Hydrated Lime Slurries for Stabilization of Highly Active Clay Soils

THOMAS M. PETRY AND TA-WEN LEE

Research is presented that was used to compare the stabilizing effects of quicklime and hydrated lime slurries when applied to three samples of highly active clay soils from each of two geologic formations from North Central Texas. In addition, slurries made of the commercial lime products used in the research were studied and compared. The results obtained included soil properties measured before and after stabilization with these two slurries. These results were compared by using statistical methods to determine the significant differences. It was found that the quicklime slurries had a less detrimental effect on compactibility of the soil, provided somewhat lower swell, caused the soil to have lower plasticity and higher strength, and allowed a lower percentage of lime to be used. In addition, significant differences in time-related changes in properties are discussed in the analyses and conclusions.

Recognizing the severe damage that can be caused to transportation facilities by highly active or expansive clay soils, engineers have often chosen to stabilize these materials. The most common stabilizing agent applied to expansive clays to reduce or eliminate their problematic behavior is lime. This is especially true for the soils, site situations, and climate of the North Central Texas region.

Initially, lime was added to soils as hydrate powder, but as more projects have been built in urban areas, the prudent choice has become slurries of lime and water. Recently, the availability of slurries made in the field with quicklime has raised some questions as to how well these relatively new mixtures stabilize highly active clay soils compared with hydrated lime slurries. There are those who believe that the relatively high-temperature quicklime slurries should perform better, because chemical reactions would be accelerated, but others disagree. The research study reported here was undertaken to investigate the nature of the slurries mentioned earlier and to determine their stabilizing effects when applied to two highly active clay soils of North Central Texas.

SOILS AND LIME REACTIONS

For this study six soil samples were taken from two geologic formations: the Eagle Ford and Austin formations. These were sampled at relatively widespread locations within the Dallas–Fort Worth metroplex. These highly active clay soil samples, which were expected to be lime reactive, were taken from within the top 9 ft of the subgrade. The results for all six samples were combined during analyses, because these samples were thought to be representative of all the metroplex highly active clay soils.

The expected reactions between these clays and the lime slurries included cation exchange, ion crowding, dissolution of clay, flocculation and agglomeration, carbonation, and pozzolanic reactions (*1–5*). These mechanisms would normally cause soils to have reduced plasticity indexes and shrink-swell potentials, increased shear strength and reduced compressibility, increased workability and water repellancy, reduced compactibility, and increased abrasion and erosion resistance. Even though much is known about how these mechanisms cause the foregoing changes in behavior, little has been done to compare how well quicklime and hydrated lime slurries accomplish improvements in behavior.

SLURRY STUDY

In order to provide a basis for understanding how the two lime slurries differ, some of their properties were explored. Other than the apparent differences in the lime materials, there are reported differences in slurry properties. The pH of lime slurries is lowered at higher temperatures because the solubility of lime decreases (*6*). Free calcium cations can exist only when the pH is between 11.9 and 12.4. On the other hand, quicklime slurries are known to cause the evolution of higher heat during slurry formation, requiring that precautions be taken to protect workers. Along with these chemical property differences, there are physical differences.

Physical differences of the two slurries tested were expected but not completely known. Quicklime slurries made in the field have finer gradations than hydrated lime slurries because the slaking process is increased with increasing temperatures. As much as 98.6 percent of lime particles smaller than 5 μm has been measured in quicklime slurries (*7*). These finer particles are expected to have larger specific surface areas, which cause higher reactivi-

Department of Civil Engineering, University of Texas at Arlington, P.O. Box 19308, Arlington, Tex. 76019.

ties. In addition, during this study quicklime slurries were observed to have slower sedimentation rates than hydrated lime slurries. In general, the chemical and physical properties of quicklime slurries just described should make them better stabilizers.

During the beginning phases of this work, a study was conducted on the lime slurries to be used. Sealed cans of fresh commercial pebble quicklime and powdered hydrate lime were made available by members of the Lime Association. These were mixed with distilled, demineralized water to form slurries, the properties of which were then investigated. In order to normalize the results during this slurry study and the subsequent soil-stabilizing study, the slurries used were manufactured to have a specific gravity of 1.200 at normal ambient temperature (72°F), and were tested and utilized at this temperature. This amount of lime was chosen because a solution of 31 percent solids is generally used in the field, and because 40 percent solids is the maximum amount considered pumpable (*8*). The amount of lime in the slurries can be measured in pounds of lime per gallon of slurry (PL/GS), by the specific gravity, or by percent solids. During this study, specific gravity was measured by hydrometer or mud balance or by weighing a specific volume of slurry.

Experiments were conducted to determine the required mixtures of lime and distilled, demineralized water to achieve the needed specific gravity. For every 3.62 lb of hydrated lime used, 1 gal of this water was added. The quicklime slurries were made with 1 gal of distilled, demineralized water to 2.25 lb of quicklime pebbles. It took approximately 1.5 times more hydrated lime than quicklime to produce the same specific gravity of slurry. For each case the percent solids was determined by centrifuge separation of the supernatant and drying of the material remaining. The hydrated lime slurry was found to have 29.14 percent solids, whereas the quicklime slurry had 29.52 percent solids. The difference is believed to be caused by the impurities in the quicklime slurries.

The supernatants extracted from the slurries by centrifuging were tested for their concentrations of calcium by using an atomic absorption spectrophotometer. The results of these readings indicate the presence of 22.18 meq/L of calcium in the supernatant of the hydrated lime slurry, whereas the quicklime slurry had 24.05 meq/L of calcium in its supernatant. The 8.4 percent larger concentration of calcium may very well mean that the quicklime slurry will be more effective at stabilizing.

Following the testing of slurries, the results were used to determine the required percent of each type of lime needed to achieve the lime fixation point. This percent is defined as the lowest percentage of lime needed to fully modify soil behavior, or the lime modification optimum (LMO). The Eades and Grim pH test was utilized to find the LMO for the six soils to be used in the comparison study. In general, this would be followed by a verification of lime reactivity by determination of the stabilized Atterberg limits when compared with those measured for the natural soil. This information will be presented later. Both of these test procedures were performed following ASTM standards.

The results of pH testing are shown in Table 1 for all six soils. Interpretation was done using the lowest percentage of lime that provided sustained pH values, with engineering judgment involved in some cases. The means computed for the percentages of lime were found to be 6.17 percent for the hydrated lime slurries and 5.17 percent for the quicklime slurries.

NATURAL PROPERTIES OF SOILS

The objective of this research was to determine the stabilizing effects of both slurry types on highly active clay soils. The properties chosen for the comparisons included those that would indicate the changes in the total physicochemical nature of the soils. Those measured before and after stabilization included Atterberg limits and indexes, swelling pressure and percent swell, unconfined compressive strength, relationships between dry unit weight and water content, soil pH, cation exchange capacity, porewater cations, exchangeable cations, and percent clay. Each of these was determined by using standardized test methods as delineated by ASTM or the Soil Conservation Service of the U.S. Department of Agriculture.

TABLE 1 EADES AND GRIM pH TEST RESULTS

	Hydrated Lime		Quicklime	
Soil	Dry Dry Weight	pH	By Dry Weight	pH
GSW	6%	12.53	5%	12.56
Bardin	7%	12.47	6%	12.47
Nath	4%	12.50	4%	12.48
Dallas	6%	12.54	5%	12.56
McKinney	6%	12.44	5%	12.46
Austin	8%	12.47	6%	12.52

Once the natural properties had been determined for each soil, statistical analyses were performed to find their means and standard deviations. The intent was to have a sufficient sample population size to enable statistical inferences to be made as to property changes; therefore, only sample property statistics will be shown in this paper (Table 2). From Table 2 one can note that the mean value for the liquid limit was found to be 56.62 percent, and the mean plastic limit was 27.24 percent. Subtraction of these two values does not provide the mean plasticity index of 29.20 percent because each value was determined for the entire sample population separately. On the basis of the Plasticity Chart and the Unified Soil Classification System, these materials would be classified as CH, inorganic clays of high plasticity (AASHTO classification A-7-6).

Statistical analysis of clay contents shows that the soil

TABLE 2 RESULTS OF NATURAL SOIL PROPERTIES

Property	Mean	Std. Dev.	Range
LMO (%):			
Hydrated Lime	6.17	1.33	4.00 - 8.00
Quicklime	5.17	0.75	4.00 - 6.00
Liquid Limit (%)	56.62	5.38	51.00 - 65.27
Plastic Limit (%)	27.24	3.79	23.55 - 31.90
Plastic Index (%)	29.20	2.88	27.00 - 34.55
Linear Shrink.(%)	17.24	2.34	13.93 - 20.81
Percent Clay	41.01	5.16	35.01 - 47.74
Optimum W.C. (%)	25.77	2.77	22.50 - 29.00
Max. Dry U.W. (pcf)	96.83	3.76	92.00 - 102.00
Percent Swell	8.56	2.09	6.53 - 12.33
Swell Press. (tsf)	2.63	0.24	2.20 - 2.88
Unconfined Str. (tsf)	4.29	0.50	3.54 - 4.82
pH	7.88	0.07	7.76 - 7.94
Pore Water Cations (meq/L):			
Sodium	0.46	0.31	0.187 - 1.046
Potassium	0.41	0.02	0.0001 - 0.055
Magnesium	0.0009	0.0004	0.0003 - 0.0017
Calcium	1.55	0.56	1.01 - 2.44
Exchange Complex Cations (meq/100g):			
Sodium	0.20	0.17	0.08 - 0.50
Potassium	0.29	0.07	0.22 - 0.38
Magnesium	0.01	0.007	0.007 - 0.026
Calcium	12.47	11.67	7.31 - 27.18
Cation Exchange Capacity (meq/100g)	9.75	3.59	6.10 - 15.50

samples tested contained a mean percent clay of 41.01. Based on this value and the mean plasticity index, a high volume change capacity would be assigned to these materials, according to the volume change potential classification for clay soils (*9*). The percentages of clay were not measured for stabilized soils, because this measurement would be highly dependent on the amount of pulverization done.

Further proof of the highly active nature of these soils is the swelling test results. The mean percent swell under 1 psi was found to be 8.56. This occurred as the mean water content in the soils increased from 15.02 to 36.05 percent. The mean swelling pressure was determined to be 2.63 tsf, and the material moisture change was nearly identical to that for the other swell tests, but the mean of the beginning dry unit weights was about 10 percent lower.

Although efforts were made to compact strength test samples at their optimal conditions, slightly lower water contents and dry unit weights were achieved. The mean value of unconfined compressive strength for the soils tested was 4.29 tsf at a mean strain of 7.21 percent.

The mean values of the chemical properties measured indicated that the soils have a nearly neutral pH and cation exchange capacities that are not alarmingly high. The cation analyses indicated that these soils contain predominantly calcium, especially in their exchange complexes. These values are a further indication of how soil chemistry alone cannot be used to predict soil activity and lime reactivity, but may be useful in the understanding of what is occurring in the soil.

STABILIZED SOIL PROPERTIES

The procedures used for testing the stabilized materials were the same as those for the natural soils, with the exception of the addition of the lime slurries and the mixing, mellowing, and curing periods applied. The temperatures of all slurries at the time of application were as similar as possible given the ambient situation of the laboratory. After the lime slurries were thoroughly mixed into the soils, the mixtures were sealed in containers and allowed to mellow. In most cases, 24 hr was used as the mellowing period, but, as will be indicated, this was a variable in some procedures. After mellowing, samples were either compacted before further testing or tested for selected properties uncompacted. Curing of compacted specimens was done under sealed conditions and was varied, depending on the procedure. Each of these variable situations will be outlined as the results are discussed. Because the volume of test results is too large to include in this paper, only important trends will be presented here.

Two sequences were used for Atterberg limits testing. The first was used to verify the Eades and Grim pH test results of LMO at a mellowing period of 24 hr. The other included the use of lime percentages equal to the LMO and varying mellowing periods of 1, 6, 12, 24, 36, and 48 hr. The first sequence provided results that fully verified the LMO, as shown in Table 3. These results indicate that addition of more lime above the LMO does not further modify these soils. The mean values of plasticity indexes developed for various mellowing periods, as displayed in Table 3, show some of the relative effectiveness of these stabilizers. After 1 hr of mellowing, the soils treated with quicklime had experienced a reduction of plasticity index to 7.68 percent, whereas those treated with hydrated lime had decreased to 10.71 percent. This trend is somewhat different after 48 hr of mellowing. The soils treated with quicklime had a mean plasticity index of 4.27 percent and those treated with hydrated lime had a mean of 5.09 percent. Similar results were found when the linear shrinkage of treated samples was measured for differing mellowing periods. Without a test of the statistical significance, it appears that the quicklime slurries were more effective at reducing plasticity.

One of the more interesting behavior patterns found during this study had to do with the effects of these stabilizing slurries on the changes in the compaction characteristics of these soils. The addition of lime is expected to reduce the compacted dry unit weight and increase the necessary optimum water content. These results were observed, but to a different degree for each type of slurry, as shown in Figure 1. It appears that the reduction in compactibility associated with the addition of lime is less when quicklime slurries are used.

The swelling results for stabilized soils indicate greatly reduced tendencies for volume change. The soils stabilized with hydrated lime slurries displayed a mean swell of 0.094 percent with mean changes in water content of 7.27 percent. Those treated with quicklime slurries showed a mean swell of 0.044 percent and a mean water content change of 5.92 percent. The mean water content after swell was some 7 percent higher for the soils treated with the hydrated lime slurries.

The unconfined compression results for stabilized soils

TABLE 3 STABILIZED PROPERTIES: PLASTICITY INDEX

	Hydrated Lime	Quicklime
Percent Lime	P.I. (%)	P.I. (%)
LMO - 2	11.4	11.9
LMO	5.6	5.6
LMO + 2	8.5	8.4
Cure Time	**P.I. (%)**	**P.I. (%)**
1 Hour	10.8	7.9
6 Hours	6.9	6.9
12 Hours	6.7	8.0
24 Hours	7.3	6.5
36 Hours	6.0	6.8
48 Hours	5.1	4.3

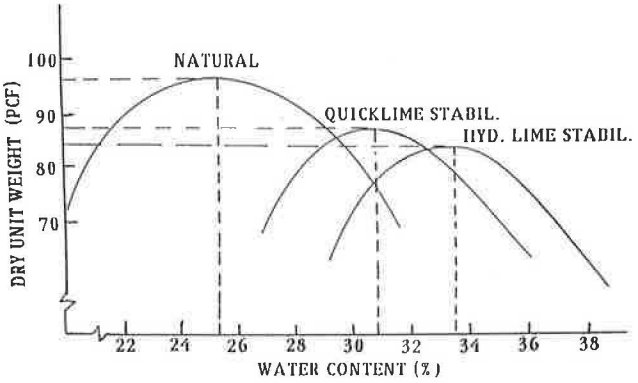

FIGURE 1 Typical compaction test results.

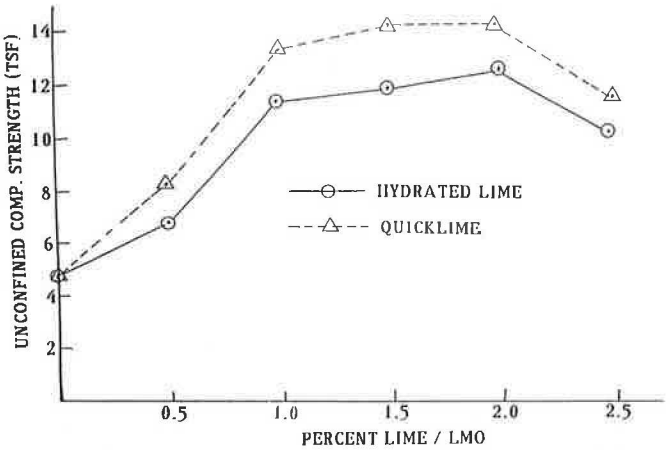

FIGURE 2 Strength comparisons.

showed dramatic increases in strength when the specimens were allowed to cure for 28 days. Both the water content after cure and the dry unit weight after cure were observed to decrease with increasing lime contents. The strength of the mixtures increased almost threefold as a result of the stabilizing action of the lime used. The mean increase in strength versus the percentage of lime added compared with each LMO is shown in Figure 2. The strength increases are most dramatic as the lime percentage reaches the LMO and continue as the amount of lime approaches two times the LMO. Above these percentages of lime there are dramatic decreases in strength. The largest mean strength gains noted were for soils treated with quicklime slurries that provide percentages of lime equal to two times the LMO. As the mean strength increased, the mean strain at failure decreased from 7.2 percent for the natural soils to 1.6 percent for the stabilized soils. This value of twice the LMO may be classed as the lime stabilization optimum (LSO) for these soils.

Soil pH values measured using the supernatants extracted from saturated samples showed little increase of mean values during the first 48 hr of mellowing when the soils were treated with percentages of lime equal to the LMO. Eventually, the mean pH of stabilized soil was found to reach 11.48. No further increases were expected to occur.

Determination of pore-water cations for these soils after stabilization revealed that there were significant increases only in calcium concentrations. The resulting mean levels of calcium in the stabilized soils are shown in Table 4. Increases were noted after just 1 hr of mellowing and continued to increase through the first 12 hr after lime application. It appears that the hydrated lime slurries caused larger increases of pore-water calcium concentrations than quicklime slurries did. On average, this amounted to a 26-fold increase over the natural mean when the percentage of lime added was the LMO.

Changes in the cation concentrations in the exchange complexes of the soils involved both calcium and magnesium. The changes in magnesium concentrations occurred during the first hour of mellowing, including a 56-fold increase for those soils treated with quicklime slurries, and a 71-fold increase occurred in soils stabilized with hydrated lime slurries. These increases are believed due to magnesium impurities in the lime. On the other hand, mean calcium concentrations increased by much greater amounts, as indicated in Table 5. The soils treated with hydrated lime had increases from the natural mean of 12.47 to 189.9 meq/100 g, whereas the concentrations in the quicklime-stabilized soils reached a mean value of 215.8 meq/100 g. These increments occurred when the percentages of lime were at the LMO, and they leveled off at these amounts within the first 6 hr of mellowing. When the lime percentages increased to two times the LMO or to the LSO

TABLE 4 STABILIZED PROPERTIES: CALCIUM IN SOIL

	Hydrated Lime		Quicklime	
Cure (Hrs)	Pore Water (meq/L)	Exch. Complex (meq/100g)	Pore Water (meq/L)	Exch. Complex (meq/100g)
1	20.8	183.6	26.8	189.1
6	34.9	189.9	30.6	215.8
12	43.5	179.7	37.7	204.6
24	41.4	196.1	35.7	204.0
36	52.1	182.4	38.7	194.1
48	42.3	200.6	39.2	203.3

TABLE 5 STABILIZED PROPERTIES: CALCIUM IN EXCHANGE COMPLEX

	Hydrated Lime		Quicklime	
Percent Lime	24 Hr Cure	28 Day Cure	24 Hr Cure	28 Day Cure
0.5 LMO	58.2	78.9	78.2	102.4
1.0 LMO	70.3	99.2	63.7	100.7
1.5 LMO	60.3	119.8	61.3	119.5
2.0 LMO	84.4	131.2	87.9	206.8
2.5 LMO	80.4	128.7	83.3	153.8

NOTE: Data are in milliequivalents per 100 g.

and 24 hr of mellowing was used, the maximum increases in calcium concentration in the exchange complexes were observed. There may likely be some tie between calcium in the exchange complex and strength gain, because these both occur at the LSO.

The data from measurements of the cation exchange capacity (CEC) of stabilized soils revealed three changes. For soils treated with lime percentages equal to the LMO and allowed to mellow 24 hr, there was a dramatic increase in CEC, and this effect was slightly more pronounced for soils stabilized with hydrated lime slurry. This trend was reversed when specimens compacted and cured for 28 days were tested. Finally, a definite decrease in CEC was measured for soils treated with percentages of lime more than two times the LMO.

The properties measured after each type of lime treatment must be compared with those determined for the natural soils in order to determine the actual meaning of the property changes achieved.

STATISTICAL ANALYSES

All experimental data were utilized during statistical analyses of comparison for each population mean difference at various confidence intervals. Hypothesis testing was used to determine the truth or falsehood of each null hypothesis. Student's *t*-statistic was used to investigate the population mean and the mean difference. The 95 percent confidence interval and results of analyses for this level of consideration are shown in Table 6. The following is a summary of the findings for all statistical analyses:

1. Even at a low 75 percent confidence level, no reduction in plasticity index can be proved as a result of using one stabilizer rather than the other.
2. At the 80 percent confidence level, quicklime slurries were found to cause lower swell potential than hydrated lime slurries.
3. At the 90 percent confidence level, quicklime slurries

TABLE 6 RESULTS OF PAIRED EXPERIMENT: *t*-STATISTICS

Hydrated Lime Treated Values - Quicklime Treated Values				
Property	Mean of Diff.	Std. Dev.	95% Confidence Interval	H_o: U=0
LMO	1.00	0.26	0.48 to 1.50	Reject
PI (%)	0.0	0.88	-1.72 to 1.82	Yes
Max. Dry Unit Weight (pcf)	-3.5	0.68	-4.88 to -2.12	Reject
% Swell	0.05	0.05	-0.05 to 0.15	Yes
Unconfined Str. (tsf)	-1.98	1.20	-4.39 to 0.43	Yes
pH	0.10	0.09	-0.07 to 0.27	Yes
Pore Water Ca (meq/L)	5.68	7.53	-9.49 to 20.85	Yes
Exch. Comp. Ca (meq/100g)	-9.08	11.53	-32.31 to 14.15	Yes
CEC - Ca (meq/100g)	99.67	159.00	-220.71 to 420.05	Yes

were found to produce more strength gain than hydrated lime slurries.

4. At the 80 percent confidence level, after 48 hr of mellowing, hydrated lime slurries were determined to cause higher soil pH than quicklime slurries.

5. At the 75 percent confidence level, within 48 hr of mellowing, hydrated lime slurries were found to provide more calcium cations in the pore water than quicklime slurries.

6. At the 75 percent confidence level, quicklime slurries were determined to provide more calcium cations to the exchange complex than hydrated lime slurries.

7. Even at this low 75 percent confidence level, no difference was found in how these stabilizers affected the CEC of these soils.

8. At the 95 percent confidence level, quicklime slurries are less detrimental to compactibility than hydrated lime slurries.

Space does not permit the listing of all statistical comparisons and results in this paper. Those interested in all the data and the statistical information should contact the authors.

CONCLUSIONS

The objective of this research was the comparison of the stabilizing effects of quicklime and hydrated lime slurries. Statistical analyses were used to test the significance of the differences in the stabilizing effects of these slurries as measured by changes in physical and chemical properties. When the conclusions below are considered, it should be taken into account that 1 percent less quicklime was used for all applications as compared with hydrated lime.

1. The LMOs determined with the Eades and Grim pH test were valid for these lime-reactive, highly active clay soils.

2. Quicklime slurries caused a more reduced plasticity and linear shrinkage, especially after the first hour of mellowing.

3. Quicklime slurries caused these soils to have less reduction in compactibility, as well as less need for water in the curing of stabilized specimens.

4. Quicklime slurries provided more strength gain in these soils, and the maximum strength gain occurred at lime percentages equal to twice the LMO.

5. When a maximum amount of calcium cations is in the exchange complex, there is an accompanying maximum strength gain.

6. Hydrated lime slurries provide more calcium in the pore water, and quicklime slurries provide more calcium to the exchange complex.

7. As short-term effects, quicklime slurries provide a larger reduction in swelling potential, more strength gain, and higher concentrations of calcium in clay soil exchange complexes.

REFERENCES

1. O. G. Ingles and J. B. Metcalf. *Soil Stabilization: Principles and Practice.* Butterworths Pty. Limited, Australia, 1972.
2. M. R. Thompson. *Influence of Soil Properties on Lime-Soil Reactions.* National Lime Association, Washington, D.C., Aug. 1965.
3. M. R. Thompson. Lime Reactivity of Illinois Soils. *Journal of Soil Mechanics and Foundation Division,* ASCE, Vol. 2, No. SM5, 1966.
4. M. R. Thompson. *Factors Influencing the Plasticity and Strength of Lime-Soil Mixtures.* Bulletin 492. Engineering Experiment Station, University of Illinois, Urbana, Ill. 1967.
5. *Lime Stabilization Construction Manual.* Bulletin 326. National Lime Association, Arlington, Va., 1982.
6. *Porta Batch—A Revolutionary New Portable Lime Slaking System.* Pozzolanic Systems, Inc., Fort Worth, Tex., 1982.
7. Q. L. Robnett and M. R. Thompson. Field Evaluation of Pressure Injection Lime Treatment for Strengthening Subgrade Soils. Presented at Roadbed Stabilization Lime Injection Conference, Little Rock, Ark., 1975.
8. *Evaluation of Railroad Lime Slurry Stabilization.* Report FRA/ORD-78/09. Federal Railroad Administration, U.S. Department of Transportation, 1978.
9. *Soil Mechanics—Design Manual 7.1.* Naval Facilities Engineering Command, U.S. Department of the Navy, May 1982.

Publication of this paper sponsored by Committee on Lime and Lime-Fly Ash Stabilization.

Effects of Pulverization on the Strength and Durability of Highly Active Clay Soils Stabilized with Lime and Portland Cement

THOMAS M. PETRY AND SUZANNE KELLY WOHLGEMUTH

This paper presents the results of a laboratory investigation exploring the effects of varying degrees of pulverization, from laboratory-quality gradations to field gradations, on the strength and durability of highly plastic clay soils stabilized with lime and portland cement. Background information is presented on the mechanisms of stabilization and on previously reported studies of other materials. A 6-yd³ sample was used to provide 198 large specimens, which were tested in unconfined compression and wet-dry tests. Considerable differences were found in the strength of a highly active clay soil, depending on the gradations used to make specimens. Significant differences were found in the durabilities of specimens, depending on the stabilizer and the gradations used. Lime appears to be a more effective stabilizer for durability and portland cement more effective for strength, provided the gradation is fine enough. Recommendations, subject to further research, include longer curing times and the use of field gradations for all mix designs.

One of the additives frequently used to stabilize heavy clay soils successfully has been high-calcium lime. There has also been some successful experimentation in the laboratory with portland cement as a stabilizer. However, the majority of this research has been performed on finely pulverized samples, usually having 100 percent passing the No. 4 sieve. The main drawback with using this type of gradation is that it does not accurately reflect the kinds of pulverization specified in the field. The differences between laboratory and field gradations are great enough that the stabilized materials in each case have vastly different properties. These differences are most critical for highly active clay soils, especially when they are exposed to cycles of wetting and drying.

The purpose of the research reported here was to investigate and evaluate the effect of soil preparation (pulverization) on the strength and durability of highly plastic clay soils that have been stabilized with lime or portland cement. This was done using materials that were pulverized according to field and laboratory gradations, then compacted and subjected to strength and durability testing.

BACKGROUND

The objective of soil stabilization by the addition of lime or portland cement is to modify the physicochemical properties of fine-grained soils to improve strength and durability. Much has been reported about how these agents affect soil physical and chemical properties, yet there has been little investigation of the effects of differences in pulverization.

The responses of soil to treatment with hydrated high-calcium lime are complex and often dramatic (*1, 2*). With the addition of lime to a fine-grained soil, several reactions occur. Cation exchange and flocculation-agglomeration reactions occur rapidly and produce immediate changes in soil plasticity and workability, and the immediate incurred strength and load deformation properties. Pozzolanic time-dependent reactions may occur, depending on the soil being stabilized. These pozzolanic reactions result in the formation of various cementing materials that increase mixture strength and durability. The exact products formed during stabilization with lime will vary depending upon the type of clay and the reaction environment, especially temperature and pH.

The stabilization of clay soils with portland cement is a two-stage process. The hydrolysis and hydration of cement, with the resulting soil hardening, are regarded as the primary processes. The cement particles bind the adjacent soil grains together to form a more-or-less continuous skeleton of hard material enclosing a matrix of unaltered soil (*3*). The clay itself participates in the secondary process by combining with the calcium ions produced by the hydration of the cement and forming new cementitious materials. Although minimal, the calcium generated during cement hydration reacts with the clay in much the same manner as if added as the stabilizing agent. The amounts of calcium hydroxide available decrease as the cement-soil reactions progress. The hardening of the soil-and-cement combination is primarily due to the hydration of cement, but it is also the result of physicochemical reactions between the soil and cement particles (*3*).

The inclusion of large clay lumps in stabilized soil has long been considered detrimental to the stabilization process and to the corresponding strengths and durabilities. Granular soils and light clays have been successfully pulverized in the field with the aid of lime and cement stabilizers. However, pulverizing heavy, highly plastic soils to meet the same specifications is difficult, and often the specifications cannot be met. Furthermore, there is very little information available or research reported concerning the durability of coarsely pulverized stabilized soils.

Department of Civil Engineering, University of Texas at Arlington, P.O. Box 19308, Arlington, Tex. 76019.

Portland cement and lime stabilizers react differently to soils with gradations that are coarser than the typical laboratory gradation (*4–9*). Construction specifications normally stipulate different gradations for portland-cement- and lime-stabilized soils, with cement-stabilized soils having a finer gradation. For example, the U.S. Department of Transportation (DOT) recommends the same degree of pulverization as that used by the Texas Department of Highways and Public Transportation: 100 percent passing the 1-in. sieve and a minimum of 80 percent passing the No. 4 sieve (*7*). In contrast, the Portland Cement Association recommends that the minimum passing a 1¾-in. sieve be 100 percent and that the minimum passing a ¾-in. sieve be 75 percent.

Felt (*5*) studied the factors influencing the physical properties of soil and cement mixtures; he used many different types of soil, from nonplastic fine-grained silts to highly plastic clays. He prepared specimens of stabilized soils that had different percentages of lumps larger than a No. 4 sieve. In some specimens these lumps were wet and in some they were dry. As the specimens were subjected to wet-dry and freeze-thaw tests the ones with dry lumps were destroyed upon contact with water. Felt concluded that the quality of the mixture was adversely affected if less than 80 percent of the clay soil was pulverized to pass a No. 4 sieve and the large lumps were dry of optimum water content.

In another study, Grimer and Ross (*6*) investigated the effects of the degree of pulverization on the quality of heavy clay soils stabilized with portland cement. Specimens were prepared using aggregations of continuous grading (retained on British Standard No. 14 sieve to retained on B.S. No. 200 sieve) and various proportions of single-sized 3/16-in. extruded aggregations. All specimens were cured in wax for 7 days and then immersed in water for 7 or 28 days before being tested in unconfined compression. Grimer and Ross found that the strength of the stabilized soils increased with decreases in aggregation size. In addition, the ratio of the strength after immersion to that after cure decreased with an increase in the percentage of the large aggregations. The considerable increase in strength found with increased pulverization suggested that pulverization, much more than mixing, was the main factor governing the strength of portland cement clay mixtures.

In a recent study, Kennedy et al.(*7*) investigated the effects of pulverization on portland-cement-treated, highly plastic clays. They compared the unconfined compressive strengths in both the wet and dry conditions of both unpulverized and well-pulverized samples. The unpulverized soils had gradations with 85 percent passing the No. 4 (U.S. series) sieve, and 15 percent passing a 1½-in. sieve and retained on a ¾-in. sieve. The well-pulverized samples had gradations with 100 percent passing the No. 4 sieve. The strengths of the mixtures of unpulverized clay and portland cement were substantially lower than those of the comparable well-pulverized materials when tested in a dry condition, a situation that was more pronounced for those in the wet condition. The study concluded that for portland-cement-modified, highly plastic clay soils, even small amounts of unpulverized materials are detrimental to the overall strength of the mixture.

Through the years efforts have been made by those who thought that lime migration into soil clods or aggregates would eventually stabilize these soils to make construction more economical by reducing the required pulverization of lime-stabilized soils. These beliefs were often been supported by field observations.

During a study by Davidson et al. (*8*), the diffusion phenomena and the effect of coarse gradations were investigated on combinations of gradations containing from 20 to 100 percent lumps passing the 1-in. sieve in a matrix of soil passing the No. 4 sieve and appropriate amounts of lime. The specimens made were cured from 7 to 270 days and tested in unconfined compression. The results of these tests showed that the presence of lumps in compacted soil-lime mixtures decreased the strength of the mixture, but that after about 150 days of curing time the strengths of all mixtures were approximately equal. This change of influence by the lumps was believed to have been caused by lime movement, which occurred in sufficient quantities to cause a pozzolanic reaction within the mixture.

Additional support for the theory of lime migration was found by Stocker (*9*). In his study specimens were prepared using field gradations. Three percent and 15 percent lime was added, and the compacted samples were cured for up to 122 days. The specimens were then alternately wetted and dried under suction while their volume changes were observed. Specimens cured 122 days showed no sign of distress, and Stocker concluded that lime migrates into the soil lumps and stabilizes them.

The majority of studies on lime and portland cement as stabilizers for plastic soils have regarded strength as the primary quality-control check. Few have investigated the relationships between strength and durability and degree of pulverization. The intent of the study reported here was to explore these relationships.

PRELIMINARY TESTING PROGRAM

The program of research reported here contained initial testing to evaluate the materials used and to determine the optimal percentages of the agents to use. Following these activities, gradations for further testing were prepared, and the compaction characteristics of both natural and stabilized materials were determined.

The soil profile for the test sample was that of soils weathered from the Taylor geologic formation at an industrial park just west of Greenville, Texas. The suitability of these soils was initially determined using Shelby tube samples taken from two 25-ft-deep borings. After the soil plasticity indexes were found to be at least 60 percent, approximately 6 yd^3 of soil was excavated from the lower A and upper B horizons at depths of 1.5 and 7.0 ft, respectively, using a front-end loader; loaded on an 8-yd^3 truck; and transported to the laboratory. These materials were randomly sampled and tested to ensure that their plasticity indexes were equal to or greater than 60. Typical values

of the Atterberg limits of these materials, which are classified as inorganic clays of high plasticity, are shown in Table 1. These tests were performed according to ASTM methods on soils that were wet-processed and passed the No. 40 sieve.

X-ray diffraction tests were performed on samples of the soil that had passed the No. 40 sieve. The primary constituents were as follows:

Mineral	Percent
Quartz	50
Montmorillonite	40
Calcite	10
Feldspar	<1
Illite	<1
Kaolinite	<1

Samples that were utilized for the Eades and Grimm lime-soil pH test, the lime percentage-PI series test, and the portland cement percentage-PI series test were processed as for Atterberg limit testing. These procedures were performed in accordance with ASTM methods. The optimum lime content based on the lime-soil pH series was selected from the curve at a pH of 12.4, which occurred at 10 percent lime content. The results of the tests in which plasticity indexes were determined for various lime additive rates indicated that the maximum reduction in the plasticity index occurred at a lime content of 10 percent, when the plasticity index was 16.8. The same type of testing, when performed on portland-cement-treated soils, resulted in an optimum portland cement additive rate of 12 percent, which corresponds to a maximum reduction in the plasticity index to 12. It was clearly evident that this soil was both lime and portland cement reactive, so the testing could proceed.

Once the suitability of the soil had been determined, the clay was air dried and sieved by hand and with a large mechanical shaker to pass the sieves chosen, forming coarse, medium, and fine gradations as follows:

Coarse:
Minimum passing 1 ¾-in. sieve = 100 percent
Minimum passing No. 4 sieve = 60 percent

Medium:
Minimum passing 1-in. sieve = 100 percent
Minimum passing No. 4 sieve = 80 percent

Fine:
Amount passing No. 4 sieve = 100 percent

TABLE 1 ATTERBERG LIMITS TEST RESULTS

Sample No.	Liquid Limit	Plastic Limit	Plastic Index
1	82	17	65
2	94	22	72
3	86	22	64
1	96	19	77
2	91	23	68
3	99	31	68

It was necessary to prepare these gradations at moisture levels slightly lower than the soil's plastic limit to prevent coalescence of individual aggregations. All the graded soils were placed in metal barrels and sealed to retard or prevent moisture loss.

The relationships between moisture and unit weight were determined for all gradations of both raw and stabilized soil. To enable the use of these coarser gradations and the highly plastic soils, a modified compaction method was chosen based on the TEX-113E testing specification. This specification was used to best represent the expected field situation, especially to prevent overcompaction. To achieve the 6,912-ft-lb/ft^3 energy level, a 6-in.-diameter mold 4 in. high was used with a 5.5-lb hammer falling 12 in. Three layers and 30 drops of the hammer per layer were used.

Moisture-unit weight relationships were determined for portland-cement-treated clay mixtures containing the optimum amount of cement as indicated by the PI reduction method. The proper amount of cement was mixed with the soil, water was added in varying amounts, and the soil mixture was immediately compacted. Similarly, soil-lime mixtures were prepared using the optimum lime contents determined from both the PI reduction and pH test methods. These mixtures were allowed to cure in sealed plastic bags for 24 hr before compaction testing. The optimum moisture contents and maximum dry unit weights determined from these compaction tests are shown in Table 2. These results seem to indicate that the addition of lime had little effect on the compaction characteristics of this soil and that portland cement acted as an apparent compaction aid, providing an increased maximum dry unit weight and lower optimum water content.

SPECIALIZED TESTING PROGRAM

The major testing program included a series of unconfined compressive tests and wet-dry tests on compacted mixtures of lime- and portland-cement-treated soil. Strength and durability testing was performed on a total of 198 cylinders of soil (6 by 12 in. each) compacted using six layers and the compactive effort explained earlier. Three specimens were prepared for each gradation and type and amount of stabilizer, which were cured for various periods in a moist

TABLE 2 RESULTS OF TESTS ON MOISTURE AND UNIT WEIGHT

Stablizer (%)	Gradation	Optimum Dry Unit Weight (lb/ft^3)	Moisture Content (%)
Raw	Coarse	79.4	34.0
Raw	Medium	76.9	33.6
Raw	Fine	75.4	35.0
7 (cement)	Coarse	86.5	29.5
12 (cement)	Medium	89.1	26.0
12 (cement)	Fine	87.8	28.6
10 (lime)	Coarse	79.0	32.0
10 (lime)	Medium	78.0	34.0
10 (lime)	Fine	75.3	36.5

environment before unconfined compressive testing. The levels of stabilizer used included the optimum and 3 percent above and below the optimum.

Two specimens were made for each gradation and type and amount of stabilizer for the wet-dry testing, as follows:

1. At the end of the cure period, the specimens were submerged in tap water at room temperature for 5 hr.
2. The specimens were removed from the water and allowed to drain.
3. Each specimen was weighed to the nearest 0.1 lb and measured to the nearest 1/16 in.
4. Each specimen was then placed in an oven set at 160°F for 42 hr and removed.
5. The specimens were again weighed and measured.
6. The previous five steps constituted one cycle of wet-dry testing.

All materials used for these tests were prepared using the same procedures as those for the compaction tests and at optimum conditions. The amounts of lime or portland cement stabilizer and the curing methods used depended on the testing situation, as will be explained later.

The procedure for the unconfined compressive tests was the same for all specimens. After they had cured for the specified length of time, which was 0, 7, or 28 days, in a wet concrete-curing room, the specimens were removed, weighed, and measured. They were then tested to failure at a constant strain rate of 0.1 in./min. The ultimate load was recorded for each of the specimens, and their moisture content was found after failure. The test results are shown in Figures 1–3. For each case of stabilizer and cure period the resulting average unconfined strength is plotted versus the percent stabilizer. On each graph a separate curve is drawn according to the gradation, which is plotted to best represent the variations in strength.

Figure 1 and the top part of Figure 3 show how lime

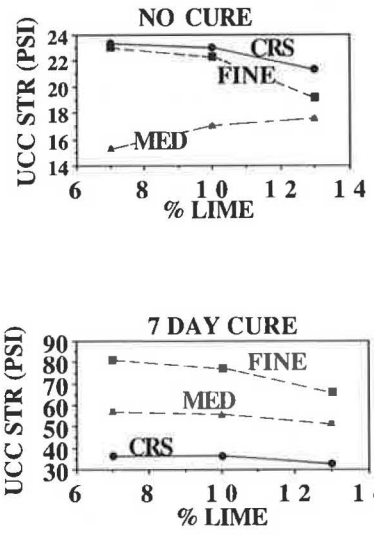

FIGURE 1 Unconfined strength of lime-treated soils: 0- and 7-day cures.

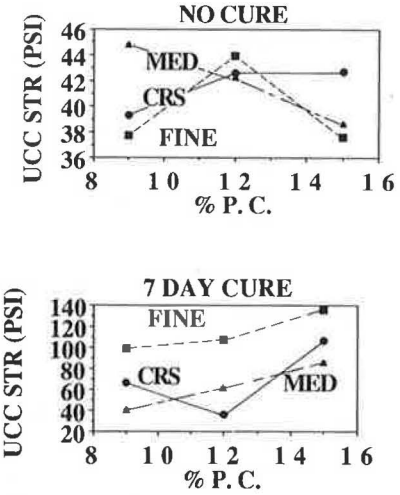

FIGURE 2 Unconfined strength of portland-cement-treated soils: 0- and 7-day cures.

treatment affected the strength for each length of curing time. Figure 2 and the lower part of Figure 3 show these same features for the portland-cement-treated soils. The results for unconfined strength following a 28-day curing period are shown for both stabilizers in Figure 3 to facilitate comparisons.

If one considers only the effects of changes in gradation, the resulting strengths measured depended greatly on the curing period involved. For both stabilizers and for immediate testing of specimens without curing, the amount of pulverization appears to have had little effect on the strength developed. After a 7-day curing period the effects of degree of pulverization on the resulting strength were mixed. The lime-treated specimens that were made from more finely pulverized materials displayed more strength. This trend was not as clearly evident for the portland-cement-treated specimens, although the most finely pulverized materials provided the specimens with highest strengths. For those

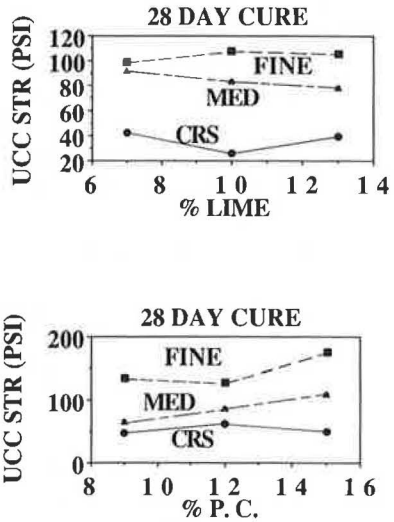

FIGURE 3 Unconfined strength of stabilized soils: 28-day cure.

specimens cured for 28 days before strength testing, strengths were very dependent on the degree of pulverization of the material before treatment and compaction. Those specimens that had been made with the most finely pulverized soil had significantly more strength than those made from the medium and especially the coarse gradation materials. The benefits of finer pulverizations are clearly evident in Figures 1–3.

Consideration of how the measured unconfined strengths of specimens changed with added amounts of the stabilizers revealed the effects of curing. Without curing, specimens stabilized with both agents had little or mixed changes of strength as the percent of the stabilizer increased. The lime-treated specimens, which had been cured for 7 days, displayed generally decreasing strengths as the percent of lime was increased. This trend was different when the lime-treated specimens were cured for 28 days. In this case the measured strengths increased as the percent of lime was increased to the optimum but remained unchanged as the lime content was increased further. The portland-cement-treated specimens, when cured for either 7 or 28 days, exhibited increases of strength as the percent of cement was increased. The largest strength gains noted were for portland-cement-treated specimens with 15 percent cement cured for 28 days.

Overall, the cement-stabilized specimens displayed higher strength than the lime-stabilized specimens, with differences ranging between 10 and 70 psi. This trend became more evident as the curing times and the percent of stabilizer increased. The most significant increases in unconfined strengths were noted in specimens made of soils stabilized by both agents as the gradations of materials used to make the specimens became finer.

Specimens to be tested in the wet-dry procedure were first cured for 7 days in the wet room. These specimens were tested according to a modified version of ASTM D 559-82. The specifics of the procedure were given at the beginning of this section. This procedure was repeated at least 12 times, or until the specimens failed, either during the wetting cycle or the drying cycle. All specimens that completed these wet-dry cycles were tested in unconfined compression.

The results of wet-dry testing revealed much about the durability of compacted stabilized materials with various gradations. The portland-cement-treated soils did not appear to perform well during this testing. After the first cycle of wet-dry testing on the cement-stabilized soils with coarse gradation, all the specimens slaked heavily. This occurred when they were stabilized at optimum, below optimum, or above optimum percent cement and during the 5-hr soaking period. At the end of the 42-hr drying period all cement-stabilized specimens crumbled as an attempt was made to remove them from the oven.

After the first 5-hr soaking period for the soil specimens prepared with medium gradation and cement treatment, those with below-optimum percentages of cement fell apart and were discarded. The remaining specimens in this category crumbled after the prescribed period of drying.

The cement-stabilized specimens made with the fine gradation soil completed one full cycle of the wet-dry test. However, when removed from the oven, all of those with 9 percent, one with 12 percent, and one with 15 percent cement crumbled. The remaining two specimens, one with 12 percent and the other with 15 percent cement, slaked to total failure after 5 min of the second soaking cycle.

Specimens stabilized with lime were much better able to endure the wet-dry testing cycles. The benefit derived from finer gradations was very apparent during this part of the testing also. All lime-stabilized specimens made with coarse gradation soil completed two cycles of the wet-dry tests. After the third soaking period, however, these samples had slaked so heavily that they crumbled when removed from the soaking tank.

The lime-stabilized specimens compacted using medium gradation soil varied in their durability to the wet-dry testing. The specimens with 7 percent lime crumbled after the fourth cycle. The samples stabilized with optimum lime contents (10 percent) completed seven full cycles of wetting and drying, and those with above-optimum percentages of lime (13 percent) completed the full 12 cycles of the test. However, after the 10th cycle, there was only one specimen with 13 percent lime to continue testing. At the end of the 12 full cycles, the remaining specimen was not considered testable in unconfined compression because it was heavily slaked.

The most durable of the lime-stabilized specimens were those made with the fine gradation. Those stabilized with below-optimum percentages of lime completed seven cycles of the wet-dry tests before disintegration. The specimens with optimum and above-optimum lime contents successfully completed all 12 cycles of the wet-dry tests. One specimen with 10 percent and one with 13 percent lime were accidentally broken before strength testing. Two viable specimens remained, one with 10 and one with 13 percent lime. They were soaked again and tested for their unconfined compressive strength. The specimen with the optimum percent of lime had a strength of 14.1 psi and the one with above-optimum lime had a strength of 33.1 psi.

The weight loss for all specimens was fairly consistent. This varied from approximately 0.5 to 1.0 lb of material per cycle lost in soaking until the specimens slaked to failure. Figure 4 shows how this weight loss occurred for a fine-gradation specimen stabilized with the optimum percent of lime.

DISCUSSION OF RESULTS

When all the results described above are considered, it becomes clear that the way in which a stabilizing agent works with and within the soil influences the way in which the stabilized soil will be affected by differences in the amount of pulverization before treatment. The results achieved for very finely pulverized samples used for the Atterberg limits and reactivity testing seem to indicate that these stabilizers are roughly similar in their stabilizing effects. Indeed, the samples treated with portland cement appeared

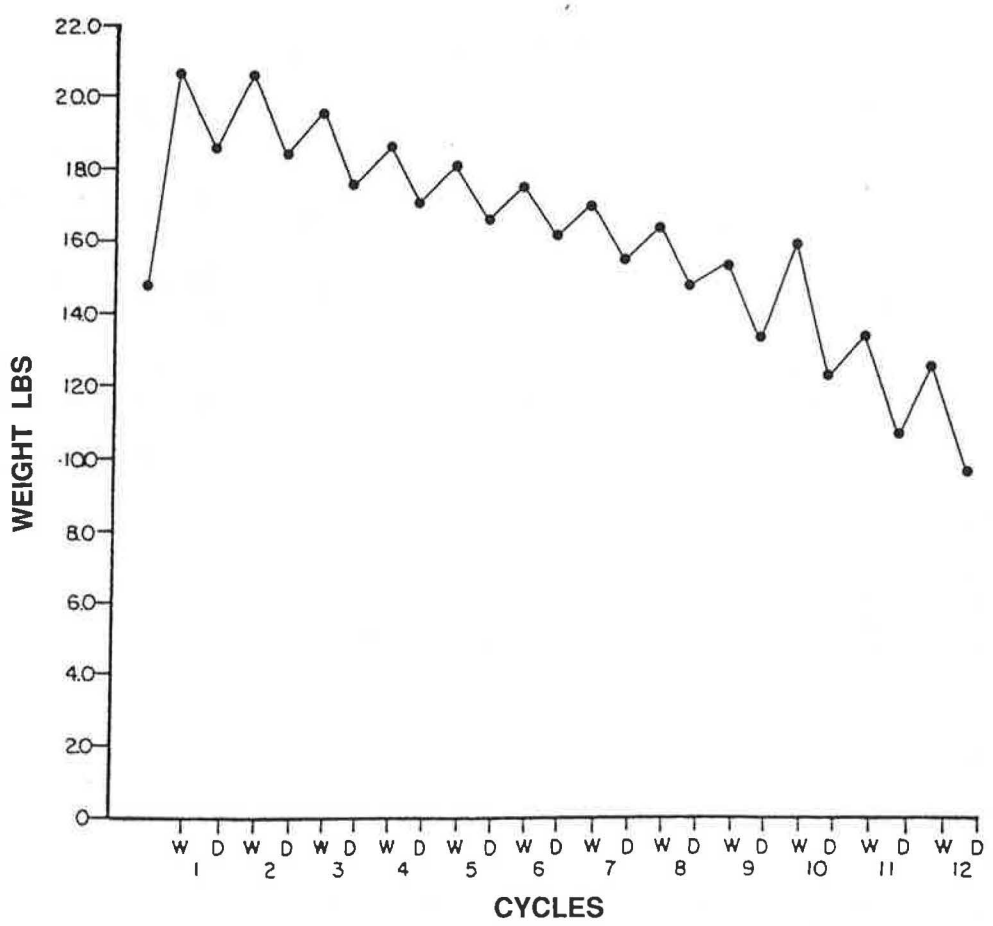

FIGURE 4 Weight variation per wet-dry cycle, 10 percent lime, fine gradation.

to be more stable as far as their PIs would indicate. However, these results did not indicate clearly what would occur during later testing.

The effects of the coarse gradation on the stabilized soil were caused primarily by the presence of large clods or aggregations of highly active clay particles that were left relatively untreated. After tests had been completed, the destroyed specimens were inspected and the following observations were made.

1. The specimens stabilized by lime had large aggregations in which the outer layers reacted with lime to form a coating that provided a degree of waterproofing but little strength. This may be the reason for the small strength gain in these samples. However, even this small amount of lime migration provided definite protection during wetting and drying cycles.
2. The specimens treated with portland cement contained large aggregations held together by the cement coatings but not fully coated to a level where they were waterproof and resistant to conditions leading to shrinking and swelling of the clods. This condition led to little strength gains for these soils and ineffective waterproofing. The strength displayed by all coarsely graded specimens was most likely dependent only on the shear strength of the clay clods or aggregations.

As the gradations became finer, stabilizing effects increased and the materials gained strength and durability. The maximum stabilizing effects occurred for the finest gradation. Those specimens stabilized with portland cement had higher dry unit weights and significant strength gains from about 39 to 176 psi. Better compaction for the cement-treated specimens may have occurred because of less flocculation than occurred in the lime-treated soils and some lubricating effects. The cementitious effects of cement hydration in forming a skeleton of binding material were also evident. On the other hand, it is evident that the waterproofing capacity of portland cement is questionable, especially where it affects the shrink-swell phenomena in clay particle aggregations.

The lime-stabilized materials displayed the kind of waterproofing needed for durability against wetting and drying. However, these materials did not display as much strength gain as those stabilized with cement. It is very possible that a good part of the difference in strength gain is because of the lower dry unit weights in the lime-stabilized soils. When the strength gains realized are nor-

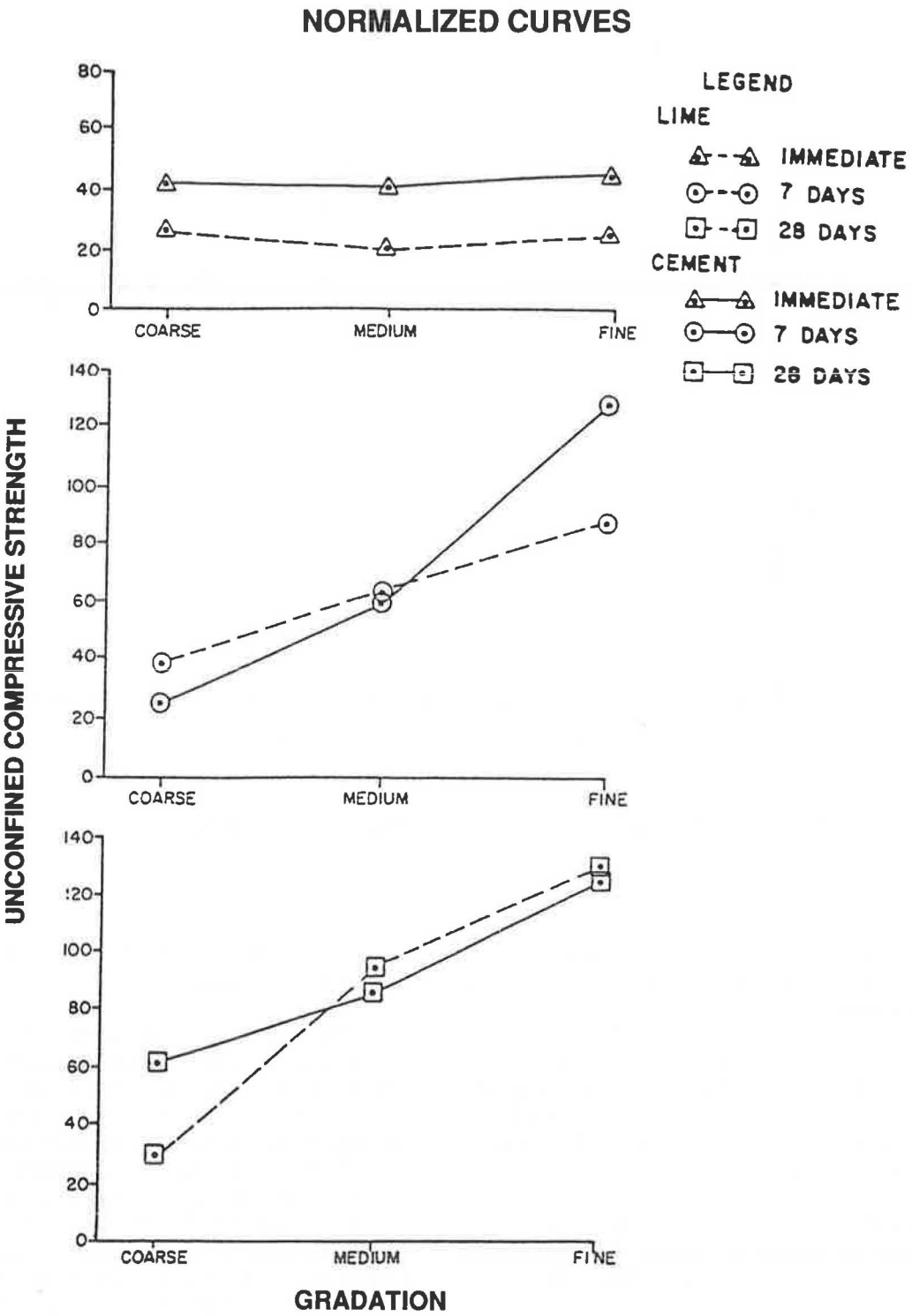

FIGURE 5 Strength versus gradation, 10 percent lime, 12 percent cement.

malized by differences in dry unit weights, the type of curves shown in Figure 5 results. It is believed that the coating and migrating effects of the lime lead to greater overall stability for these highly active clays. As the gradation approached that used in the initial laboratory testing, the strength gain effects of these stabilizers became similar.

It became evident that the differences in behavior and response to different gradations can be tied to the difference in stabilization effects of the lime and portland cement. The physicochemical action of lime provides more stability for these materials than the primarily mechanical (e.g., cementing) action of portland cement. It is interesting to note that after 12 cycles of wetting and drying and one of

saturation, specimens made with the fine gradation had significantly higher unconfined compressive strengths than the untreated soils.

CONCLUSIONS AND RECOMMENDATIONS

The objective of this investigation was to determine the effect of pulverization on the strength and durability of highly plastic clays stabilized with lime and portland cement. The objective was reached through an extensive program of testing. The conclusions are as shown below.

1. With regard to long-term durability, lime stabilization produced a better product for all gradations tested.
2. Portland cement produced a stabilized material that had better compaction characteristics and better strength, provided the gradation was fine enough.
3. Lime stabilization of coarsely graded materials required longer curing time than did fine-graded materials to reach attainable strength and durability.
4. Portland cement is not an effective stabilizer for highly plastic soils under field gradation situations. The strengths vary and are probably very dependent on the shear strength of the clay.

The following recommendations, which should be supported by further research, are a consequence of this investigation.

1. Laboratory tests for stabilizing soils should be conducted using field gradations.
2. When wet-dry tests are conducted on 6- by 12-in. specimens, the soaking and drying times should be extended to ensure complete saturation and drying.
3. Curing periods should be extended to obtain more realistic strength values for specimens made with coarser gradations.

REFERENCES

1. S. Diamond and E. B. Kinter. Mechanics of Soil Lime Stabilization. In *Highway Research Record 92,* HRB, National Research Council, Washington, D.C., 1965, pp. 83–101.
2. *Transportation Research Circular 180: State of the Art: Lime Stabilization Reactions, Properties, Design, Construction.* TRB, National Research Council, Washington, D.C., Sept. 1981.
3. A. Herzog and J. K. Mitchell. Reactions Accompanying Stabilization of Clay with Cement. In *Highway Research Record 36,* HRB, National Research Council, Washington, D.C., 1963, pp. 146–171.
4. *Soil Stabilization in Pavement Structures: A User's Manual,* Vol. 1. FHWA, U.S. Department of Transportation, Oct. 1979.
5. E. J. Felt. Factors Influencing Physical Properties of Soil-Cement Mixtures. *Bulletin 108,* HRB, National Research Council, Washington, D.C., 1964, pp. 138–162.
6. F. J. Grimer and N. F. Ross. The Effect of Pulverization on the Quality of Clay-Cement. *Proceedings, 4th International Conference on Soil Mechanics and Foundation Engineering,* Vol. 2, 1957, pp. 109–113.
7. T. W. Kennedy, R. Smith, R. J. Holmgreen, Jr., and M. Tahmoressi. An Evaluation of Lime and Cement Stabilization. In *Transportation Research Record 1119,* TRB, National Research Council, Washington, D.C., 1987, pp. 11–25.
8. D. T. Davidson, T. Demirel, and R. L. Handy. Soil Pulverization and Lime Migration in Soil-Lime Stabilization. In *Highway Research Record 92,* HRB, National Research Council, Washington, D.C., 1965, pp. 103–126.
9. P. T. Stocker. *Diffusion and Diffuse Cementation in Lime and Cement Stabilized Clayey Soils.* Special Report 8. Australian Road Research Board, Vermont South, Victoria, Australia, 1972.

Publication of this paper sponsored by Committee on Lime and Lime-Fly Ash Stabilization.

Minimum Requirements for Temporary Support with Artificially Frozen Ground

HUGH S. LACY AND CARSTEN H. FLOESS

Use of artificially frozen ground to provide temporary support is increasing in the United States. Temporary frozen ground structures are usually designed by contractors experienced in this type of construction. However, there is an absence of accepted requirements for artificially frozen ground. Sheeting and shoring are typically designed by a professional engineer, stress levels are regulated by code, and computations are often reviewed. Similar standard design procedures do not exist for temporary frozen walls. As a result, the owner and the engineer cannot readily ascertain the adequacy of the design of a project or the risk undertaken by the contractor. This paper describes the ground-freezing process and proposes performance and monitoring requirements for artificial ground freezing. Engineers can then judge whether the design is commensurate with project needs. Case histories are included.

Use of frozen ground to provide excavation support has increased in the United States in recent years. Although it has been used for the construction of deep vertical shafts in soils for more than 100 years, recent applications include much larger circular shafts as well as irregular-shaped structures, emergency measures to stabilize soil, and mining beneath critical structures.

Artificially frozen ground has been used for projects in which it was necessary to limit exterior groundwater drawdown. It has also provided temporary support, which can be completed before excavation, for tunnels extending beneath mainline railroad tracks. It has been used to provide early support for excavations of various shapes, including circular shafts, located near existing structures at shallow depths in a manner similar to that for structural slurry walls. Temporary structures of artificially frozen ground meet safety requirements for some geometric configurations and soil conditions that cannot be met by most other cofferdam methods, even at much higher cost. Increased use of this procedure is enhancing competitiveness, particularly for deeper circular shafts. Because of the significant expense of energy and rental of the refrigeration plant, the economy of this method depends on the duration of construction within the excavation.

Most analysis and design of frozen ground systems are performed by contractors experienced in this type of construction. Some projects have been attempted by contractors with little experience in ground freezing, sometimes with somewhat unsatisfactory results. The purpose of this paper is to summarize the information needed by engineers who consider artificially frozen ground for their projects and to establish minimum performance and monitoring requirements to avoid damage to structures, construction delays, or contractor claims.

There is a lack of accepted minimum requirements for artificially frozen ground. Industry practice for a contractor-designed sheeting and shoring usually requires design by a professional engineer that is submitted for review. Codes limit allowable stresses, and industry standards guide design. Specifications often require that the excavation contractor demonstrate minimum experience. Soil-freezing contractors have widely varying experience, and some are willing to take greater risks than the engineer or owner wants to accept.

Failure of an artificially frozen barrier because of marginal procedures or inadequate knowledge of soil conditions could cause loss of life, subsidence, and damage to adjacent structures or a structure within the excavation. Failure may result in project delay or contractor claims. Catastrophic failures are, in the writers' experience, rare. More common are partial failures due to an unfrozen zone or unplanned delay in forming the frozen structure, sometimes because of equipment breakdown. Minimum performance requirements for a particular project should be tailored to the project's specific needs and be a function of the impact of possible failure.

FREEZING SYSTEM

An installation for ground freezing is composed of a refrigeration plant and a distribution system for controlled circulation of coolant to the ground. Ground-freezing technology was introduced by Poetsch in Germany in 1883. Ground freezing is described in several publications (*1–3*), and only the most common freezing systems are briefly summarized here.

System Components

The most common refrigeration source is a conventional ammonia or freon plant, available in various capacities and typically trailer or skid mounted. It is powered by 100- to 300-hp motors providing freezing capacities ranging between 40 and 120 tons of refrigeration (1 ton of refrigeration =

Mueser Rutledge Consulting Engineers, 708 Third Avenue, New York, N.Y. 10017.

3.5 kW). Rated tonnage for ground freezing is highly dependent on brine temperature and is often based on cooling the circulating brine to −20°C. The evaporating temperature of the refrigerant in the chiller will be about −25°C before this brine temperature is obtained. The authors recommend that this relationship be established as a standard in artificial freezing construction. A refrigeration plant will produce more than twice the rated tonnage during startup when the brine is warm and only 70 percent to less than 50 percent of the rated value after the ground is frozen and brine temperatures are approaching practical lower limits. Rated tonnage also depends to a lesser degree on atmospheric conditions and refrigerant temperature.

It is difficult to establish the rated capacity of the refrigeration plant in the field. Refrigeration plants are often modified and may have replacement components differing from the initial assembly. Although the basic components of an appropriate freezing plant are available from many manufacturers dealing with various aspects of refrigeration, these components are usually selected and assembled by a few refrigeration specialists familiar with the particular design and construction requirements for ground freezing. The contractor should always be required to submit data that clearly establish the manufacturer of the refrigeration plant and its rated capacity.

Several plants can be combined if greater capacity is required for a given project. A backup refrigeration unit should be available during all phases of excavation to ensure stabilization of the frozen ground in case of breakdown. A backup unit should also be required during the initial freeze if breakdown delays cannot be tolerated by the project's schedule.

The refrigeration plant comprises a compressor, a condenser, and an evaporator, shown schematically in Figure 1. The compressor liquifies gaseous refrigerant as it is pressurized to several atmospheres. Pressurization raises the temperature of the refrigerant, which is then cooled as it passes through water-cooled coils in the condenser. The refrigerant next passes through an expansion valve and is sprayed onto the coils of the evaporator. Coolant is chilled as it passes through the evaporator coils, which act as a heat exchanger. The ammonia or freon gas then flows into the compressor, where the cycle is repeated. The refrigeration plant is a closed system in which the ammonia or freon refrigerant is continuously circulated.

In the classic ground-freezing system, the coolant is brine. Generally this is a solution of calcium chloride and water that has a specific gravity of 1.24 to 1.28. The brine is pumped into freeze pipes in the ground by means of a supply header. Freeze pipes that are accessible at only one end, such as in a shaft, contain a concentric feed pipe that supplies chilled brine to the end of the pipe. The chilled brine returns back through the annulus formed by the two pipes, extracting heat from the ground as it flows. Brine can be pumped directly from one freeze pipe into another if both ends of the freeze pipes are accessible, as in a tunnel. The warmed brine is collected in a return header and rechilled at the refrigeration plant. The cycle is then repeated. The freeze pipes and headers form a closed system in which the brine is continuously circulated. Calcium chloride brine begins to gel at about −40°C.

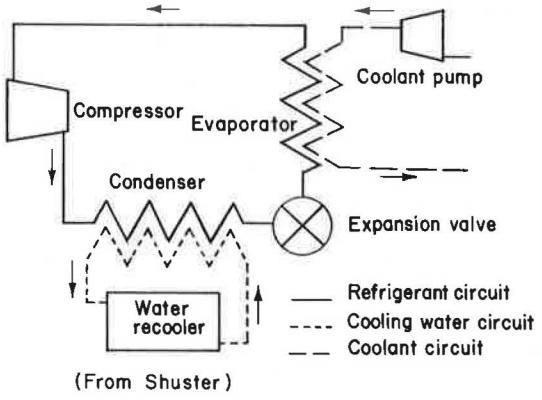

FIGURE 1 Refrigeration plant schematic (*2*).

The closed brine circulation system is simple and is the most commonly used system in ground freezing. Heat transfer is by convection; there is no phase change in the coolant. Time required for freezing is measured in weeks.

Another system that is less frequently used entails the direct injection of a refrigerant, typically liquid nitrogen, into the freeze-pipe assembly, where it evaporates. The resulting gas, still at a very low temperature, is released into the atmosphere. The nitrogen system will freeze soil considerably faster than chilled brine, and the freezing time is typically measured in days rather than weeks. Expandable refrigerants, such as nitrogen, have been used mainly for small projects of short duration or in which emergency stabilization is needed. The principal difficulty with expandable refrigerants is control of the open system. Unconfined venting of the refrigerant often results in a very irregular frozen ground zone. Liquid nitrogen has also been used as a refrigeration plant backup system to cool the brine. This use requires careful control to avoid localized overcooling of the brine.

Other possible freezing systems involve the recovery of evaporated refrigerants and their subsequent reliquification and recirculation. Shuster (*2*) describes these closed refrigeration systems in greater detail. They are not being used at this time.

Freezing Procedures

A wall of frozen ground is created by freeze pipes positioned at a predetermined spacing along the perimeter of the planned excavation. Freeze pipes are generally made of metal and are 80 to 100 mm in diameter. Larger pipe, up to about 250 mm in diameter, is sometimes used, particularly when alignment control is important.

Freeze pipes are installed by either soil removal methods or soil displacement methods. Examples for horizontally installed pipe are (a) rotary wet drilling with following casing, (b) air track drilling with following casing, (c) pipe jacking with interior soil removal, (d) using a pneumatic mole with following casing, (e) using a dry auger with

following casing, (f) jacking closed-end pipe, and (g) using a steerable, larger-diameter casing. It is generally easier to control and adjust the alignment of larger-diameter pipe, so it should be considered for horizontal freeze pipes because alignment control is more difficult in horizontal installations than it is in vertical holes. Vertical pipes are usually installed in holes advanced with drilling mud or wet drilled with a following casing.

Following installation, the actual position of the freeze pipes is measured using inclinometers for vertical holes and deflectometers for horizontal holes. A deflectometer measures angle changes between two sections of small pipe sliding inside the freeze-pipe casing. Inclinometer and deflectometer data are used to determine whether the spacing of adjacent freeze pipes exceeds design values at any point along their length. Additional freeze pipes should be installed where spacing exceeds design values. Use of electronic data collection and modem transmission for microcomputer analysis and plotting of the relative location of a series of freeze pipes at various depths has expedited analysis of inclinometer measurements.

Figure 2 is a cross section through a tunnel showing horizontal freeze pipes and the approximate frozen ground envelope at the critical location directly beneath overlying railroad trackage. The measured deviation of the freeze pipe from the intended position is shown with arrows. Such deviations are typical for most freeze-pipe installations.

Freeze pipes should be pressure tested to check for leaks; then freezing is started by circulating brine through the pipes. Flow through individual pipes should be adjusted with valves to provide equal flow along the frozen ground structure. Bleed-off valves should be provided to remove air from the freeze-pipe system.

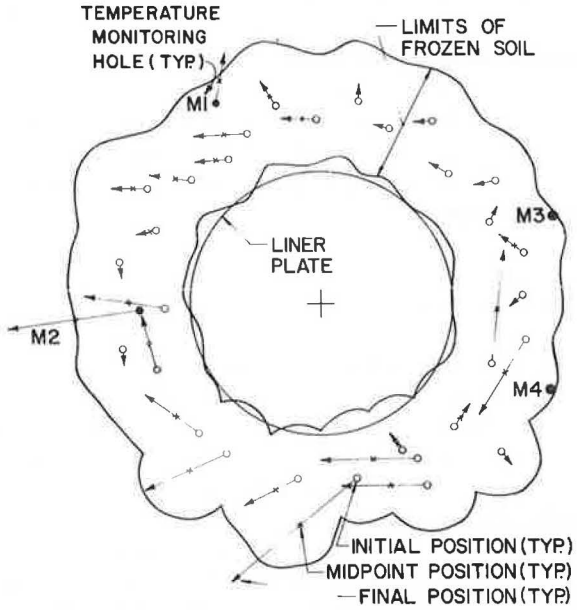

FIGURE 2 Cross-section view through tunnel showing horizontal freeze pipes and approximate frozen ground envelope beneath railroad trackage.

Design of Frozen Soil Walls

Wall thickness is based on limiting stresses in the frozen ground structure. Allowable stress levels are time and temperature dependent. Frozen soil creeps under steady load. Strength is based on plastic failure and Coloumb's law. Deformation is estimated by means of simple equations for creep. Table 1 presents typical frozen-soil properties at −10°C, representing an average soil temperature that varies from about −25°C at the coolant pipe to 0°C at the boundary between frozen and unfrozen soils. These values are not intended to be used for design but to aid in evaluating feasibility of a frozen ground alternative. Formulations for frozen ground strength and deformation are reviewed elsewhere (*4–6*).

Once the design thickness and temperature of the frozen ground wall have been achieved, interior excavation can begin.

HEAVE AND SETTLEMENT

Frost heave and thaw settlement of the ground can be small and, unless carefully measured, may not be noticed during and following construction on artificially frozen ground. However, there have been several projects in which movement of the soil during and following ground freezing has been significant.

Soil movement from ground freezing is generally insignificant in clean sands and very stiff to hard clays, even when the groundwater table is close to the surface. Low-plasticity silts and silty fine sands are much more susceptible to frost heave and postconstruction thaw settlement. Soft clays may not experience large heave but may be subject to significant settlement during thaw.

Soil movement from freezing is caused by two distinct but related phenomena. Frost heave, beyond the small volume increase resulting from the phase change of pore water to ice, is caused by the formation of ice lenses along the freezing front that draw water from nearby, more

TABLE 1 TYPICAL FROZEN-SOIL PROPERTIES

	Sand[a]	Clay
Short-term strength		
Tsf	95–160	50–95
MPa	9.1–15.3	4.8–9.1
Stress causing failure at 60 days of load (%)	±70	±70
Allowable strength at 60 days (% of 1)	30–50	—
Elastic modulus		
Frozen soil		
Tsf	6,000	—
MPa	575	—
Unfrozen soil		
Tsf	500	—
MPa	48	—

[a]Saturated soil (partially saturated soils have reduced strength).

permeable soils by negative water pressure (*7*). Thawing of incompressible soil that has experienced frost heave will result in settlement approximately equal in magnitude to the frost heave caused by escape of thawed water from the ice lenses.

The magnitude of heave due to ice lensing can be estimated from laboratory tests. Frost heave tests are performed by subjecting undisturbed samples to a controlled negative heat gradient with vertical confining pressures approximating in situ values. The sample is frozen while access is allowed to free water at its bottom, which permits the formation of ice lenses. The segregation potential method has been used to estimate frost heave (*8, 9*). The segregation potential of soil is determined by measuring the volume of water absorbed by the soil sample during freezing. The estimated magnitude of frost heave is a function of the segregation potential and soil porosity.

Although this test more closely models freezing from the ground surface down rather than radial freezing from a freeze pipe, it is a way of determining relative heave potential for various soils. The magnitude of frost heave can be minimized by rapidly freezing the ground. Because of time constraints in construction, ground is normally frozen rapidly, thus resulting in minimal ice lensing and small amounts of frost heave.

The second phenomenon occurs when compressible soils with natural moisture contents significantly above their plastic limits are frozen (*10*). Ice lenses form during freezing because of segregation of contained pore and film water within the clayey soils. If there is no external source of water, such ice lensing results in small volume increases and heave. However, significant settlement will occur during thaw when water in the ice lenses escapes. The thawed soil finally reaches a lower water content and is denser than it was before freezing. Freezing, in effect, preconsolidates the soil between ice lenses (*10*). If the soil is also susceptible to frost heave from intake of external water, the two phenomena are additive. Thaw consolidation includes both settlement from frost heave and settlement from freeze-thaw preconsolidation.

The term "thaw consolidation" is really a misnomer, because the actual densification of soil occurs during freezing. However, thaw consolidation becomes evident only when the soil thaws. An example of severe thaw consolidation will be described in detail in one of the case histories presented in the next subsection.

Thaw consolidation can be estimated by measuring thaw strain of samples that had been frozen using a controlled negative heat gradient. Thaw consolidation of clay soil can also be estimated from its plastic limit and natural water content (*10*). Special laboratory testing to determine heave and final settlement potential is normally not required for a project. Tests should be performed, however, in special circumstances, such as a frozen tunnel extending beneath critical structures or highly frost-susceptible soil. Testing may aid in quantifying the risk in employing frozen ground construction and the magnitude of soil movement.

The following case histories are not typical of most frozen ground projects, but are presented to illustrate cases of significant soil movement. In some examples, the movement was anticipated and not detrimental. Heave and thaw consolidation often can be accommodated if anticipated. Projects 3 and 4 demonstrate that potential for thaw consolidation must be given consideration.

Project 1

A 3.3-m-diameter tunnel (*11*) was constructed beneath mainline railroad tracks; the soil above the springline was primarily a cinder fill. Below the groundwater table and springline, the soil was a silty fine sand. The crown of the mined tunnel was less than 2.3 m from the surface, and frozen ground extended to less than 0.6 m from the base of the railroad ties. Horizontal freeze pipes were placed 2.3 to 2.6 m from the tunnel center. Some timber and boulder obstructions were encountered in the cinder embankment fill when freeze pipes were installed. Figure 3 shows typical heave of the tracks and postconstruction settlement. The track was periodically reballasted to compensate for settlement following construction. Settlement continued for approximately 7 months following termination of freezing. Thawing was probably prolonged after shutdown of the freeze units by the cold temperatures during the winter months.

Project 2

A second tunnel, about 30 percent larger in diameter, was recently constructed beneath railroad tracks with the crown of the excavated tunnel about 3.3 m below the ground surface and the frozen ground extending to within about 1.5 m of the base of the railroad ties. Subsoils were composed of silty clay fill extending to approximately the tunnel crown and underlain by soft to hard lacustrine silty clay deposits that extended approximately to the tunnel invert. During installation of the freeze pipes, a shallow, buried stone rubble wall was encountered. An estimate of the probable magnitude of frost heave of the tracks based on the range of soil porosities and the segregation potential determined from laboratory tests is shown in Figure 4. The soil characteristics and laboratory test data indicated a larger potential for frost heave here than in Project 1. This was confirmed by actual measurement of track heave. Rapid soil freezing was required on this project, and the actual magnitude of frost heave is superimposed on the estimated magnitude in Figure 4. Figure 5 gives the typical time rate of heave and postconstruction settlement. Tracks were periodically reballasted to compensate for these movements.

Project 3

A shaft was excavated through 17 m of soft marine clay to the top of glacial till. Nine meters of sand and gravel backfill was placed in the excavation, and a pump station was placed on the top of this backfill. Freeze pipes were

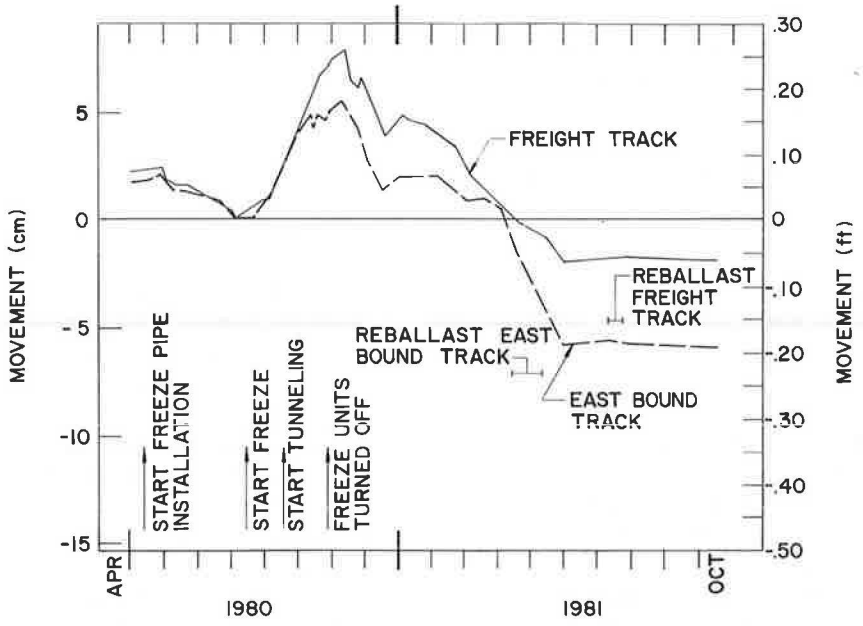

FIGURE 3 Typical heave of tracks and postconstruction settlement.

installed at 0.9-m horizontal spacing in a 16-m-diameter circle to depths of about 21 m to form the artificially frozen ground cofferdam supporting this excavation.

No heaving of the ground surface was observed during soil freezing. Approximately 1 year after construction was completed, settlement of a corner of a one-story building located 3.7 m from the line of refrigeration pipes was noted. Two and a half years later, measured settlement of the ground surface at this location totalled about 0.9 m and was still continuing. One interesting aspect of these measurements is that the most rapid settlement occurred during the last year of measurement. Soil samples obtained more than 3 years after construction revealed that although the soil had completely thawed, some ice lenses were still frozen. It appears that the salty marine clay thawed before the closely spaced ice lenses, which had formed by drawing fresh water from the clay. The fresh-water ice lenses thawed at a higher temperature than the surrounding salty soil. This would explain the relatively slow initial rate of settlement followed by more rapid settlement as the ice lenses thawed.

The soil that had been frozen reached a lower water content and higher strength than adjacent soil that had never been frozen. The decrease in water content in the frozen soils accounted for the total surface settlement. The settlement also caused damage to piping leading into the pump station and as much as 0.4 m of settlement of the pump station because of lateral movement of the supporting sand and gravel fill into the adjacent marine clays that contained thawing ice lenses. Slope inclinometers were used to measure horizontal movement toward the thawing ground from both inside and outside the frozen cylinder.

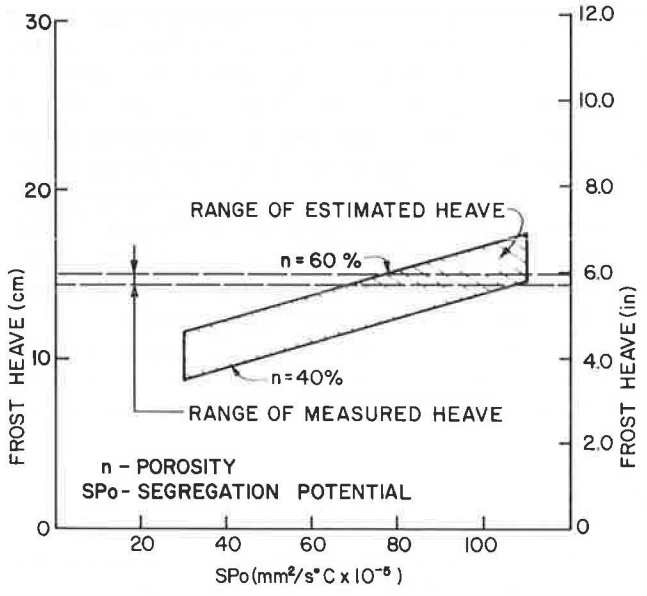

FIGURE 4 Estimated frost heave of tracks based on soil porosities and segregation potential.

Project 4

A second shaft was excavated through medium stiff to stiff clays and silts to a compact sand and gravel layer at 15 m depth. This 29- by 33-m excavation was formed by four parabolic arches that were buttressed at their flat angle corners. The resulting shape approaches a rectangle but has curving walls between corners. There was no noticeable heaving of the ground during freezing; however, no measurements were made. Movement of groundwater from adjacent pumping caused partial wall failure, exposure of freeze pipes, and rupture of brine piping. Automatic shutoff valves minimized brine contamination of the soil. Back-

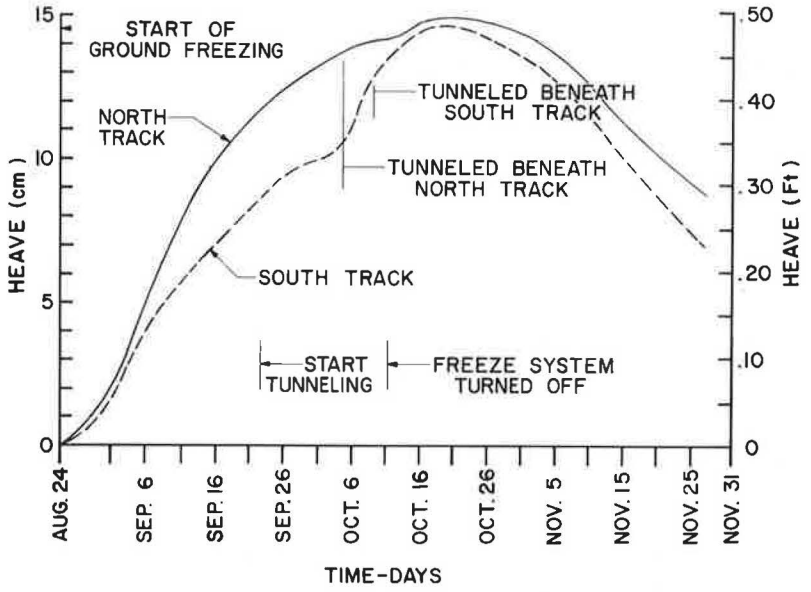

FIGURE 5 Time rate of heave and postconstruction settlement.

filling the hole with loose sand and refreezing the wall to a greater thickness extended the period of freezing substantially. Since completion, there has been nearly 80 mm of settlement of a shallow-supported retaining wall from the new structure across the line of the formerly frozen ground. There is also evidence of pavement cracking and up to 230 mm of pavement settlement, concentrated over the line of the formerly frozen ground. Ground cracks up to 80 mm wide form a circle about 9 m outside the new structure that was constructed in the shaft. Field data indicated that compaction of backfill met normal standards and should not have resulted in such large postconstruction settlement. However, a 1-m-wide band of backfill placed after partial failure was frozen in a loose condition.

REQUIREMENTS FOR ARTIFICIALLY FROZEN GROUND

The following suggested requirements are generalized for average project conditions. Different requirements may be necessary depending on the importance of maintaining a rigid frozen ground structure, the proximity of adjacent structures, and the consequences of failure of the frozen ground structure.

Freeze-Pipe Installation Methods

A variety of freeze-pipe installation methods were described in a previous section. Ground movement during installation of these elements is usually insignificant when pipes are being installed vertically. There is greater potential for ground surface settlement in installing horizontal freeze pipes. This is of particular concern when pipes are passing beneath an existing structure where settlement may be detrimental.

Rotary wet drilling methods should be used, with the casing closely following the drill bit or with drilling mud to stabilize the hole. Soil displacement methods minimize ground settlement, but pipes installed by these methods tend to be more severely misaligned than pipes installed with other methods. Rotary wet drilling must be performed carefully to avoid loss of surrounding soil. Washing a casing into the ground and having the water return outside the casing is generally not permitted for horizontal pipes. Installation of fewer large-diameter horizontal pipes is generally preferable when the pipes are long, when there may be obstructions, and when the soils are variable or dense, because their alignment is easier to control. Smaller-diameter pipes are suitable for lengths less than 30 m in low-strength soils.

Freeze-Pipe Spacing

Pipes for ground freezing are normally spaced 0.9 to 1.2 m apart. A rule of thumb for smaller freeze pipes is that the ratio of spacing to diameter should be ≤ 13. This simple formula appears to apply for pipes that are about 120 mm or less in diameter. The contractor should normally be required to meet this criterion for installed freeze pipes.

Brine Temperatures

Brine temperatures during freezing drop during the first several days of freezing and approach an equilibrium between $-20°$ and $-30°C$. A required brine temperature of $-25°C$ or less is suggested to ensure that the soil is frozen rapidly, which minimizes frost heave and expedites construction. However, temperature requirements will vary with strength requirements for individual structures, which, in turn, vary with soil type and water content.

Size of Refrigeration Plant

Refrigeration plant size in the United States is normally measured in tons of refrigeration. Some ground-freezing contractors prefer to measure plant size in terms of horsepower because rated tonnage is dependent on several factors, including air temperature, relative humidity, and brine temperature.

Typically, about 4 to 7 tons of refrigeration per 93 m^2 of interior frozen ground surface is required to form the wall of shafts. This corresponds to about 0.013 to 0.025 tons of refrigeration per lineal foot of freeze pipe. Tunnels sometimes have a double row of freeze pipes above the springline, and refrigeration requirements have typically been higher. Refrigeration capacity for a particular project depends on many factors, including desired speed of freezing, design temperatures, and so forth. Formulations to estimate tonnage requirements have been presented by Sanger (*5*). About 50 to 70 percent of the estimated tonnage requirement is typically needed to maintain the frozen ground structure after it is formed. Backup units should be made available in case of refrigeration plant breakdown.

Special Design Considerations at Shallow Depths

When the ground around a vertical shaft is frozen, heat from flowing air inhibits freezing near the ground surface. The cylinder of frozen ground around an individual freeze pipe becomes progressively smaller within 0.9 to 1.2 m of ground surface. This tapering can result in incomplete freezing of the soil between freeze pipes at shallow depths. If this unfrozen soil ravels from the top into the excavation, it will expose underlying frozen soil, which may then gradually melt. To alleviate this problem, contractors often install a horizontal freeze pipe along the center line of the vertical pipe ring 0.3 to 0.6 m below ground.

The strength of frozen soil depends on sufficient moisture between the soil grains to form ice bonds. Saturated soil below groundwater normally obtains high strength when frozen. Clay soils above the groundwater table are nearly saturated and normally obtain high frozen strength. Silty soils near the water table usually have high moisture contents as a result of capillarity, and therefore will also have high frozen strengths.

Evaporation at shallow depths tends to dry the soil, often resulting in low frozen strengths. Sands above the water table are normally too dry to form strong ice bonds when frozen, and may require the addition of moisture to obtain adequate frozen strength. This is accomplished by wetting the soil surface from a ditch or by installing slotted polyvinylchloride (PVC) pipe along the circle of freeze pipes to act as a soaker. Excessive application of water will delay formation of the frozen ground wall. Horizontal slotted pipes have been installed above tunnel alignments to add moisture where the groundwater table is low. In one instance (*11*), a bentonite slurry was used to increase moisture in a highly permeable cinder fill when it was found that moisture content was too low and that water drained away too rapidly to obtain the intended frozen strength.

Strength Testing for Design

The strength of the frozen ground is more critical at certain locations. An example would be the need for consistent frozen ground strength across the crown of a tunnel when it is immediately beneath a heavy structure. Other examples include heavy train loads above a tunnel, a highly variable rock level in a large-diameter shaft causing unbalanced loadings, a shaft that has rather flat curvature or straight walls along one or more of its sides, structures that require penetration through frozen ground walls, and curved frozen shaft segments buttressed against separate frozen shafts.

A general knowledge of the soils and their degree of saturation is usually adequate for most projects to estimate frozen soil strength with sufficient accuracy using published information. However, it is sometimes necessary to determine the frozen strength of a particular soil for design of a critical frozen ground structure. It is then necessary to obtain undisturbed samples of the in situ soils for laboratory frozen strength testing.

Strength of frozen ground is generally a function of its temperature below freezing. In other words, frozen soil at −10°C is significantly stronger than frozen soil at −5°C. Frozen soil creeps under load. As a result, strength of frozen ground decreases with time of loading (*11*). The rate of creep deformation is a function of the stress level. Creep parameters can be determined from laboratory testing. Repetitive train loading above a frozen tunnel has been simulated in the laboratory (*11*). High repetitive loads cause creep deformation and a reduction from the short-term strength in a manner similar to a smaller load applied over a long period of time.

Another method of establishing frozen strength and modulus is by artificially freezing a small test section of ground to perform in situ testing (*11*). A soil auger is used to make a hole through the frozen ground, and a pressuremeter appropriate for rock testing is inserted into the hole and expanded against its sides. Results of such tests correlate reasonably well with tests performed on soil samples frozen in the laboratory.

It is sometimes necessary to determine the elastic modulus of both the frozen ground and the surrounding unfrozen soil to analyze the distribution of unbalanced load such as a train or other moving vehicle above a frozen ground tunnel. When the frozen ground structure is close to these moving loads and the track or roadway has heaved during freezing, the dynamic loads will be attracted to the stiff frozen soil structure. The ratio of frozen to unfrozen soil modulus, as determined by laboratory test, is commonly about 12 but could be 40 or more (*11*).

Analyses of stresses within a frozen ground structure can vary from relatively simple empirical methods to elaborate finite-element techniques, which produce detailed contours of stress levels throughout the structure. An

example of the results of the latter type of analysis for the first tunnel project described earlier is shown in Figure 6.

Protection of Frozen Ground Structures

Sunlight and high air temperatures at some sites can thaw frozen ground exposed in an excavation. It is then necessary to protect the frozen ground from deterioration. White plastic or canvas tarpaulins can be draped over exposed areas or foam insulation sprayed on 50 to 75 mm thick and lightly reinforced with wire mesh anchored to the exposed frozen wall.

An important requirement for a frozen ground shaft or tunnel is to prevent surface water from contacting the frozen ground structure. Normal-temperature water flowing over the top of a shaft and into the excavation can rapidly cause the frozen ground to deteriorate. It is necessary to divert drainage around the shaft and prevent inflow if there is a possibility of flooding during wet weather.

Groundwater Control

Artificial ground freezing is often used where the groundwater table cannot be lowered, typically where existing structures are underlain by compressible deposits or where watertight cofferdams cannot readily be installed. Design of frozen ground structures must consider existing groundwater conditions. Frozen ground shafts normally penetrate an aquiclude below the subgrade, if practical. If the shaft extends to or below the bedrock surface, freeze pipes are toed into the rock to ensure a good seal. Bedrock within the shaft can be grouted to minimize water inflow, depending on rock jointing and its permeability.

The stability of soil subgrades in shafts must be analyzed in the same way as that for normal shaft construction. If necessary, underlying aquifers should be depressurized by pumping before excavation. If no aquicludes exist, the shaft interior must be dewatered with wells. Groundwater inflow from below a frozen ground shaft because of a dewatering system malfunction can cause rapid deterioration of frozen ground.

Flowing groundwater will impede formation of the ice wall. If the flow velocity through the soil pores exceeds about 1 to 2 m per day, formation of a continuous frozen ground wall may be inhibited (*12, 13*). This seepage velocity refers to the resultant actual seepage velocity in the soil pores, and not to the superficial velocity as defined by Darcy for flow through soils. Seepage velocity is simply the superficial Darcy velocity divided by the soil porosity.

It is essential to determine the groundwater gradient at a given site and to estimate its magnitude. This can be done by installing several observation wells across the site and measuring areawide water levels. The seepage velocity in an aquifer with known gradient can be estimated if the permeability and porosity of the aquifer are also known.

In a recently completed frozen ground shaft, a window in the frozen ground wall was discovered as the shaft was excavated. The window was attributed to groundwater flow, which prevented closure on the upstream side of the shaft. The window was eventually closed by adding extra freeze pipes and grouting the soil on the upstream side to block water movement through the frozen wall.

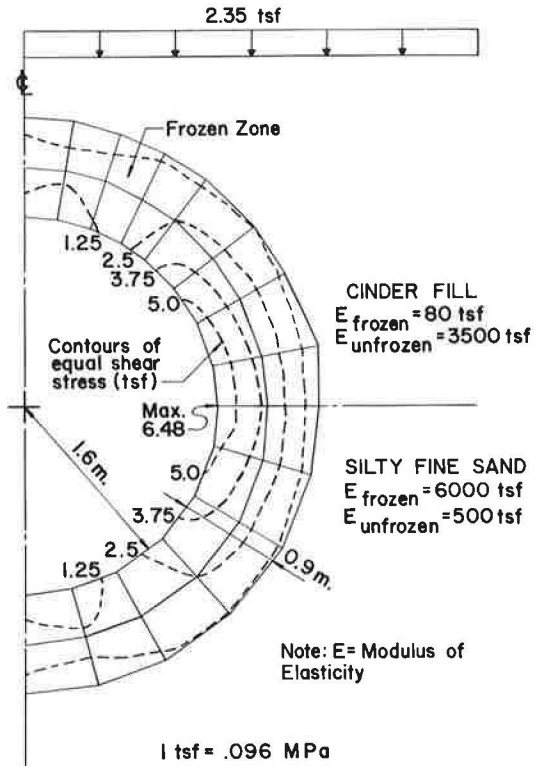

FIGURE 6 Finite-element analysis of tunnel Project 1.

MONITORING

Every frozen ground project should be carefully monitored to evaluate the performance of the system and to track growth and temperature of the ice wall.

For a chilled-brine system, both the brine flow and the brine temperature are normally monitored, as well as ground temperatures within and adjacent to the frozen ground wall. For shafts, the groundwater level inside the frozen ground ring should be monitored for a characteristic rise in interior water level, which indicates closure of the frozen cylinder. Heave and settlement of adjacent and new structures should be monitored by establishing survey points on the structures. Suggested monitoring procedures and requirements for typical projects are outlined in the following paragraphs. Monitoring for any given project will vary depending on site-specific conditions.

Brine Flow

Brine flow into and out of freeze pipes or groups of freeze pipes is measured to identify blockage or air pockets in a

pipe. Air is normally bled from high points on a daily basis to ensure efficient circulation. Brine flow data are used to balance the freezing system; that is, flow into individual freeze pipes or groups of freeze pipes is regulated with valves to ensure approximately uniform rates of growth along the ice wall.

Brine flow rates should, as a minimum, be monitored shortly after startup of the system to check for blockage and to tune the system. Thereafter, the flow rate could be checked periodically. It is also prudent to recheck brine flow shortly before excavation to ensure that there is no blockage and that brine is being distributed evenly to all parts of the frozen ground wall. Brine flow in segments of the system is commonly estimated by measuring brine temperature differences as described in the following subsection.

Brine Temperature

Brine delivery temperatures from the refrigeration plant and brine return temperatures to the plant should be monitored daily. Brine delivery temperatures will drop gradually during the freeze and thereafter stabilize at a temperature largely dependent on the volume of soil to be frozen and the plant capacity. When two or more refrigeration plants are operating together in series, the brine delivery temperature will rise dramatically if one of the plants is shut down temporarily. The difference between brine delivery and return temperatures, indicating the amount of heat transfer, will narrow as the frozen ground wall develops.

It is also instructive to monitor delivery and return temperatures at each freeze pipe or group of freeze pipes. These data can be used to pinpoint inefficient or overcooled pipes. Groundwater flow that is preventing freezing may be identified by large temperature differentials in individual pipes or groups of pipes, indicating a heat source. Brine temperatures in individual freeze pipes or groups of freeze pipes should be measured periodically, and as a minimum, just before excavation.

A temperature profile can also be obtained in a freeze pipe by temporarily disconnecting it from the system and then profiling the temperature of the brine with a thermocouple or other temperature sensor. Usually it is informative to leave individual pipes disconnected for several hours to monitor changes in the temperature profile with time. Warm spots or windows of unfrozen ground can readily be detected by this method. The freeze pipe must be disconnected from the system for a sufficient time to allow the brine temperature in the pipe and the temperature of the surrounding frozen ground to equilibrate. Such temperature profiling is not done routinely but is useful if there is a problem or a suspected problem with a frozen ground wall.

Soil Temperature

Ground temperature measurement by thermocouples in probe holes is the primary control system for ground freezing. Temperature probe holes are not installed until all freeze pipes have been completed and inclinometer surveys have been made in each freeze-pipe hole to measure deviation from the intended position. The probe holes are then installed at locations where freeze-pipe spacing is maximum. Sets of probe holes should be installed at a minimum of two locations; each set should be made up of at least two probe holes. Probe holes are normally positioned midway between freeze pipes and near the center and exterior of the zone to be frozen.

Temperatures should be monitored in each probe hole at given intervals, say every 1.5 to 7 m, with at least one thermocouple located in each soil stratum. Extra ther-

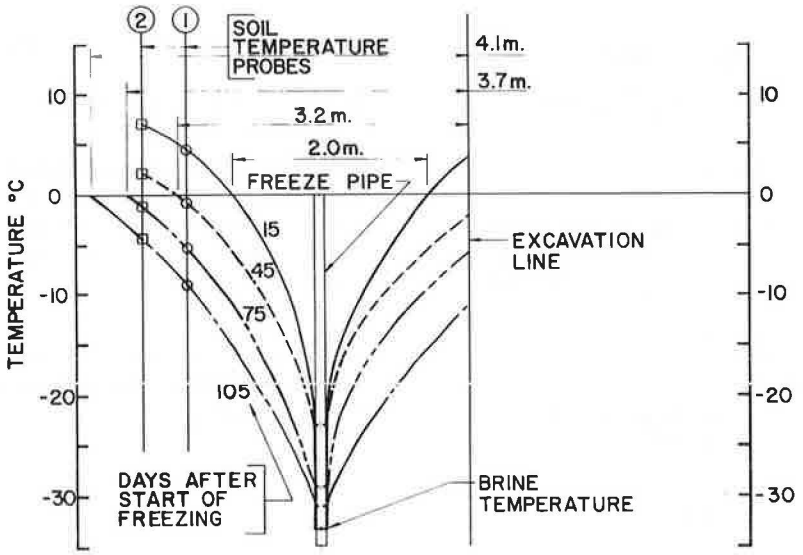

FIGURE 7 Temperature versus radial distance from freeze pipe.

mocouples can be positioned at critical locations, such as where closure is expected to take the longest.

Measured temperatures are plotted versus radial distance from the freeze pipe as shown in Figure 7. These data can be used to estimate the approximate thickness of the freeze wall, as shown. Progressive expansion of frozen ground around a freeze pipe in a shaft is shown in Figure 8. Because the wall thickness will be minimal midway between freeze pipes, this is where the probe holes should ideally be positioned. Electronic data collection of large volumes of soil and brine temperatures is now being used to speed microcomputer evaluation of the variation in temperatures with time and to permit more detailed analysis of the growth of frozen ground with time.

Other methods of determining the thickness of artificially frozen ground include frost indicators and test pits. Both are best suited for shallow frozen ground structures. Simple frost indicators consist of small-diameter (about 25 mm) plastic pipe installed in the ground. A smaller-diameter clear plastic tube, which is filled with a mixture of water and methylene blue, is then inserted into the pipe. As the mixture freezes, the blue fluid turns white. The level of adjacent frozen ground can be determined by periodically removing the insert tubes and measuring the location of the color change. This low-cost measuring device can provide a detailed profile of the freeze boundary.

Test pits can be used to directly determine the limits of frozen ground where it is shallow. This technique is particularly suited to examining the crown of shallow frozen ground tunnels. Test pits allow direct visual examination of the extent and quality of frozen soil.

Locations of temperature probe holes may be dictated by special conditions of the project. For a tunnel excavation, for example, the thickness and temperature along the crown would be of primary importance, because this area may carry heavy loads. In a tunnel project recently constructed beneath railroad tracks, four horizontal temperature probe holes were specified to be distributed across the tunnel crown to the springline. Vertical temperature probes and frost indicators were also used to measure the top of the frozen tunnel at regular intervals.

Another example is where known groundwater flow conditions exist. Under these circumstances, it is most important to place probe holes on the up-gradient side of the frozen barrier. In a recent frozen-shaft project, for example, temperature probes were placed at the widest freeze-pipe spacing, which happened to be on the downstream side of the groundwater flow. A window in the ice wall, apparently caused by the flowing groundwater, was discovered only after excavation had begun. This window might have been discovered earlier and a blow-in prevented had temperature probes been placed on the upstream side of the shaft.

Settlement

Ice lensing and resulting heave and thaw consolidation and settlement are most severe for silt-sized soil. Because of potential heave and settlement, survey monitoring points should be established before construction on all nearby structures and major utilities, including new structures after their completion. These survey points should be monitored periodically during ground freezing and subsequent thaw.

MINIMUM DATA NEEDED BY CONTRACTOR

For proper design of a frozen ground structure, the exploration should meet normal requirements for the particular project, including number and type of borings, undisturbed samples, groundwater measurements, and so on. Obstructions should be identified, because they may slow installation of freeze pipes and affect the cost of construction and the schedule.

Of great importance in ground freezing is the water content of the soils to be frozen, particularly cohesive soils. A large amount of heat energy must be removed to change pore water to ice, and freezing typically develops slowest in high-water-content cohesive soils. Of secondary importance is the density of the soils to be frozen. This can readily be determined by measuring and weighing undisturbed samples of cohesive soils. As a minimum, the water content of each soil type encountered in the exploration should be determined. Densities of cohesive soils should also be measured directly if they cannot be reliably es-

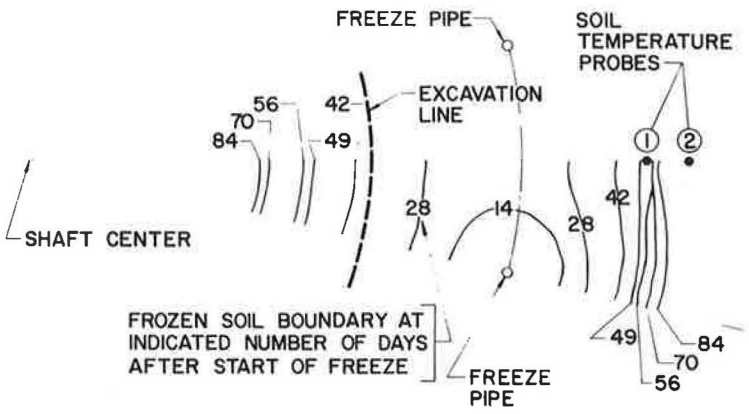

FIGURE 8 Progression of frozen ground around freeze pipe in shaft.

timated. Densities of granular deposits can generally be estimated with sufficient accuracy. The degree of saturation of granular soils above the water table should be determined.

A detailed investigation should be made of groundwater conditions to determine the gradient across the site as well as the grain size and permeability of each aquifer. These data are used to estimate seepage velocity through the soil pores. Temperature of the ground and groundwater should also be determined. If ground freezing is contemplated during design, consideration should be given to obtaining undisturbed samples of critical strata for laboratory testing of both frozen and unfrozen strength and deformation. Frost heave and thaw consolidation tests should be performed if heave or settlement will adversely affect existing or new structures.

CONCLUSIONS

Use of artificially frozen ground to provide temporary support of excavations has increased in the United States in recent years. It is commonly used for projects on which it is required that support be completed before excavation and on which the water table must not be depressed during construction. Ground freezing is occasionally specified for a project, but more commonly it is proposed and designed by the contractor when project requirements make this method of temporary support cost-effective.

This paper establishes general performance and monitoring requirements for artificial ground freezing. These are intended to enable the engineer to review a proposed frozen ground design for a particular project.

Artificial ground freezing has been successfully used for numerous projects. Nevertheless, unexpected problems have occurred even on successful projects. Examples of possible problems are presented. These can generally be anticipated by thorough subsurface investigation at the project site.

REFERENCES

1. J. P. Powers and D. Maishman. Ground Freezing. In *Construction Dewatering: A Guide to Theory and Practice,* Chap. 20, John Wiley & Sons, New York, 1981, pp. 349–359.
2. J. A. Shuster. Controlled Freezing for Temporary Ground Support. In *Proceedings, North America Rapid Excavation and Tunneling Conference,* Chicago, Ill., June 1972, pp. 863–895.
3. A. R. Jumikis. *Thermal Soil Mechanics.* Rutgers University Press, New Brunswick, N.J., 1966.
4. F. J. Sanger. Ground Freezing in Construction. *Journal of the Soil Mechanics and Foundations Division,* ASCE, Vol. 94, No. SM1, Jan. 1968.
5. F. J. Sanger and F. H. Sayles. Thermal and Rheological Computations for Artificially Frozen Ground Construction. Presented at International Symposium on Ground Freezing, Germany, March 1978.
6. J. M. Konrad and N. R. Morgernstern. A Mechanistic Theory of Ice Lens Formation in Fine Grained Soils. *Canadian Geotechnical Journal,* Vol. 17, 1980, pp. 473–486.
7. J. M. Konrad and N. R. Morgernstern. The Segregation Potential of a Freezing Soil. *Canadian Geotechnical Journal,* Vol. 18, 1981, pp. 482–491.
8. J. F. Nixon. Field Frost Heave Predictions Using the Segregation Potential Concept. *Canadian Geotechnical Journal,* Vol. 19, 1982, pp. 526–529.
9. .J. F. Nixon. Field Frost Heave Predictions Using the Segregation Potential Concept. *Canadian Geotechnical Journal,* Vol. 19, 1982, pp. 526–529.
10. E. J. Chamberlain. Overconsolidation Effects of Ground Freezing. In *Proceedings of Second International Symposium on Ground Freezing,* Trondheim, Norway, 1980, pp. 325–337.
11. H. S. Lacy, J. S. Jones, and B. Gidlow. Tunnel Constructed Through Cinders By Ground Freezing. In *Proceedings of Third International Symposium on Ground Freezing,* June 1982, pp. 389–396.
12. T. Takashi. Influence of Seepage Stream on the Joining of Frozen Soil Zones in Artificial Soil Freezing. In *Special Report 103,* HRB, National Research Council, Washington, D.C., 1969, pp. 273–286.
13. H. T. Hashemi and C. M. Sliepcevich. Effect of Seepage Stream on Artificial Soil Freezing. *Journal of the Soil Mechanics and Foundations Division,* ASCE, Vol. 99, No. SM3, March 1973.

Publication of this paper sponsored by Committee on Frost Action.

Behavior of Frozen and Unfrozen Sands in Triaxial Testing

H. YOUSSEF AND A. HANNA

Frozen and unfrozen soils are natural composite materials composed of soil particles and voids that can be partly or totally filled with ice or water. When the temperature of the soils decreases below 0°C, its water phase crystallizes to ice, which changes its mechanical behavior. The purpose of this paper is to present the results of an experimental investigation of the behavior of frozen and unfrozen sands in triaxial testing. The results are presented in the form of a comparative analysis of the relationships among stress, strain, and volume change of these materials tested under the same conditions of confining pressure and strain rate. In the conclusion, emphasis is given to structures that are usually subjected to such changes in behavior because of seasonal temperature changes.

Because of the high viscosity of intergranular ice, the strength of frozen sand is due to its ice cohesion as well as its frictional components. This strength is time dependent; unfrozen sand is a cohesionless material, and because of the low viscosity of the intergranular water, its shear behavior is basically time independent.

Triaxial testing of frozen sands is essentially of one type—closed-system conditions—because the intergranular ice is not free to move out of the samples during testing in shear. However, these samples exhibit volume changes (*1–3*). Triaxial testing of unfrozen sands is mainly of two types (*4, 5*): drained and undrained.

This paper presents the basic difference between the mechanical behavior of unfrozen sand and its state when it is frozen to −5°C during triaxial testing.

TERMINOLOGY

The following terms are used in this paper:

C = cohesion component of shearing resistance of frozen sands,
D_r = relative density,
DU = unfrozen sand sample tested in drained conditions,
e = voids ratio,
F_S = frozen soil sample,
n = porosity,
p = hydrostatic (normal) stress = $\frac{1}{2}(\sigma_1 + \sigma_3)$,
q = shear stress = $\tau = \frac{1}{2}(\sigma_1 - \sigma_3)$,
S_i = degree of saturation of ice,
S = degree of saturation of water,
US = unfrozen sand sample tested in undrained conditions,
U_f = pore-water pressure at failure,
V_s = volume of sand grains in the frozen sample,
V_i = volume of ice in the frozen sample,
W_i = ice content,
W = water content,
ε_{if} = axial strain corresponding to the peak stress,
ε_v = volumetric strain,
ε_1 = axial strain rate,
ϕ = angle of shear resistance,
γ_T = total unit weight,
γ_D = dry unit weight,
τ_{oct} = octahedral shear stress = $(\frac{2}{3})\frac{1}{2}(\sigma_1 - \sigma_3)$, and
σ_{oct} = octahedral normal stress = $\frac{1}{3}(\sigma_1 + 2\sigma_3)$.

EXPERIMENTAL STUDY

A series of triaxial tests was performed on frozen and unfrozen cylindrical samples of silica sand (average grain size, 0.06 to 0.80 mm) with nominal dimensions of 38.10-mm diameter by 76.20-mm length. The physical properties of the tested samples are reported in Tables 1–3 (*2, 6*), from which it can be seen that the voids ratio for both frozen and unfrozen samples varies in the same range of 0.53 to 0.72. This permits the use of these samples to perform a quantitative comparison between frozen and unfrozen test results.

The testing procedures carried out on unfrozen soils followed the conventional methods described by Bishop and Henkel (*4*) and Bowles (*5*). The procedures followed for sample preparation and testing of frozen sands were essentially the same as those utilized at the U.S. Army Corps of Engineers Cold Regions Research and Engineering Laboratory (*7*) and modified by Youssef (*2, 3*); the tests were performed at a temperature of −5°C. The test results are summarized in Table 4. Typical test results for frozen and unfrozen sands are shown in Figures 1–3.

ANALYSIS OF TEST RESULTS

Referring to Table 4 and Figure 1, it can be observed that the short-term strength is influenced to a high degree by

Department of Civil Engineering, Concordia University, 1455 de Maisonneuve Boulevard West, Montreal, Quebec H3G 1M8, Canada.

TABLE 1 PHYSICAL PROPERTIES OF FROZEN SANDS (*2*)

Test Number	Void Ratio, e	Ice Content, W_i %	Degree of Saturation S_i %	Volume of Sand Grains, $V_s \times 10^{-6}$ m^3	Volumetric Ratio of Ice to Sand Grains, V_i/V_s	Total Unit Weight, γ_T kN/m^3	Dry Unit Weight γ_D kN/m^3
FS 1	0.6	21	95	54	0.6	19.6	16.3
FS 2	0.6	20	98	54	0.6	19.9	16.5
FS 3	0.7	22	92	50	0.6	19.0	15.7
FS 4	0.6	21	95	54	0.6	19.5	16.2
FS 5	0.7	28	92	50	0.6	19.3	15.9
FS 6	0.7	22	99	53	0.7	19.6	16.0
FS 7	0.6	19	94	52	0.5	19.9	16.8
FS 8	0.7	20	90	53	0.6	19.3	16.0
FS 9	0.7	20	90	53	0.6	19.3	16.0
FS 10	0.6	21	93	55	0.6	19.5	16.2
FS 11	0.7	23	100	55	0.7	19.7	16.1
FS 12	0.6	21	94	55	0.6	19.5	16.1
FS 13	0.6	20	93	55	0.6	19.6	16.3
FS 14	0.7	21	93	52	0.6	19.3	15.9
FS 15	0.6	19	93	56	0.5	20.0	16.8

TABLE 2 PHYSICAL PROPERTIES OF CONSOLIDATED DRAINED UNFROZEN SANDS (*6*)

Test No.	Dry Unit Weight γ_D kN/M^3	Void Ratio, e	Porosity n %	Relative Density D_r %	Cell Pressure σ_3, kPa	Deviator Stress $(\sigma_1-\sigma_3)_f$ kPa	Volumetric Strain ε_{vf}%	Axial Strain ε_1%	Angle of Shearing Resistance ϕ^omax
DU 1	17	0.6	37	78	167	557	1	4	38
DU 2	17	0.6	39	68	334	997	1	4	36.
DU 3	17	0.6	38	75	434	1234	1	5	34.
DU 4	17	0.6	39	71	167	667	1	6	37
DU 5	16	0.7	42	45	334	848	0.4	8	34
DU 6	18	0.5	35	93	167	512	2	3	39
DU 7	18	0.5	35	92	334	1083	1	4	38
DU 8	18	0.6	36	88	434	1339	1	4	38
DU 9	17	0.6	38	73	334	1001	1	3	37
DU10	18	0.5	35	93	434	1419	1	4	39

TABLE 3 PHYSICAL PROPERTIES OF CONSOLIDATED UNDRAINED UNFROZEN SANDS (*2*)

Test No.	Void Ratio, e	Water Content, W %	Degree of Saturation S %	Volume of Sand Grains, $V_S \times 10^6$ m^3	Vol. Ratio of Water to Sand, V_W/V_S	Total Unit Weight γ_T, kN/m^3	Dry Unit Weight γ_D, kN/m^3
US1	0.7	25	98	67	0.7	19.7	15.80
US2	0.6	24	99	69	0.6	20.0	16.30
US4	0.7	24	99	71	0.6	20.0	16.00
US5	0.6	22	99	70	0.6	20.4	16.80
US6	0.6	21	100	72	0.6	20.6	17.00
US7	0.7	25	100	68	0.7	20.0	16.00
US8	0.6	23	100	69	0.6	20.3	16.50
US9	0.6	23	100	69	0.6	20.3	16.60
US10	0.6	24	99	69	0.6	20.0	16.20
US11	0.7	25	100	68	0.7	19.9	15.90
US12	0.8	25	99	68	0.7	19.8	15.80

TABLE 4 TEST RESULTS: FROZEN SANDS (*2*)

Test Conditions				Maximum Stresses, kPa						
Test No.	Strain Rate, $\varepsilon \times 10^{-5}$ sec^{-1}	Failure Strain, ε_f %	Confining Pressure σ_3 kPa	$(\sigma_1 - \sigma_3)$	σ_1	(σ_1/σ_3)	τ_{oct}	σ_{oct}	p	q
FS1	3.20	4	277	9100	9381	33.35	4290	3315	4831	4550
FS2	3.25	4	138	8041	8182	58.03	3791	2821	4162	4021
FS3	3.40	3	345	5057	5409	15.37	2384	2038	2880	2528
FS4	161.00	2	448	11440	11893	26.02	5391	4269	6175	5718
FS5	170.00	3	448	10200	10656	23.32	4808	3857	5557	5100
FS6	162.00	2	448	10510	10967	24.00	4954	3960	5712	5255
FS7	3.50	4	448	9590	10047	21.99	4520	3653	5252	4795
FS8	3.25	3	448	7180	7637	16.71	3384	2850	4047	3590
FS9	3.25	3	448	7030	7430	16.38	3314	2800	3972	3515
FS10	3.20	3	448	7235	7692	16.83	3410	2869	4074	3617
FS11	3.20	5	448	10543	11000	24.07	4922	3938	5678	5221
FS12	3.20	5	138	8488	8629	61.20	4001	2970	4385	4244
FS13	3.20	4	277	7859	8141	28.87	3705	2901	4211	3930
FS14	3.30	5	553	11190	11749	20.87	5273	4292	6156	5593
FS15	3.25	2	448	5618	6075	13.29	2649	2330	3266	2809

the applied strain rate (ε_1) and the level of confining pressure (σ_3). In addition it is a function of its physical properties, mainly the initial voids ratio (e_i) and the degree of saturation. The effect of the applied strain rate on the strength of the frozen sand is noted by comparing Samples FS4 and FS10, both of which have similar physical properties (Table 1) and are subjected to identical testing conditions of confining pressure and temperature (Table 4). Sample FS4 was tested under an applied strain rate of 1.61×10^{-3} sec^{-1}, whereas Sample FS10 was tested at a strain of 3.19×10^{-5} sec^{-1}. The resulting shear stress ratio is $\tau_4/\tau_{10} = 1.58$, which indicates that the higher the strain rate, the higher the peak shear strength of the tested frozen sand. This is due to the high viscosity of the intergranular ice phase.

The variation of the voids ratio influences the shear strength of frozen sands. In general, the smaller the voids ratio, the higher the shear strength, as shown in Tables 1 and 4.

The increase of the confining pressure from 345.31 to 552.30 kPa (Tests FS3 and FS14) causes an increase in the shear strength of 22 percent. This is in agreement with Goughnour and Andersland (*8*) and Chamberlain et al. (*9*), who found that increasing the confining pressure increases the strength of the sand. This is due to the fact that increasing the confining pressure causes the sand particles to be held in more intimate contact, which makes the grain boundary adjustment more difficult and consequently increases the intergranular strength.

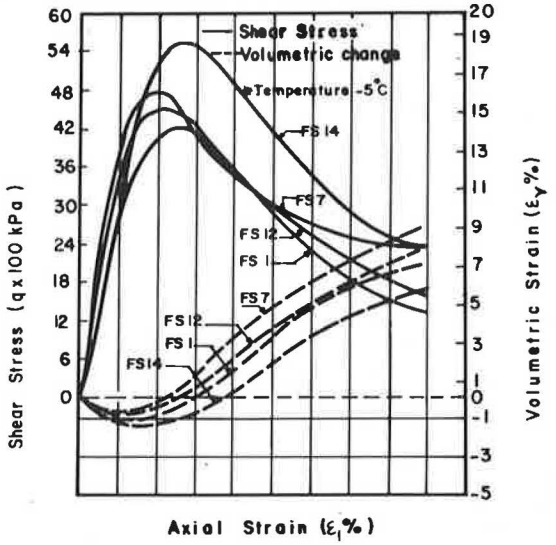

FIGURE 1 Test results for frozen sands.

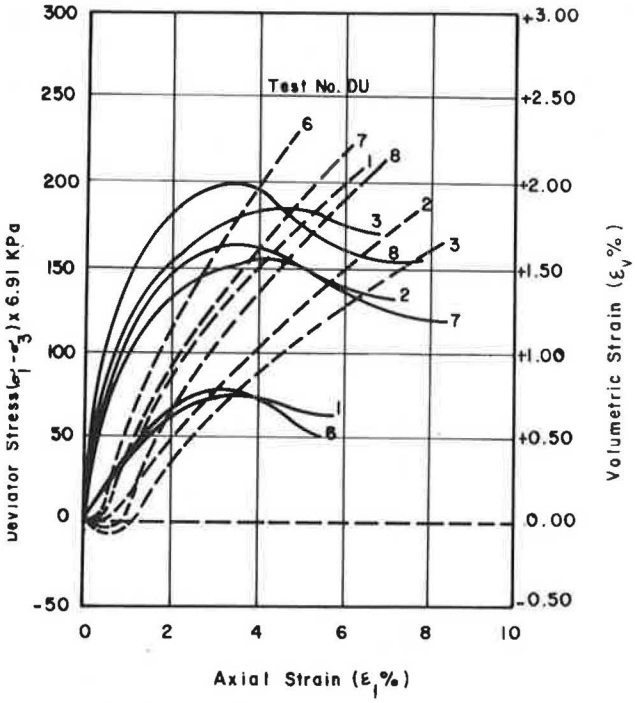

FIGURE 2 Test results for drained unfrozen sands.

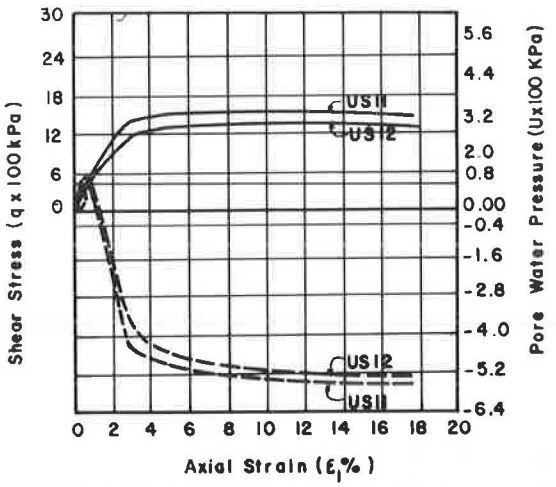

FIGURE 3 Test results for undrained unfrozen sands.

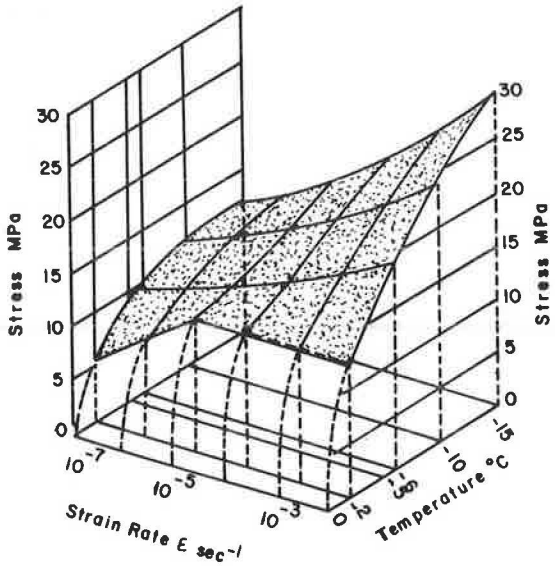

FIGURE 4 Variation in strength of frozen sand with temperature and applied strain rate ε_1 [after Parameswaran (*10*)].

The influence of the degree of saturation (S_i) on the shear strength can also be traced from Table 4. The higher the degree of saturation, the higher the shear strength of the frozen sands. As previously mentioned, the increase in the shear strength because of the increase in the degree of saturation is attributed to the increase in the area of contact between the sand particles and the ice. This in turn causes intensification of the cementation bond.

As can be seen in Figure 1, the volumetric change behavior for all samples was tested under frozen conditions. The volume initially decreases with an increase in the axial strain; it shows a rapid increase up to the failure strain; then it continues to increase with a milder slope to the end of the test (strain level, 20 percent).

The stress-strain behavior shows one peak at a strain level in the range of 3.94 to 5.30 percent, depending on the applied confining pressure, strain rate, and physical properties of the sample (see Table 4 and Figure 1). In general, the applied strain or deformation rate affects the magnitude of the failure strain because of the high viscosity of the intergranular ice in the frozen sample.

Parameswaran (*10*) presented the dependence of the uniaxial strength of frozen soils as a function of temperature and strain rate (Figure 4). As can be seen from this diagram, increasing the confining pressure as well as decreasing the temperature results in increasing the frozen soil strength.

The test results of drained unfrozen sand (Figure 2 and Tables 2 and 5) show that increasing the confining pressure increases the drained shear strength. The failure strain (ε_{1f}) varies from 2.95 to 8 percent depending on the voids ratio after consolidation (e) and the applied confining pressure (σ_3). The maximum deviatoric stress was taken as the failure criterion, which was similar to those for frozen and undrained unfrozen results. The maximum deviatoric stress ($\sigma_1 - \sigma_3$) at failure depends on the voids ratio (e), and the confining pressure (σ_3) varies from 512.08 to 14.53 kPa. The volumetric strain (ε_v) during the shearing stage initially shows compressive behavior at small strain levels up to and close to an axial strain of 1 percent and then starts to increase progressively as the samples dilate, first with

TABLE 5 TEST RESULTS: DRAINED UNFROZEN SANDS (*6*)

Test Conditions*				Maximum Stresses, kPa						
Test No.	Axial Strain ε_1 %	Vol. Strain ε_v %	Confining Pressure σ_3 kPa	$(\sigma_1 - \sigma_3)$	σ_1	(σ_1/σ_3)	τ_{oct}	σ_{oct}	p	q
DU1	4	1	167	557	724	4.34	262	353	445	279
DU2	4	1	334	997	1030	3.10	469	566	682	498
DU3	5	1	434	1234	1668	3.85	581	845	1051	617
DU4	5	1	167	667	834	5.00	314	389	500	334
DU5	8	0.40	334	848	1181	3.54	399	616	607	424
DU6	3	2	167	512	679	4.10	241	338	423	256
DU7	4	1	334	1083	1417	4.25	510	695	875	541
DU8	4	1	434	1339	1773	4.10	631	880	1103	670
DU9	3	1	334	1001	1334	4.00	471	667	834	500
DU10	4	1	434	1419	1852	4.27	668	907	1143	709

* Strain Rate $[\varepsilon] = 0.25 \times 10^{-5}$ sec^{-1}

TABLE 6 TEST RESULTS: UNDRAINED UNFROZEN SANDS (*2*)

Test	Test Conditions			Maximum Total Stresses [KPa]						
Number	ε_1%	σ_3	U_b	$[\sigma_1 - \sigma_2]$	σ_1	p	q	σ_{oct}	σ^{oct}	σ_1/σ_3
US 1	13	277	504	1984	*2765	1773	992	1442	935	3.54
					**2260	1268				
US2	8	277	804	2669	3750	2415	1334	1971	1259	3.47
					2946	1346				
US3	7	448	602	3038	4089	2570	1519	2064	1432	3.89
					3487	1968				
US4	7	448	602	3006	4056	2553	1503	2051	1417	3.86
					3453	1951				
US5	4	448	601	3304	4354	2702	1652	2151	1558	4.15
					3752	2100				
US6	21	448	906	2960	4314	2834	1480	2341	1395	3.19
					3408	1929				
US7	19	139	600	1915	2654	1696	958	1377	885	3.59
					2053	1096				
US8	14	138	600	2088	2826	1783	1044	1435	984	3.83
					2226	1182				
US9	20	277	600	2503	3380	2128	1251	1711	1179	3.85
					2779	1528				
US10	7	552	501	3062	4115	2584	1530	2073	1443	3.90
					3614	2084				
US11	8	552	501	2668	3722	2388	1334	1943	1258	3.53
					3222	1887				

* values do include U_b

** values do not include U_b

a relatively steep slope up to the strain level (ε_{1f}) (corresponding to the sample shear strength) followed by a milder slope of increase to the end of the test. The values of (ε_v) at failure vary from 0.40 to 1.50 percent, depending on (e_1) and (σ_3). In general, the volumetric strain at failure decreases with an increase in the confining pressure because of the decrease in the interlocking of the sand particles and also with the increase in porosity for the same confining pressure. The denser the sample, the higher the dilatancy (interlocking among particles) observed.

As can be seen from the typical results of tests on undrained unfrozen sands (Table 6 and Figure 3), the shear stress increases up to a strain level of 6.67 percent (Test US10) and then decreases slightly. The residual stress at a strain level of 20 percent is more than 90 percent of the maximum strength. The pore-water pressure initially displays a small increase at a small strain level of less than 1 percent and then decreases as the sand particle skeleton tends to dilate. This is typical behavior for dilatant soils. The current experimental results (*2*) support the results obtained by Atkinson and Bransby (*11*) on medium dense (e = 0.75) brasted sand tested at a confining pressure (σ_3) of 73 kPa (0.744 kg/cm^2). It should be mentioned that the particle size and shape (round or angular), as well as the arrangement of the sand particles inside the sample (sand structure), also affect stresses and pore-water pressures.

COMPARATIVE STUDY BETWEEN FROZEN AND UNFROZEN SAND

The changing ground temperature in seasonally frozen geographical areas changes the mechanical behavior of the soil. It is important to know the effect of freezing and thawing of the water in the ground on the shear stress-strain volume change behavior of the soil. This mechanical behavior of the soil provides the basis for design and construction of structures built on seasonally frozen ground.

This section presents a comparative study of frozen and unfrozen sand. Figure 5 shows the shear stress and strain curves for both frozen and water-saturated sands (samples FS8, US6, FS9, and US4). In general, the shear strength of frozen sand is much higher than that of unfrozen sand. Freezing the water-saturated sand, even at a temperature of −5°C, will result in an increase of the shear strength by a factor of more than 2.5 and increase its modulus of

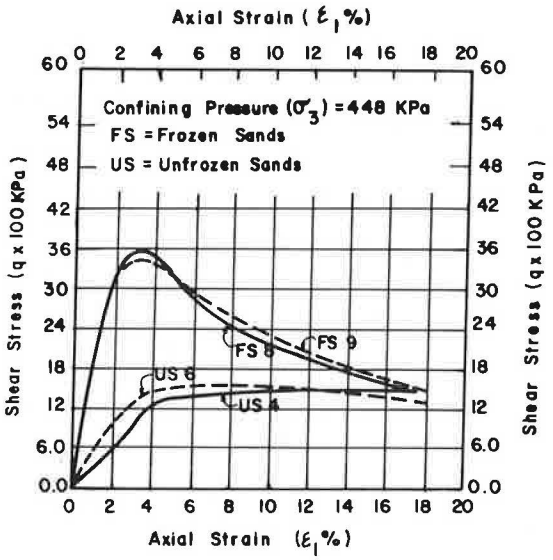

FIGURE 5 Shear stress and strain curves for frozen and unfrozen sands.

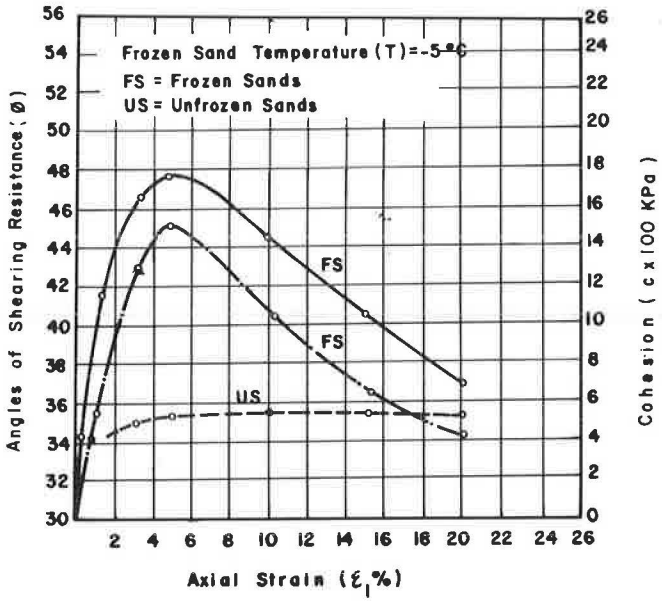

FIGURE 6 Shear strength components of sands versus strain.

elasticity by a factor of about 4. Transformation of the water to its solid state (ice) increases the brittleness of the sand samples.

The residual strength (at 20 percent strain or higher) of frozen sand approaches that of unfrozen soil. This indicates that at higher strain levels (longer time duration of loading), the contribution of the ice matrix to cohesion and friction will decrease to a negligible value. The higher strength of the frozen samples is due to the contribution of the intergranular ice shear strength. Because of the high viscosity of the ice inclusion, the strength of the frozen sample can be made higher by increasing the strain rate during testing.

The variation in the frictional and cohesion components of the shear strength is shown in Figure 6 as a function of strain. The apparent average cohesion of frozen sand (ice cohesion) increases rapidly to 15.30 kg/cm^2 (1.50 MPa) at an average strain level of 4.60 percent and then decreases rapidly to 4.38 kg/cm^2 (0.43 MPa) at a strain level of 20 percent. Because unfrozen sand samples are cohesionless materials, the contribution of the cohesion in the strength of frozen sands is solely due to the intergranular ice, which acts as a cohesive bond.

The variation of the effective angle of friction (ϕ) for frozen and unfrozen sand samples is also shown in Figure 6 for comparison purposes. The friction angle of frozen sand increases to 47.70 degrees and then decreases to 36.93 degrees at a strain level of 20 percent. It could be noted that at higher strain levels, the angle ϕ approaches that for unfrozen sand (ϕ = 35.43 degrees), and the value of cohesion approaches zero. This indicates that at higher strain levels (i.e., with the passing of time) the contribution of the ice matrix to the shear strength for both friction and cohesion components appears to dissipate, and the shear strength of the frozen sand tends to approach the values for unfrozen undrained tests.

Figure 7 shows typical volume change behavior during triaxial testing on frozen and unfrozen sands. It can be seen that the apparent volume change behavior of both frozen and unfrozen sands is similar; it first starts to decrease and then increases progressively until the end of the test. However, the mechanisms of deformation are different for frozen and unfrozen sands.

Very little work has been reported on triaxial testing of frozen soils with volume change (*7*) because of the assumption that frozen soils are tested in closed systems (similar to the undrained tests of unfrozen sands). Furthermore, because of the high viscosity of ice, it is not free to move in or out of the samples during shearing. Goughnour and Andersland (*8*), O'Connor (*12*), and Lade et al. (*1*) have presented data on volume change measurements of frozen soils; however, the mechanism controlling the behavior of this composite material was not explained. On the basis of results of compression and triaxial tests on frozen samples tested with and without a rubber membrane (*2, 3*), it was concluded that the initial volume decrease is due to the compressibility of both the frozen sample and the air bubbles entrapped between the rubber membrane and the sample (which are very difficult to avoid in testing of frozen soil). In addition, the volume increase is due to initiation and progress of cracks in the frozen soil.

APPLICATIONS

The objectives of this paper are to present the results of an experimental investigation of frozen and unfrozen sands using triaxial equipment and to report on the changes in the mechanical behavior of unfrozen soils caused by freezing. The results of this study demonstrate the advantages of freezing soils for construction purposes. As can be seen from Figure 5, freezing the ground, even at a temperature of -5°C, results in an increase of the shear strength by a factor of more than 2.50. The study also shows (Figure 4) that the strength of frozen sand increases because of the decrease in temperature. In essence, artificially freezing the ground to a very low temperature (-196°C can be achieved by utilizing liquid nitrogen) will sharply increase the strength of the soil to the strength of rock or concrete. Thus, one of the advantages of ground freezing for construction purposes is the ability to use the ground itself (outside the cold regions) as a temporary construction material, for example, in building retaining walls, deep mine shafts, and tunnels. This will simplify the site work, cut construction costs, and reduce construction time.

CONCLUSIONS

This paper describes the changes in shear stress and strain and the volume change of sand in its thawed and frozen states. Emphasis is given to the mechanical behavior of particulate and composite materials during shearing in triaxial apparatus. It was possible to show from the experimental results that freezing water-saturated sand to -5°C

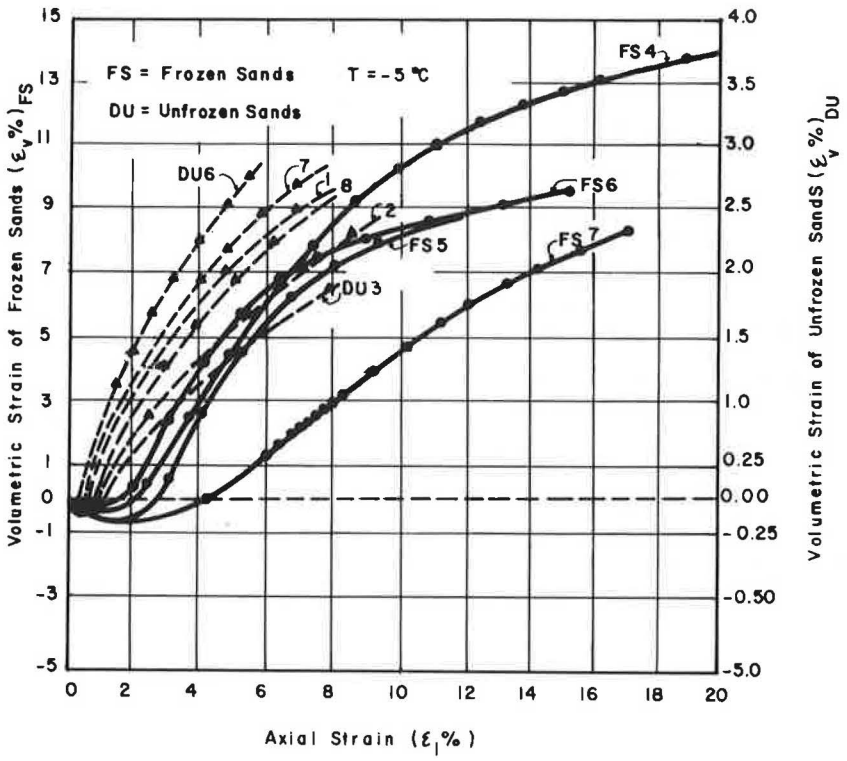

FIGURE 7 Comparison of volume change between frozen and unfrozen sands.

increases its shear stress and modulus of elasticity by factors of 2.50 and 4.00, respectively, compared with unfrozen samples. This increase is time (strain-rate) dependent: the faster the strain rate, the higher the shear strength. This is due mainly to the high viscosity of ice. In addition, as shown by the shear stress and strain curves, freezing the sand causes more brittle behavior. Water-saturated sands compress when subjected to isotropic consolidation, whereas this effect is almost negligible for a sand-and-ice system, especially when subjected to a relatively low confining pressure.

During the shearing stage under triaxial stress conditions, unfrozen (and relatively dense) sands subjected to low confining pressures show initial compression at lower strain levels followed by a volume increase because of dilatancy (interlocking among particles).

Under the same stress conditions, frozen sands exhibit apparent similar volume change behavior during shearing. An initial decrease in volume is observed, followed by progressive volume increases until the end of the test.

From the analysis of these test results, it was possible to illustrate the influence of the voids ratio and the applied confining pressures on the magnitude of the volume increase of water-saturated sands. For the same voids ratio, increasing the confining pressure decreases the dilatancy, and for the same confining pressure, increasing the porosity also decreases the dilatancy. It was possible to separate the ice cohesion component of strength and the frictional component for frozen sands and to explain their development during deformation as a function of strain. Although unfrozen sand is a cohesionless particulate material, the freezing process (even to -5°C) causes it to become a cohesive frictional composite material (sand-ice system). This change is attributed to the cohesion of the ice matrix to the sand particle skeleton.

It is of interest that although the volumetric strain behavior of the thawed and frozen sands is apparently similar, the mechanisms controlling the behavior, especially during the volume increase phase, are different. The results of tests on frozen sand samples showed that the volumetric increase is mainly due to initiation and progressive development of cracks (void gaps) rather than to interlocking among the sand particles. This change is also due to the cohesion and high viscosity of the pore-ice matrix.

In practice, in seasonal frozen (geographical) areas above the frost line, building foundations will be subjected to thaw settlements, which result from changes in the soil behavior from winter to summer, that is, from the frozen to the unfrozen state. Therefore, it is recommended that foundations be constructed below the frost line. In the case of highways, coarse material that is not frost susceptible (i.e., gravels) should be used for the subgrade in order to provide sufficient drainage. In addition, outside the cold regions, the advantages obtained in the soil behavior by artificially freezing the soil (i.e., increasing its shear strength) enable utilization of the ground as a construction material, for example, for deep mine shafts and tunnels.

ACKNOWLEDGMENT

The financial support of the National Science and Engineering Research Council of Canada is gratefully acknowledged.

REFERENCES

1. P. V. Lade, H. L. Jessberger, and N. Dickman. Stress-Strain and Volumetric Behaviour of Frozen Soils. Presented at Second International Symposium on Ground Freezing, Trondheim, Norway, 1980.
2. H. Youssef. Indirect Determination of Intergranular Stresses in Frozen Soils. Ph.D. thesis. Department of Civil Engineering, Ecole Polytechnique, University of Montreal, Quebec, Canada, 1984.
3. H. Youssef. Development of a New Triaxial Cell with Self-Cooling System (TCWSCS) for Testing Ice and Frozen Soils. Presented at Fourth International Symposium on Ground Freezing, Sapporo, Japan, 1985.
4. A. W. Bishop and D. Henkel. *The Measurements of Soil Properties in the Triaxial Test,* 4th ed. Edward Arnold Ltd., London, 1978.
5. J. E. Bowles. *Engineering Properties of Soils and Their Measurements*. McGraw-Hill, New York, 1978.
6. N. F. Massoud. Shear Strength Characteristics of Sands. M.Sc. thesis. Department of Civil Engineering, Concordia University, Montreal, Quebec, Canada, 1981.
7. F. Sayles. *Triaxial Constant Strain Rates and Triaxial Creep Tests on Frozen Ottawa Sand*. Technical Report 253. U.S. Army Engineer Cold Regions Research and Engineering Laboratory, Hanover, N.H., 1974.
8. R. Goughnour and O. Andersland. Mechanical Properties of a Sand-Ice System. *Journal of the Soil Mechanics and Foundation Division,* ASCE, No. SM4, July 1968.
9. E. Chamberlain et al. The Mechanical Behaviour of Frozen Earth Materials Under High Pressure Triaxial Test Conditions. *Géotechnique,* Vol. 22, 1972.
10. V. Parameswaran. Deformation Behaviour and Strength of Frozen Sands. *Canadian Geotechnical Journal,* Vol. 17, 1980.
11. H. J. Atkinson and L. P. Bransby. *The Mechanics of Soils: An Introduction to Critical State Soil Mechanics*. McGraw-Hill, London, 1978.
12. M. J. O'Connor. Triaxial and Plane Strain Experiments on a Frozen Silt. Ph.D. thesis. Queen's University, Kingston, Ontario, Canada, 1975.

Publication of this paper sponsored by Committee on Frost Action.

Model Simulations of Winchendon Freeze-Thaw Field Data

LEWIS EDGERS AND LAURINDA BEDINGFIELD

This paper describes theoretical studies of the Winchendon field performance data using a computer model, FROST1, developed by the U.S. Army Corps of Engineers Cold Regions Research and Engineering Laboratory (CRREL). The Winchendon field test site was constructed by the Massachusetts Department of Public Works (MDPW) during the fall of 1977. Data on frost heave, frost depth, and thaw weakening were then obtained during the next three winter seasons. FROST1 assumes one-dimensional vertical heat and moisture flux, and is intended for use on problems of seasonal freezing and thawing of nonplastic soils that range from silts to silty sands and gravels above the water table. These simulations have shown that the computations are sensitive to the input thermal and hydraulic soil parameters, porosities, and boundary temperatures and pressures. Nevertheless, they provide guidance in the selection of input parameters for FROST1. Parametric studies were made to provide design curves that show, for two water-table depths, the reduction in maximum heave with increasing amounts of frost protection. These curves will assist designers in evaluating the required depth of frost protection and in particular the effects of only partial frost protection in situations where factors such as buried utilities or economics preclude the use of non-frost-susceptible (NFS) materials to the full frost depth.

This paper describes theoretical studies of the Winchendon field performance data using a computer model, FROST1, developed by the U.S. Army Corps of Engineers Cold Regions Research and Engineering Laboratory (CRREL). One objective of these studies was to develop relationships between physical properties of the soil and model input parameters so that the theoretical model could then be used as a design tool to predict frost heave and frost penetration versus time for trial design pavement cross sections. Computations of pore pressures and settlements during the thaw period might then be incorporated into mechanistic design approaches such as those described by AASHTO (*1*).

A second objective of these theoretical studies was to first calibrate the model to the Winchendon field performance data and then compute the effects on frost heave of variations in the depths to frost-susceptible (F) materials and the groundwater table. These studies will assist designers in evaluating the required depth of frost protection and in particular in evaluating the effects of only partial frost protection in situations where factors such as buried utilities or economics preclude the use of non-frost-susceptible (NFS) materials to the full frost depth.

The following sections of this paper include discussions of the Winchendon field test site, the computer model, theoretical studies of three of the Winchendon soils, parametric studies of idealized highway cross sections, and a summary, including design curves.

L. Edgers, Department of Civil Engineering, Tufts University, Medford, Mass. 02155. L. Bedingfield, Massachusetts Department of Public Works, 10 Park Plaza, Boston, Mass. 02116.

DESCRIPTION OF WINCHENDON FIELD TEST SITE

The Winchendon field test site, located in north-central Massachusetts, was constructed by the Massachusetts Department of Public Works (MDPW) during the fall of 1977. The site consists of 12 test cells, each a minimum of 28 ft wide (by 8 ft long in plan view) and consisting of a lower roadway and an upper roadway (Figure 1). The base of the test soils extended to a minimum of 6 in. below the groundwater level. The paved surface of the lower roadway of the cell was approximately 3 ft above the groundwater level and of the upper roadway, approximately 5 ft above the groundwater level. A bituminous concrete paved surface 8 ft wide and 3 in. thick was placed on both the upper and lower roadways of the test cells.

Test soils were selected to represent a wide range of soils with varying degrees of frost susceptibility. Table 1 gives the laboratory index property data. Edgers and Bono (*2*) have assembled the complete data in a separate data report.

Freezing data were obtained by the MDPW during three consecutive winter seasons, 1977–1978, 1978–1979, and 1979–1980 (*3*). Pavement surface deflections due to frost heave were measured at nine control points on both the upper and lower roadways over each soil by means of an engineer's transit. Frost penetrations were measured using a frost-depth indicator consisting of a transparent pipe containing a dye that turns colorless upon freezing at 32°F. Figure 2 shows typical plots of the frost heave, frost penetration, and groundwater observation data.

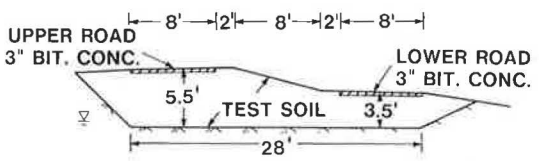

FIGURE 1 Transverse profile of typical test cell.

TABLE 1 LABORATORY INDEX PROPERTIES OF WINCHENDON TEST SOILS

	Test Soil	% Finer By Weight .02 mm	.075 mm	Uniform Coeff.	Plasticity Index
Many Fines	Moulton Pit Silt	52-69	96-99	3.4-4.2	N.P.
	Graves Silt Sand	8-12	44-47	5.2-6.2	N.P.
	Morin Clay	77-82	95-98	--	10.8
	Hyannis Sand	4-20	32-90	2.7-5.1	N.P.
	Ikalanian Silt-Sand	6-10	38-57	4.0-4.2	N.P.
	Sibley Till	17-21	32-37	Over 100	4.2
Intermed. Fines	Worcester Till	7-8	14-21	Over 100	N.P.
	Keating Stone Dust	~12	17-20	~100	N.P.
	Hart Brothers Sand	4-5	15-18	6.0	N.P.
Few Fines	Mason Pit Sand	1-3	5-9	5.8-6.7	N.P.
	Keating Dense Graded	~6	6-10	25-100	N.P.
	Corbosiero Sand	2-4	12-16	4.0-4.3	N.P.

N.P. = Non-plastic

CRREL MODEL OF FROST HEAVE AND THAW SETTLEMENT

The CRREL theoretical model is described in detail by Berg et al. (*4*), Guymon et al. (*5, 6*), and Johnson et al. (*7*). This model was developed as part of a cooperative research program begun in 1975 and involving the U.S. Army Corps of Engineers, the Federal Highway Administration, and the Federal Aviation Administration. The theoretical model serves as a basis for the computer program, FROST1, made available to the project by CRREL.

The CRREL model assumes one-dimensional vertical heat and moisture flux and is intended for use on problems of seasonal freezing and thawing of nonplastic soils that range from silts to silty sands and gravels above the water table. The model assumes that moisture transport in the unfrozen zone is governed by the unsaturated-flow equation based on Darcy's law and that moisture flow in the frozen zone is negligible. Heat transport in the entire soil column is governed by the sensible heat transport equation, which includes a convective term, and freezing or thawing is approximated as an isothermal phase change process. Detailed features and assumptions embodied in the model are described by Johnson et al. (*7*).

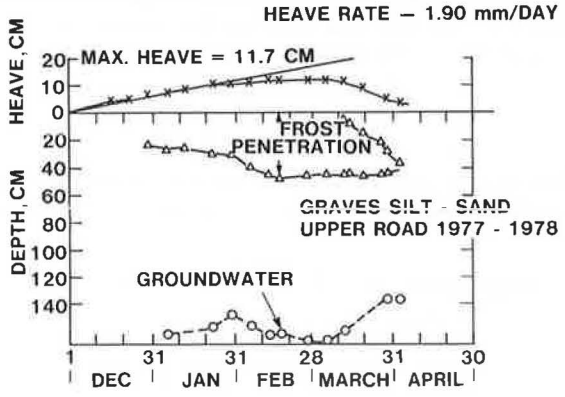

FIGURE 2 Typical frost depth, groundwater depth, and heave data.

Figure 3 shows a typical model simulation at a given time and defines the major variables. These include

- Head—water pressure (h_p) and overburden (σ_o)
- Temperature—T, T_u, and T_L
- Porosity
  - —Initial (n)
  - —Unfrozen water (θ_r)
  - —Variable with pressure (θ_u)
  - —Ice (θ_i)
  - —Segregated ice (θ_s)

FROST1 assumes that the variations of porosities (θ_u) and unsaturated permeabilities (K_u) with pressure are accurately described by Gardner functions (*8*). The unfrozen permeability K_u is reduced because of ice formation in soil pores in accordance with the following equation:

$$K_f = K_u \cdot 10^{-E\theta_i} \quad (1)$$

where K_u and θ_i have already been defined, K_f is the frozen permeability, and E is an empirically determined factor. No rigorous theoretical principles or laboratory tests are available for determining E. At present, this parameter must be determined by calibrating, or tuning, FROST1 with either laboratory freezing-column data (*9*) or field data.

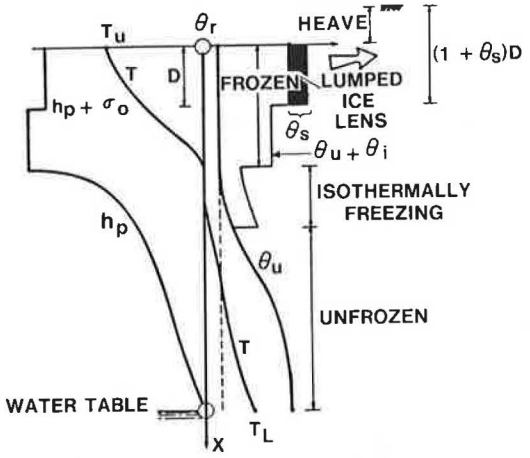

FIGURE 3 Typical model simulation result at a given time (*7*).

The thaw settlement portion of the model is an extension of early work by Morgenstern and Nixon (*10*). FROST1 uses probabilistic concepts to consider the effects of uncertainties in the input soil parameters and the nodal domain integration method. The soil profile is represented by a sequence of elements and nodes as shown in Figure 4, and the time-domain solution is by the well-known Crank Nicolson or fully implicit method.

FROST1 requires the following input:

1. Volumetric parameters
   a. Porosity n and Gardner moisture parameters A_w and α for porosity
   b. Unfrozen water content factor, θ_r
   c. Soil density
2. Hydraulic parameters
   a. Unsaturated permeability K_u
   b. Gardner's parameters A_k and β for permeability
   c. A multiplier factor for permeability (usually 1.0)
   d. Permeability correction factor for freezing soil E

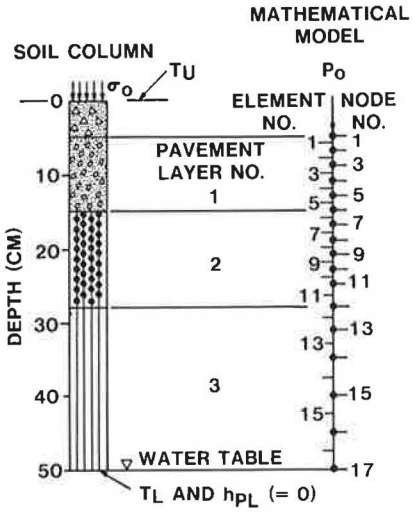

FIGURE 4 Example soil profile divided into finite elements (*6*).

3. Thermal parameters
   a. Volumetric heat capacity of soil C_s
   b. Thermal conductivity of soil K_s
   c. Freezing-point depression of soil water T_f

In addition, the following boundary and initial conditions must be specified:

1. Initial pore pressure, ice content, and temperature;
2. Soil surface boundary conditions for temperature (T_u), determined from air temperature multiplied by a factor to represent soil surface temperature (*11*); and
3. Lower boundary pressure (h_{pL}) and temperature (T_L)—if the bottom of the profile is at the water table, h_{pL} equals zero.

Output from the model includes frost heave at the surface, frost depth, thaw depth, subsurface temperature, and pore pressure. The computed frost heave can be used directly to aid in selection of an appropriate pavement design by relating it to pavement roughness criteria. Pore-water pressure may be used in empirical equations developed from laboratory tests to estimate resilient modulus values of layers within the pavement system at various times of the year. The resilient modulus data may then be used in a pavement structural response model, where output can be related to pavement performance criteria.

In the last half-dozen years, development efforts have included simulation studies of Fairbanks silt (*5*); evaluations of model uncertainties, parameter errors, and boundary condition effects (*6*); and initial model calibrations with laboratory soil column and field data on a number of soils, including six of the Winchendon soils (*6*). There are still, however, major uncertainties regarding selection of soil input parameters, especially E, the calibration factor that accounts for the effects of freezing on soil permeability.

Johnson et al. (*7*) discuss the shortcomings of the model and, in particular, the inability to derive some of the necessary input parameters from basic concepts of soil physics. The modeling requires calibration of the hydraulic conductivity correction factor E and estimates moisture tension in the freezing zone from laboratory relationships between moisture tension and unfrozen water content. The studies described in the following sections of the paper will assist in the evaluation of these input parameters.

FROST1 STUDIES OF THREE WINCHENDON SOILS

Initial calibrations of FROST1 described by Guymon et al. (*6*) included simulations of the field performance during the winter of 1978–1979 of six of the Winchendon soils. Calculations were made for the upper roadway only, and computed frost heave and frost penetration agreed well with measured values once the CRREL model had been tuned by using the frozen hydraulic conductivity factor E.

CRREL provided Tufts University with a version of FROST1 that has been modified to make it compatible

with the university's Vax 11/780 computer system. Preliminary FROST1 runs were then made (*12*) to verify that the Tufts version of the program was operating correctly; to familiarize the researchers with the operation of FROST1, especially the preparation of input; and finally, to evaluate the sensitivity of the computations to variations in mesh formulation and the input parameters. These runs established that FROST1 computations are sensitive to the volumetric and hydraulic soil parameters, including the permeability correction factor E. Initial pore pressure and temperature do not strongly influence the computed frost heave and frost penetration, provided the soil is initially unfrozen. The lower boundary pressures (h_{pL}) and temperatures (T_L) strongly influence the computed frost heave if the frost penetrates more than halfway to three-fourths of the way into the finite-element mesh.

After these preliminary FROST1 runs, three of the Winchendon soils were selected for detailed study. Graves silt sand was selected as representative of highly frost-susceptible materials; Keating dense graded stone was selected as representative of low-frost-susceptible materials; and Hart Brothers sand was selected as representative of materials of intermediate frost susceptibility. In situ, Hart Brothers sand was strongly affected by the water-table location, with about three times greater heave on the lower roadway (high water table) than on the upper roadway (low water table). One objective of this series of runs was to first simulate the field performance of these three soils at the upper roadway and then test FROST1 by using the same thermal, volumetric, and hydraulic parameters to simulate the performance of these three soils at the lower roadway.

Initial ground temperature, pore-water pressure, and lower boundary temperature were determined from the field measurements. Initial ice content was assumed to equal zero. Ground surface temperature was estimated from mean daily air temperatures using the Corps of Engineers n-factor method (*11*). The grid depth was taken to the average groundwater table depth; 150 cm (upper) and 100 cm (lower) for Graves silt sand and Hart Brothers sand; and 120 cm (upper) and 60 cm (lower) for dense graded stone. Thus the lower boundary pressure head (h_{pL}) was approximated as zero, and fluctuations in groundwater table during the simulation period were neglected. The grids were divided into 43 to 61 variable-length segments, from 0.5 cm at the top to 5 cm at the column bottom. Table 2 gives the soil parameters used in these analyses. These parameters were taken from the laboratory measurements or are based on the initial CRREL analyses (*6*).

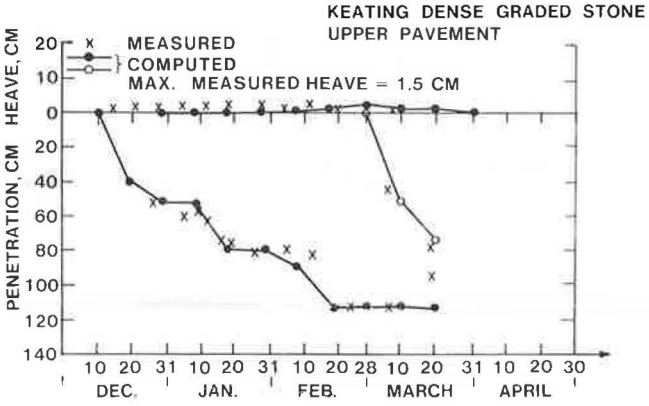

FIGURE 5 Computed frost heave and frost penetration for Keating dense graded stone, upper roadway, 1978–1979.

The results of these computations are shown in Figures 5 through 11. For the dense graded stone (Figures 5 and 6) and Hart Brothers sand (Figures 7 and 8), computed values of frost heave, frost penetration, and thaw penetration show excellent agreement with measured values. Some differences in detail between measured and computed values occur because the lower boundary ground-

TABLE 2 SOIL PARAMETERS FOR REMOLDED WINCHENDON TEST SITE SOILS USED IN TUFTS UNIVERSITY STUDIES

Parameter	Graves Silty Sand	Hart Bros. Sand	Dense Graded Stone
Soil density (g/cm^3)	1.49	1.69	1.87
Soil porosity (cm^3/cm^3)	0.460	0.282	0.334
Soil-water freezing point dep. (^oC)	0	0	0
Vol. heat cap. of soil ($cal/cm^3\ ^oC$)	0.2	0.2	0.2
Thermal cond. of soil (cal/cm hr ^oC)	17.0	17.0	17.0
Unfrozen water cont. factor (cm^3/cm^3)	0.12	0.04	0.15
Soil water characteristics [A_w,(α)]	.00560 (.900)	.022 (.867)	.053 (.462)
Permeability characteristcis [A_k,(β)]	.00081 (2.536)	2.681 (1.2)	2.681 (1.3)
Saturated hydraulic cond. (cm/hr)	1.92	4.08	5.54
Frozen soil hydraulic cond. factor-E	6 (upper road) 9 (lower road)	10.0	23.0

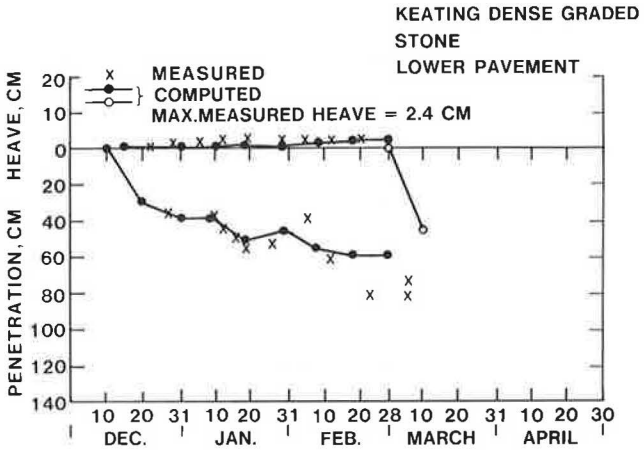

FIGURE 6 Computed frost heave and frost penetration for Keating dense graded stone, lower roadway, 1978–1979.

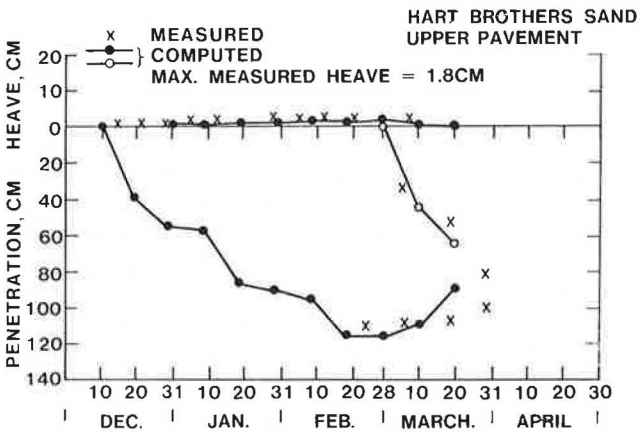

FIGURE 7 Computed frost heave and frost penetration for Hart Brothers sand, upper roadway, 1978–1979.

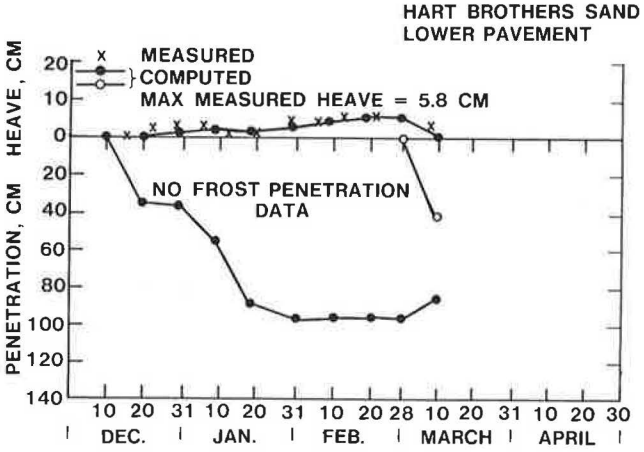

FIGURE 8 Computed frost heave and frost penetration for Hart Brothers sand, lower roadway, 1978–1979.

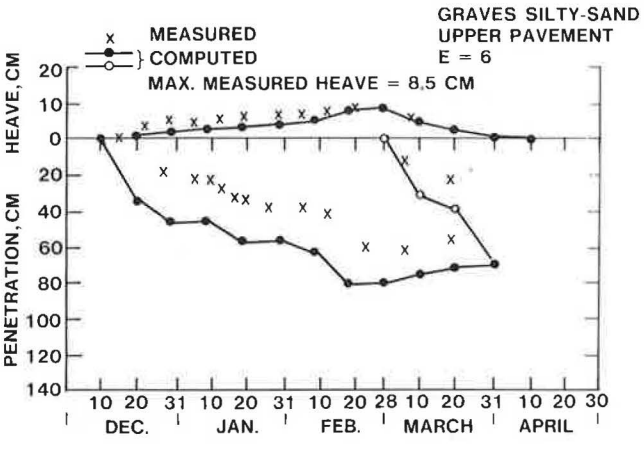

FIGURE 9 Computed frost heave and frost penetration for Graves silty sand, upper roadway, 1978–1979 (E = 6).

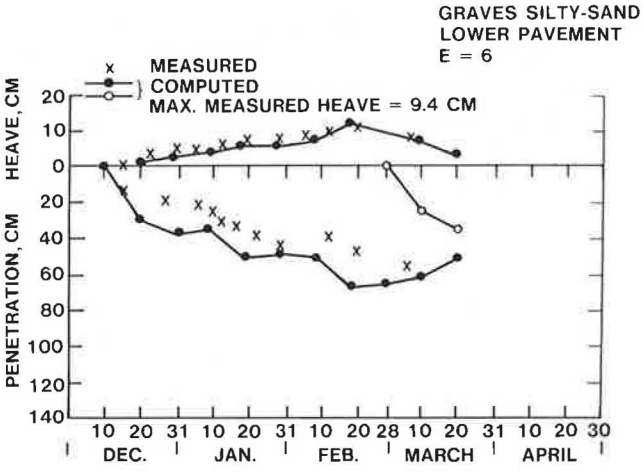

FIGURE 10 Computed frost heave and frost penetration for Graves silty sand, lower roadway, 1978–1979 (E = 6).

water condition was assumed constant with time. Comparison of Figure 5 with Figure 6 and Figure 7 with Figure 8 shows that the same soil parameters accurately simulate the field performance of both the upper and lower roadways.

The analyses of Graves silt sand (Figures 9 through 11) show poorer agreement with field performance. The computed frost penetration depths are larger than measured values, especially for the upper roadway. Also, a value of 6 for E best simulated the performance of the upper roadway (Figure 9); this value was used to compute a heave-versus-time curve for the lower roadway (Figure 10), which agreed in general with the measured heaves but resulted in a maximum computed heave for the lower roadway that is slightly too large (Figure 10). Figure 11 shows a FROST1 simulation of the lower roadway of Graves silt sand that uses a value of 9 for E. The computed maximum heave shows good agreement with the measured maximum heave.

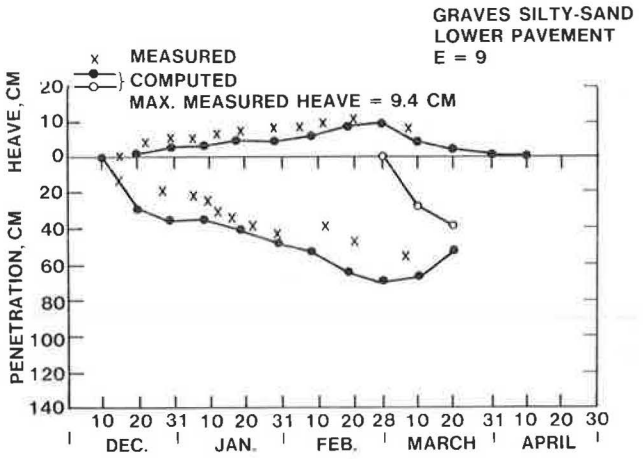

FIGURE 11 Computed frost heave and frost penetration for Graves silty sand, lower roadway, 1978–1979 (E = 9).

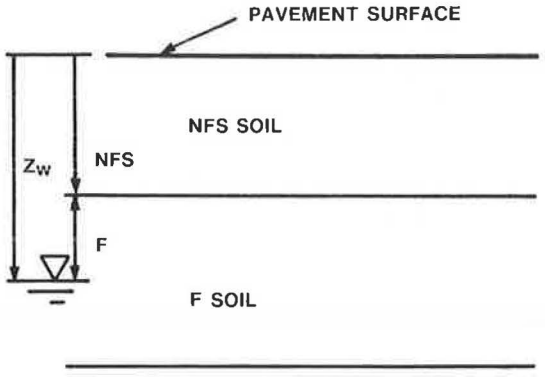

FIGURE 12 Geometry of two-layer roadway system for FROST1 parametric study.

Guymon et al. (*6*) further discuss difficulties in using FROST1 to model the Winchendon field performance data. They identify the possibility of errors due to incorrect thermal conductivity, incorrect surface moisture flux boundary condition (assumed zero), and variations in soil parameters due to freeze-thaw cycles. They conclude that "the most likely problem with the Winchendon soils simulation is that the pavement surface temperature was used as a boundary condition. More accurate results will have been possible if soil surface temperatures below the pavement were used."

It is believed that in addition to these, errors in estimating the input soil parameters, especially the unfrozen water content factor, θ_r, and the unsaturated permeabilities and porosities may also have contributed to differences between the computed values and measured performance data. Nevertheless, these analyses show reasonable agreement between the computer simulations and the Winchendon field performance.

PARAMETRIC STUDIES OF TWO-LAYER SYSTEM

Parametric studies were made to evaluate the effects on frost heave of variations in the depth to frost-susceptible materials and the groundwater table. These studies will assist designers in evaluating the required depth of frost protection and, in particular, the effects of only partial frost protection in situations where factors such as buried utilities or economics preclude the use of NFS materials to the full frost depth.

These parametric studies were performed on a two-layer system (Figure 12) consisting of NFS material underlain by a highly frost-susceptible material. The thickness of the NFS material, *NFS*, was varied from zero to the full groundwater table depth, Z_w. Computer runs were made for two groundwater table depths, 3.1 and 5 ft. The properties of the NFS material were represented by those of the Keating dense graded stone, and the frost-susceptible material by those of the Graves silt sand (Table 2). Thus, these parametric studies have been calibrated to the preceding Winchendon field simulations. The initial and boundary temperatures and pore pressures were idealized from the field measurements. The air temperatures correspond to the normal average daily temperatures recorded at Winchendon, providing a freezing index (FI) of 835 °F-days.

Figures 13 and 14 show for Z_w of 3.1 ft and 5 ft, respectively, computed frost heave and frost penetration versus time. The families of curves correspond to the different thicknesses of NFS material. These curves are summarized by Figure 15, which plots maximum heave versus thickness of NFS soil.

Figure 15 shows that at NFS = 0 (full thickness of Graves silty sand), the maximum heave computed in this parametric study, 10.5 and 11.9 cm for Z_w equal to 5 and 3.1 ft, respectively, is about 20 percent larger than the corresponding values computed for Graves silt sand in the simulations of Figures 9 and 11. This is because of differences in the initial and boundary conditions in these parametric studies.

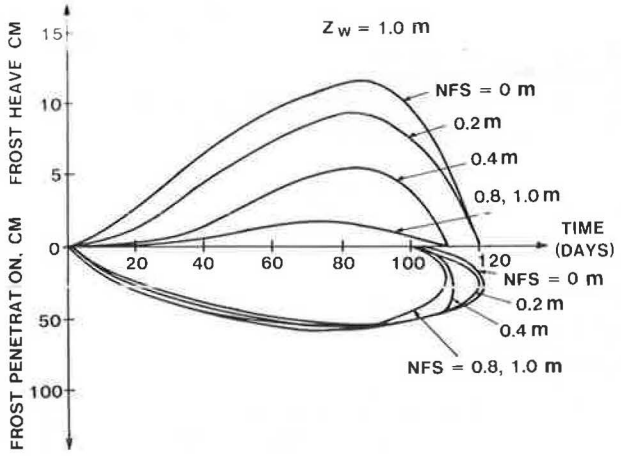

FIGURE 13 Computed frost heave and frost penetration versus time, two-layer parametric study (Z_w = 3.1 ft).

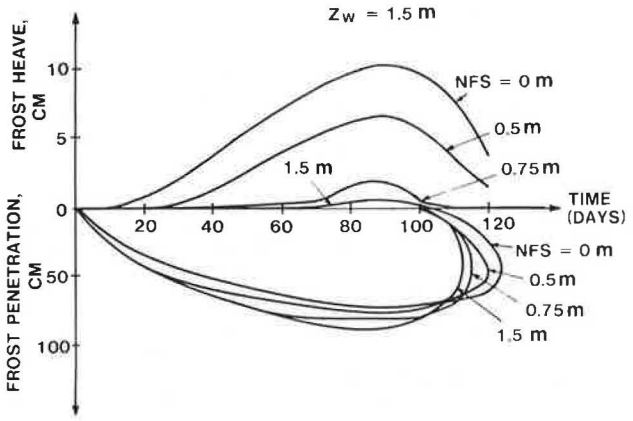

FIGURE 14 Computed frost heave and frost penetration versus time, two-layer parametric study (Z_w = 5 ft).

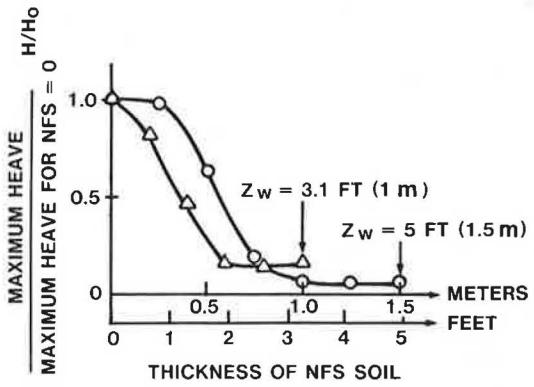

FIGURE 16 Normalized maximum heave versus thickness of NFS soil.

For Z_w = 5 ft, the maximum heave decreases gradually with increasing thickness of NFS material, until *NFS* = 3 ft. This depth is slightly greater than the computed frost penetration depth (Figure 14). NFS material of 2 ft reduces the maximum heave to about 5 cm, only about a 50 percent reduction. Little additional benefit is obtained by placing more than 3 ft of NFS material over the frost-susceptible material.

For Z_w = 3.1 ft, the maximum heave decreases much more rapidly with increasing thickness of NFS material, until *NFS* = 2 ft. This depth is approximately the computed frost penetration depth (Figure 13). NFS material of 2 ft reduces the maximum heave to about 2 cm, about an 80 percent reduction. Little additional benefit is obtained by placing more than 2 ft of NFS material over the frost-susceptible material.

The comparison for the two water-table depths is shown also in Figure 16, which plots the reduction in normalized heave versus thickness of NFS soil. Figures 15 and 16 show that there is more heave for the shallow water table, as expected, for a large thickness of NFS soil, corresponding to full-section thicknesses. Figures 15 and 16 also show that as *NFS* increases from zero, that is, as the thickness of protective NFS soil placed over the frost-susceptible soil (F-soil) is increased, more relative benefit is obtained by an equal thickness of NFS material when the water table is at the shallower depth (3.1 ft) than when the water table is at the greater depth (5 ft). The more rapid decrease in heave with increasing thickness of NFS soil for the shallower water table occurs because for an equal NFS, less frost-susceptible material is left in the ground within the zone of frost penetration. In fact, Figure 17 plots the normalized heave versus the thickness of frost-susceptible soil penetrated by frost and shows almost the same normalized relationship for the two water-table depths analyzed.

SUMMARY AND CONCLUSIONS

The theoretical studies of the Winchendon field performance data using the CRREL computer model FROST1 have shown that the computations are sensitive to the input thermal and hydraulic soil parameters, porosities, and boundary temperatures and pressures. FROST1 computations were made to simulate the field performance of Graves silt sand, Keating dense graded stone, and Hart

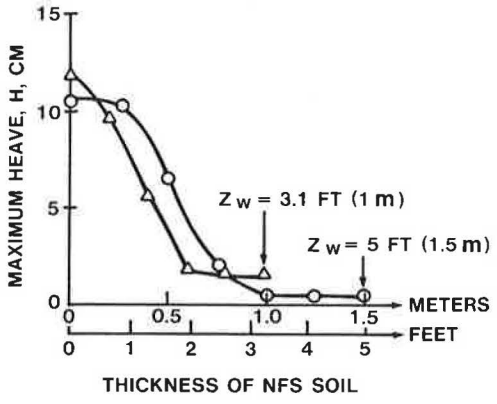

FIGURE 15 Maximum heave versus thickness of NFS soil.

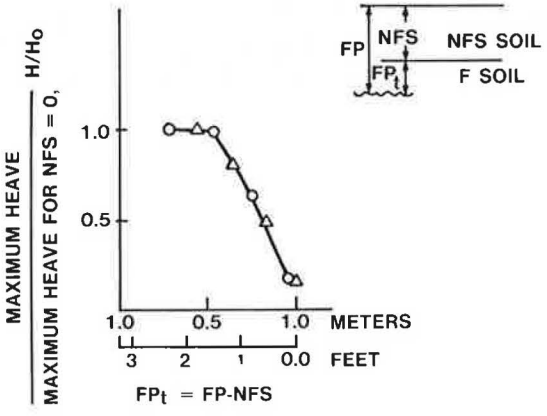

FIGURE 17 Normalized heave versus thickness of frost-susceptible (F) soil penetrated by frost.

Brothers sand. Computed and measured values of frost heave, frost penetration, and thaw penetration showed excellent agreement, especially for Keating dense graded stone and Hart Brothers sand. For Graves silt sand, the computed frost penetration depths are larger than measured values, and it was necessary to use different values of E to accurately simulate the performance of the upper ($E = 6$) and lower ($E = 9$) roadways. Table 2 gives the input thermal and hydraulic soil parameters used in these simulations. Except for the slight variations in E described above, the same parameters accurately simulated the field performance of both the upper and lower roadways of a particular soil.

Parametric studies were made to evaluate the effects on frost heave of variations in the depth to frost-susceptible materials and the groundwater table. The parametric studies were performed on a two-layer system consisting of non-frost-susceptible material underlain by a highly frost-susceptible material. The properties of these materials were represented by those found in the FROST1 simulations described above, and thus these have been calibrated to the Winchendon field performance data.

These parametric studies are summarized in Figure 16, which shows, for two water-table depths, the reduction in maximum heave with increasing amounts of frost protection. Figure 16 evaluates the required depth of frost protection and in particular the effects of only partial frost protection in situations where factors such as buried utilities or economics preclude the use of non-frost-susceptible materials to the full frost depth. It shows, for example, that for equal thicknesses of non-frost-susceptible soils, more relative benefit is derived for the shallow groundwater condition. No benefit is derived from placement of additional non-frost-susceptible material below the depth of frost penetration.

ACKNOWLEDGMENTS

This research was supported by the Department of Public Works (MDPW), Commonwealth of Massachusetts. The authors acknowledge the assistance of numerous MDPW personnel. The assistance of Richard Berg and Edwin J. Chamberlain of the U.S. Army Corps of Engineers Cold Regions Research and Engineering Laboratory in making FROST1 available and helping in its use is greatly appreciated.

REFERENCES

1. *Proposed Guide for Design of Pavement Structures*. National Cooperative Highway Research Program (Project 20-7/24); Joint Task Force on Pavements, American Association of State Highway and Transportation Officials, Washington, D.C., 1986.
2. L. Edgers and N. Bono. *Highway Design for Frost Susceptible Soils, Laboratory and Field Data: Winchendon Soils*. Massachusetts Department of Public Works, Boston, 1985.
3. *Full Depth Testing of Frost Susceptible Soils: Final Report and Appendices*. HPR Research Study R-12-9. Massachusetts Department of Public Works, Boston, 1982.
4. R. L. Berg, G. L. Guymon, and T. C. Johnson. *Mathematical Model To Correlate Frost Heave of Pavements with Laboratory Predictions*. CRREL Report 80-10. U.S. Army Corps of Engineers Cold Regions Research and Engineering Laboratory, Hanover, N.H., 1980, 49 pp.
5. G. L. Guymon, R. L. Berg, T. C. Johnson, and T. V. Hromadka II. Results from a Mathematical Model of Frost Heave. In *Transportation Research Record 809*, TRB, National Research Council, Washington, D.C., 1981, pp. 2–6.
6. G. L. Guymon, R. L. Berg, T. C. Johnson, and T. V. Hromadka II. *Mathematical Model of Frost Heave in Pavements*. CRREL Report. U.S. Army Corps of Engineers Cold Regions Research and Engineering Laboratory, Hanover, N. H. (in preparation).
7. T. C. Johnson, R. L. Berg, E. J. Chamberlain, and D. M. Cole. *Frost Action Predictive Techniques for Roads and Airfields: A Comprehensive Summary of Research Findings*. CRREL Report 86-18. U.S. Army Corps of Engineers Cold Regions Research and Engineering Laboratory, Hanover, N. H., 1986, 52 pp.
8. W. R. Gardner. Some Steady-State Solutions of the Unsaturated Moisture Flow Equation with Application to Evaporation from a Water Table. *Soil Science*, Vol. 85, 1958, pp. 223–232.
9. R. L. Berg, J. Ingersoll, and G. L. Guymon. Frost Heave in an Instrumented Soil Column. *Cold Regions Science and Technology*, Vol. 3, Nos. 2 and 3, 1980, pp. 211–221.
10. N. R. Morgenstern and J. F. Nixon. One-Dimensional Consolidation of Thawing Soils. *Canadian Geotechnical Journal*, Vol. 8, 1971, pp. 558–565.
11. R. L. Berg. *Design of Civil Airfield Pavements for Seasonal Frost and Permafrost Conditions*. Report FAA-RD-74-30. FAA, U.S. Department of Transportation, 1974.
12. R. Ghazzaoui. Parametric Studies Using FROST1 To Predict Frost Heave. Master's report. Department of Civil Engineering, Tufts University, Medford, Mass., 1986.

Publication of this paper sponsored by Committee on Frost Action.

Field Evaluation of Criteria for Frost Susceptibility of Soils

LEWIS EDGERS, LAURINDA BEDINGFIELD, AND NANCY BONO

Field data on frost heave, thaw weakening, and frost penetration acquired over a period of 3 years at the Winchendon field test site are analyzed. These data show that simple grain-size criteria such as the percent of particles smaller than 0.075 or 0.02 mm correlate weakly with field performance. Although soils with few fines (particles smaller than 0.075 mm) performed well in the field test, some of those with intermediate and many fines performed well and some poorly, with a great deal of scatter. The U.S. Army Corps of Engineers Frost Design Classification System and tabulated freeze test data provided very wide ranges of frost susceptibility compared with the field performance of the 12 test soils. Comparisons of the field frost heave data with data on soils in freezing conditions from the Massachusetts Department of Public Works heave stress test on nonplastic soils and with data from the new freeze-thaw test of the U.S. Army Corps of Engineers Cold Regions Research and Engineering Laboratory (CRREL) show excellent correlations. The thaw-weakening California bearing ratio (CBR) data from the CRREL freeze-thaw test correlated well with the resilient deflections from repeated plate bearing (RPB) tests in the field. Frost penetration depths calculated by the modified Berggren formula are in general agreement with, but somewhat larger than, the frost penetrations measured at the Winchendon field test site. This may possibly be due to the effects of freezing-point depressions of soil moisture, approximations in the adjustment of air to ground surface temperatures, and other factors not accounted for in the field test.

In order to develop field performance data on various New England soils, the Massachusetts Department of Public Works (MDPW), in a cooperative effort with the Federal Highway Administration (FHWA), constructed a field test site in Winchendon, Massachusetts, where 12 representative soils were subjected to three winters of freezing temperatures (*1*). Temperature (ground and air), precipitation, groundwater level, frost heave, frost penetration, and frozen water content at the site were monitored during the winters of 1977–1978, 1978–1979, and 1979–1980. The resulting 3 years' worth of field test data are analyzed and interpreted in detail.

The purpose of this research is an improved understanding of the mechanics of frost action in various soils leading to implementation of improved highway design criteria, guidelines, and specifications. This research may lead to reduced highway construction and maintenance costs from the reduced use of special borrow to replace natural soils that do not satisfy existing overconservative criteria and possible reductions in present requirements for base and subbase thicknesses.

L. Edgers, Department of Civil Engineering, Tufts University, Medford, Mass. 02155. L. Bedingfield, Massachusetts Department of Public Works, 10 Park Plaza, Boston, Mass. 02116. N. Bono, Tufts University, Medford, Mass. 02155. Current affiliation: Haley and Aldrich, Inc., 58 Charles Street, Cambridge, Mass. 02141.

WINCHENDON FIELD TEST SITE AND TEST SOILS

The Winchendon field test site, located in north-central Massachusetts, was constructed by the MDPW during the fall of 1977. The site consists of 12 test cells, each a minimum of 28 ft wide (by 8 ft long in plan view) and consisting of a lower and an upper roadway (Figure 1). The base of the test soils extended to a minimum of 6 in. below the groundwater level. The paved surface of the lower roadway of the cell was approximately 3 ft above the groundwater level and that of the upper roadway, approximately 5 ft above the groundwater level. A bituminous concrete paved surface 8 ft wide and 3 in. thick was placed on both the upper and lower roadways of the test cell.

A wide range of test soils was selected with varying degrees of frost susceptibility. The data in the summary of laboratory index properties (Table 1) suggest that the soils may be placed into three groups: few fines (less than about 15 percent smaller than 0.075 mm); intermediate fines (between about 15 and 25 percent smaller than 0.075 mm), and many fines (more than 25 percent smaller than 0.075 mm). Edgers and Bono have assembled the complete data in a separate data report (*2*).

WINCHENDON FIELD TEST DATA

Data on soils in freezing conditions were obtained by the MDPW during three consecutive winter seasons, 1977–1978, 1978–1979, and 1979–1980 (*1*). Pavement surface deflections caused by frost heave were measured at nine control points on both the upper and lower roadways over each soil by means of an engineer's transit. Frost penetrations were measured using a frost-depth indicator consisting of a transparent pipe containing a dye that turns colorless upon freezing at 32°F. Figure 2 shows typical air temperature and precipitation data at the Winchendon test site. Figure 3 shows typical plots of the frost heave, frost penetration, and groundwater observation data. The maximum amounts of heave, average heave rates, and frost

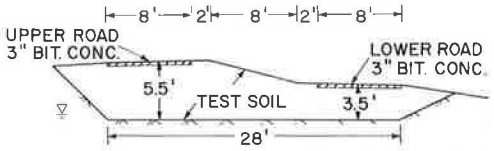

FIGURE 1 Transverse profile of typical test cell.

penetration depths for both upper and lower roadways for each winter are summarized in Table 2. The average heave rate was determined by taking the average slope of the heave-versus-time curves during the active freeze period, approximately 6 weeks after heaving began, as shown in Figure 3.

The average heave data in Table 2 demonstrate the effects on field performance of the depth to the groundwater table. For all but one of the soils (Morin clay), the maximum amount of heave was greater for the lower roadway than for the upper roadway, where the pavement was farther from the groundwater table. For three soils—Hart Brothers sand, Keating stone dust, and Worcester till—the difference between the two roadways is large. For the other nine soils, there are smaller differences in heave from the upper to the lower roadway.

Repeated plate bearing (RPB) tests were performed by the U.S. Army Corps of Engineers Cold Regions Research and Engineering Laboratory (CRREL) to determine the

TABLE 1 LABORATORY INDEX PROPERTIES OF WINCHENDON TEST SOILS

	Test Soil	% Finer By Weight .02 mm	% Finer By Weight .075 mm	Uniform Coeff.	Plasticity Index
Many Fines	Moulton Pit Silt	52-69	96-99	3.4-4.2	N.P.
	Graves Silt Sand	8-12	44-47	5.2-6.2	N.P.
	Morin Clay	77-82	95-98	--	10.8
	Hyannis Sand	4-20	32-90	2.7-5.1	N.P.
	Ikalanian Silt-Sand	6-10	38-57	4.0-4.2	N.P.
	Sibley Till	17-21	32-37	Over 100	4.2
Intermed. Fines	Worcester Till	7-8	14-21	Over 100	N.P.
	Keating Stone Dust	~12	17-20	~100	N.P.
	Hart Brothers Sand	4-5	15-18	6.0	N.P.
Few Fines	Mason Pit Sand	1-3	5-9	5.8-6.7	N.P.
	Keating Dense Graded	~6	6-10	25-100	N.P.
	Corbosiero Sand	2-4	12-16	4.0-4.3	N.P.

N.P. = Non-plastic

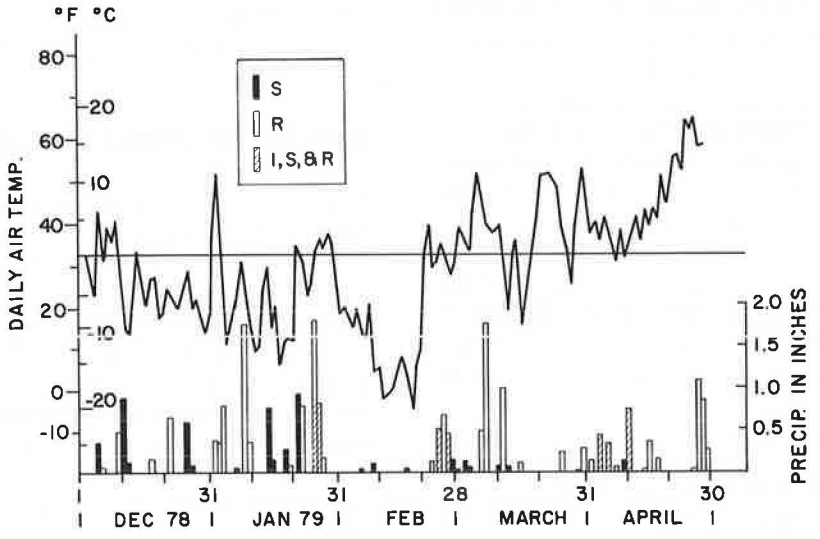

FIGURE 2 Weather data for 1978–1979 frost season.

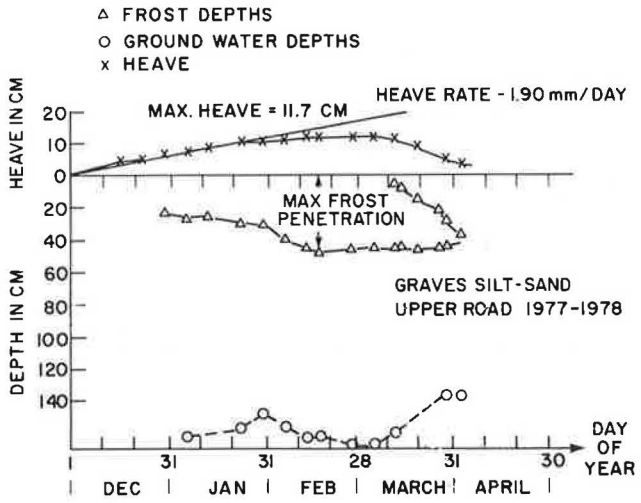

FIGURE 3 Typical frost depth, groundwater depth, and heave data.

seasonal changes in the supporting capacity of the soils as they freeze, thaw, and recover from the thaw-weakened condition (*3*). The RPB test applies loads through a 304-mm-diameter plate, repeating the load 50 to 1,000 times. The pulse duration was about 1 sec and the cycle time about 3 sec (20 cycles per minute). Figure 4 shows typical measured vertical displacements from RPB tests conducted at various stages of the freeze-thaw cycle.

Preliminary analyses of the effect of the severity of the winter on the observed field performance data (Table 2), showed a general trend of larger amounts and rates of heave with a larger freezing index and a great deal of scatter. Factors such as preconditioning of the soil structure during the first freezing season and detailed water-table and temperature variations before and during the freezing season may strongly influence the observed field performance. Thus the maximum amounts of heave and heave rates were averaged over the three seasons for the detailed analyses.

It is not clear whether maximum heave or average heave rate is a more useful summary of field performance. The maximum amount of heave serves as an index of the amount of pavement distress and surface roughness observed in the field and can be easily related to a performance criterion. However, the heave rate for any one soil may be less sensitive to the length of the active freeze period and may permit easier comparison of data collected during freezing seasons of different lengths. Detailed analyses performed with both maximum amounts of heave and heave rates showed, as will be discussed later, that there is no apparent statistical advantage to using either heave or heave rate in analyzing the Winchendon data. For the sake of brevity, the remainder of this paper will emphasize the analyses of maximum field heave data.

CRREL (*4*) has proposed field performance criteria including an adjective classification scale based on heave rates (Table 3). The maximum heave presented in Table

TABLE 2 FIELD PERFORMANCE MEASUREMENTS

	1977-78 WINTER			1978-79 WINTER			1979-80 WINTER			AVERAGE		
	Heave Rate (mm/ day)	Frost Pene. (cm)	Max. Heave (cm)	Heave Rate (mm/ day)	Frost Pene. (cm)	Max. Heave (cm)	Heave Rate (mm/ day)	Frost Pene. (cm)	Max. Heave (cm)	Heave Rate (mm/ day)	Frost Pene. (cm)	Max. Heave (cm)
UPPER ROAD												
Moulton Pit Silt	1.90	39	16.3	1.93	-	14.6	1.71	-	10.1	1.85	39	13.7
Graves Silt Sand	1.90	48	11.7	0.88	62	8.5	1.27	40	6.4	1.35	50	8.9
Morin Clay	1.19	55	8.7	1.22	-	6.7	0.71	42	4.6	1.04	48.5	6.7
Ikalanian Silt Sand	0.73	64	4.6	0.54	78	2.4	0.32	-	2.1	0.53	71	3.03
Worcester Till	0.95	88	5.6	0.98	105	4.9	0.59	74	3.3	0.84	89	4.6
Keating Stone Dust	0.66	97	2.6	0.76	109	3.4	0.68	53	4.3	0.70	86.3	3.4
Hart Brothers Sand	0.76	87	3.7	0.34	-	1.8	0.19	-	1.2	0.43	87	2.2
Sibley Till	0.54	108	2.1	0.49	128	1.5	0.42	86	1.5	0.48	107.3	1.7
Mason Pit Sand	0.34	85	1.7	0.29	96	1.5	0.27	66	0.9	0.30	82.3	1.4
Hyannis Sand	0.43	80	1.8	0.24	95	1.2	0.11	56	0.6	0.26	77	1.2
Dense Graded Stone	0.49	93	1.7	0.32	113	1.5	0.22	88	0.6	0.34	98	1.3
Corbosiero Sand	0.24	75	0.8	0.51	91	1.8	0.27	68	0.3	0.34	78	0.97
LOWER ROAD												
Moulton Pit Silt	2.19	34	18.3	2.00	47	14.9	1.90	-	8.2	2.03	40.5	13.8
Graves Silt Sand	2.15	43	15.7	1.00	-	9.4	1.02	34	6.1	1.39	38.5	10.4
Morin Clay	0.95	53	6.9	1.41	72	6.4	0.66	40	3.3	1.01	55	5.5
Ikalanian Silt Sand	0.93	46.5	6.5	0.93	64	4.0	0.52	-	1.8	0.79	55.3	4.1
Worcester Till	1.17	-	7.8	1.22	-	7.0	1.71	96	4.9	1.37	96	6.6
Keating Stone Dust	1.15	68	9.2	1.44	86	7.6	0.98	54	7.3	1.19	69.3	8.0
Hart Brothers Sand	1.44	67	9.3	1.75	-	5.8	0.71	55	4.6	1.3	61	6.6
Sibley Till	0.44	84	3.0	0.58	100	3.7	0.54	64	2.1	0.52	82.7	2.9
Mason Pit Sand	0.73	69	2.7	0.80	88	2.1	1.24	48	2.4	0.92	68.3	2.4
Hyannis Sand	0.60	71	3.3	0.49	88	1.5	0.38	-	1.2	0.49	79.5	2.0
Dense Graded Stone	0.54	67	2.4	0.97	83	2.4	0.24	66	1.2	0.58	72.0	2.0
Corbosiero Sand	0.56	74	2.5	0.46	86	1.5	0.27	52	2.1	0.43	70.7	2.0

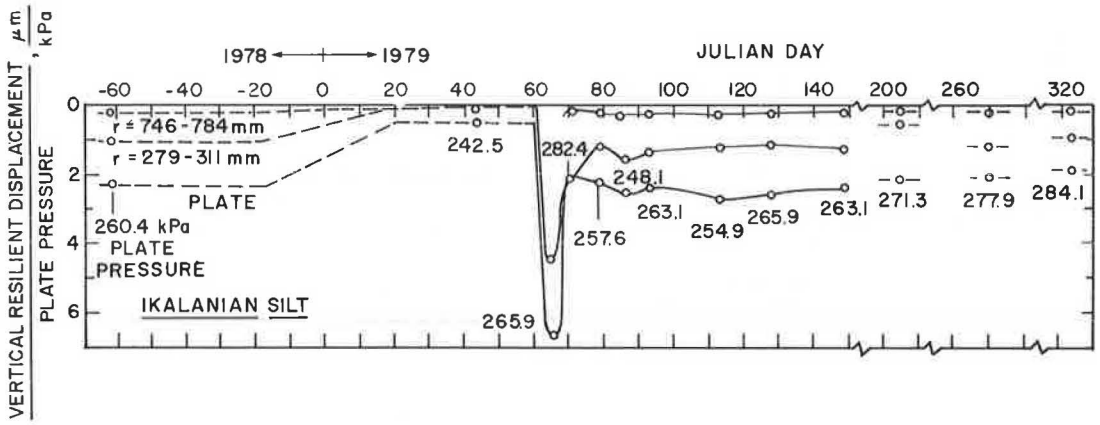

FIGURE 4 Example of resilient pavement deflections from RPB tests (*3*).

3 was computed by multiplying these heave rates by an assumed average active freeze period of 50 days. The data in Table 2 may be compared with the criteria for Table 3 to give a general impression of the relative field performance of the 12 soils tested. For example, soils that heaved less than 2.5 cm or at an average heave rate of less than 0.5 mm/day indicate negligible to very low frost susceptibility in Table 3, and thus show satisfactory performance.

LABORATORY DATA VERSUS FIELD PERFORMANCE

Introduction

Chamberlain (*5*) provides a comprehensive review of index tests for evaluating the frost susceptibility of soils, which has been updated by Bono (*6*). On the basis of these reviews, the following index tests and classification methods were selected for further evaluation in the analysis of the Winchendon field performance data:

1. Grain-size correlations of 0.02 and 0.075 mm,
2. U.S. Army Corps of Engineers Frost Design Classification System,
3. Correlations with tabulated freeze-test data,
4. MDPW heave stress test, and
5. New CRREL freeze-thaw test.

The grain-size correlations consist of relating the percentage of particles finer than 0.02 or 0.075 mm by weight in each soil to the observed field behavior. For example, the Casagrande (*7*) frost susceptibility criterion, based on the percent finer than 0.02 mm, states:

> One should expect considerable ice segregation in non-uniform soils containing more than three percent of grains smaller than 0.02 mm, and in very uniform soils containing more than ten percent smaller than 0.02 mm.

This type of grain-size criterion is easy to apply, commonly used, but generally imprecise (*8*).

The U.S. Army Corps of Engineers Frost Design Classification System is based on the percent finer than 0.02 mm by weight, the Unified Soil Classification, data collected from extensive laboratory freeze tests, and field observations of reduced bearing capacity during thaw. The system organizes soils by frost design groups such as NFS, F1, F2, F3, and F4, based on the classification data, and then assigns a frost susceptibility classification, from negligible to very high, based on the collected laboratory heave and field thaw data.

Correlations with tabulated freeze test data (*5*) use the same laboratory data base as the U.S. Army Corps of Engineers Frost Design Classification System. However, the correlations use the original data from the freezing tests directly rather than grouping the soils into frost design groups. The correlation method and the classification sys-

TABLE 3 PERFORMANCE CRITERIA FOR WINCHENDON FIELD TEST DATA (*4*)

	Heave Rate(mm/day)	Maximum Heave(cm)
Negligible	< 0.25	< 1.25
Very Low	0.25-0.50	1.25-2.5
Low	0.50-1.0	2.5-5.0
Med	1.0-2.0	5-10
High	2.0-4.0	10-20
Very High	> 4.0	> 20

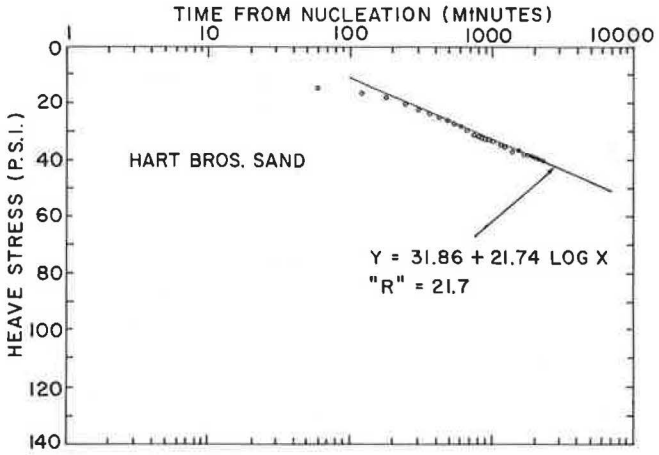

FIGURE 5 Heave stress versus log time (*9*).

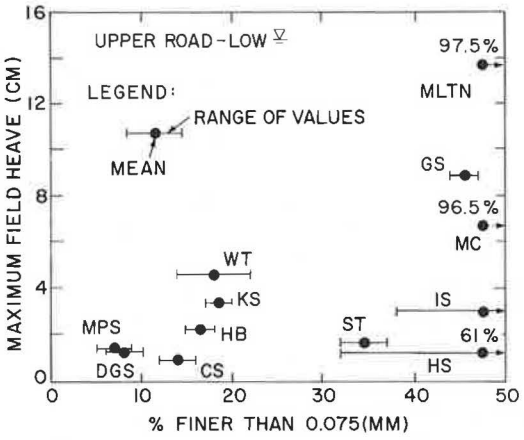

FIGURE 7 Maximum heave versus percent finer than 0.075 mm, upper roadway.

tem were selected for further study because they are inexpensive, easy to use, and possibly more accurate than grain-size correlations.

The MDPW heave stress test and the new CRREL freeze-thaw test were selected for comparison with Winchendon field performance because they offer the possibility of more accurate predictions of field performance. The MDPW heave stress test (*9, 10*) produces a plot of heave stress versus the log of time (Figure 5). The linear slope of this relationship, defined as the *R*-parameter, is taken as an index measure of in situ frost susceptibility. A high *R*-value indicates rapid development of heave stress with log time and hence high heave potential.

The new CRREL freeze-thaw test (*4*) is an improved version of earlier tests in that it is performed in an apparatus with low side friction, has a shorter duration, and measures thaw-weakening susceptibility. The test is performed in a multiring freezing cell (Figure 6), with a rubber membrane liner designed to minimize side friction. The standard test consists of two freeze-thaw cycles and requires only 5 days to complete. After the second thaw, California bearing ratio (CBR) tests are conducted to evaluate thaw-weakening susceptibility. The soil samples are then removed to determine the moisture content profile. The new CRREL freeze-thaw test is one of the simplest and most rapid freezing tests available and has great promise in making accurate predictions of frost heave and thaw-weakening behavior in the field.

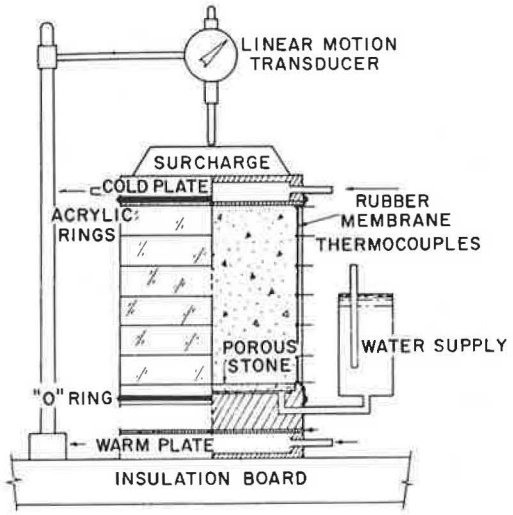

FIGURE 6 New CRREL freeze-thaw test apparatus (*4*).

Grain-Size Correlations: 0.075 mm

Figures 7 and 8 are plots of maximum field heave from the upper and the lower roadways versus percent of particles finer than 0.075 mm. The data show a large amount of scatter, indicating that the percent finer than 0.075 mm is not accurately related to field performance. For all the soils except Morin clay, the heaves were greater for the lower roadway (3 ft to groundwater) than for the upper roadway (5 ft to groundwater).

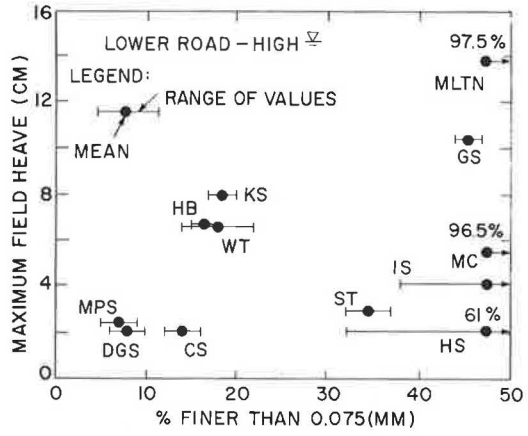

FIGURE 8 Maximum heave versus percent finer than 0.075 mm, lower roadway.

These plots also reveal differences in performance among the soils with few, intermediate, and many fines. The first group, which consists of the three soils with less than 14 percent fines, heaved small amounts, less than 2.5 cm, and performed satisfactorily according to the criteria in Table 3. The variation in depth to the groundwater table has only a small effect on these three soils. The second group, which consists of the three soils with from 15 to 21 percent fines, is sensitive to depth to the groundwater table. For the upper roadway these three soils heaved from 2 to 5 cm (Figure 7), whereas for the lower roadway they heaved from 6 to 9 cm (Figure 8). The last group, soils with more than 30 percent fines, shows a large range in field performance—from approximately 2.0 to 14.0 cm total heave. The depth to the groundwater table had little effect on the performance of these six soils. Two of the six [Morin clay (MC) and Sibley till (ST)] have plastic fines (Table 1), and the other four [Moulton pit silt (MLTN), Graves silt-sand (GS), Ikalanian silt-sand (IS), and Hyannis sand (HS)], nonplastic fines.

The establishment of a critical percentage of fines that, if exceeded, would result in some amount of frost action and thaw weakening is difficult. This critical percentage depends on the plasticity of fines, void ratio, and depth below the pavement surface. For example, uniform fine sands such as the Hyannis and Corbosiero sands can have much higher void ratios than dense well-graded soils. These sands can tolerate a much higher fines content before they become frost susceptible. On the other hand, Esch et al. (*11*), in a very extensive field study of 120 pavement structures in Alaska, show that for dense-graded aggregates typically used in pavement structural layers, fines contents in excess of 6 percent begin to result in some degree of thaw weakening as well as some level of frost heaving in laboratory tests.

Grain-Size Correlations: 0.02 mm

Figure 9 shows maximum amounts of heave versus percent finer than 0.02 mm by weight from the upper roadway. These data show a large amount of scatter, indicating that the percent finer than 0.02 mm is not accurately related to field performance. Comparison of Figure 9 with Figures 7 and 8 shows no apparent difference in the amount of scatter. This suggests that the additional work required to determine the percent finer than 0.02 mm (e.g., a hydrometer test) does not necessarily provide a stronger correlation with field performance measure than the use of the percent less than 0.075 mm.

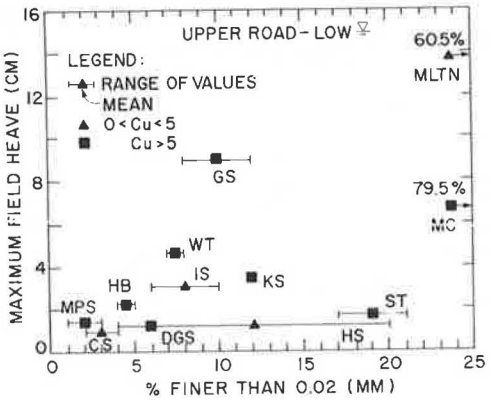

FIGURE 9 Maximum heave versus percent finer than 0.02 mm, upper roadway.

The uniformity of the 12 soils is coded in Figure 9 by different symbols. According to the Casagrande 0.02-mm criterion, Corbosiero sand (CS), Mason pit sand (MPS), and Ikalanian silt-sand (IS) would be classified as acceptable soils. However, the field performance of Ikalanian silt-sand does not quite meet the requirements of negligible to very low frost susceptibility (Table 3). Also, dense graded stone was rejected by the Casagrande criterion even though it has few fines and performed well at the field test site. These data therefore show some inconsistencies between the 0.02-mm Casagrande criterion and the Winchendon field data.

U.S. Army Corps of Engineers Frost Design Classification System

The frost susceptibility according to the U.S. Army Corps of Engineers Frost Design Classification System was determined for each of the 12 Winchendon soils, as shown in Figure 10 for Ikalanian silt-sand. The frost susceptibility classification was then used as a prediction of field performance. Table 4 gives the frost groups, percent finer than 0.02 mm, and frost susceptibility predicted by the Corps of Engineers system.

Figure 11 shows a comparison of the frost susceptibility classifications of Ikalanian silt-sand by the Corps of Engineers system and observed field heave rates and maximum amounts of heave using the field performance criteria of Table 3. The data show that the Corps of Engineers classification system provides a large range of frost classifi-

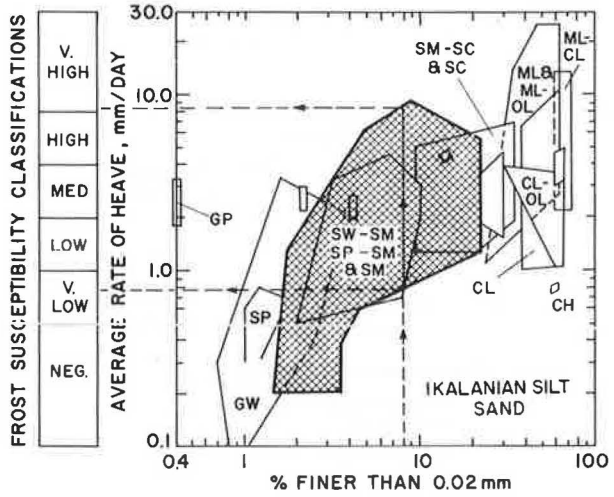

FIGURE 10 Corps of Engineers frost susceptibility classification, Ikalanian silt-sand.

TABLE 4 U.S. ARMY CORPS OF ENGINEERS FROST DESIGN CLASSIFICATION SYSTEM

Soil	Unified Class.	AASHTO Class.	% finer than 0.02 mm	Frost Group	Frost Susceptibility
Moulton Pit Sand	ML	A-4(0)	73	F4	Med to Very High
Graves Silt Sand	SM	A-4(0)	12	F2	Low to High
Morin Clay	CL	A-6(8)	82	F4	Low to Very High
Sibley Till	SM-SC	A-2-4(0)	19	F3	Low to High
Worcester Till	GM	A-1-b(0)	8	F1	Very Low to Medium
Hyannis Sand	SM	A-4(0)	9.5	F2	Very Low to Very High
Ikalanian Silt Sand	SM	A-4(0)	7.5	F2	Very Low To High
Hart Bros. Sand	SP-SM	A-2-4 (0)	4.7	S2	Very Low to High
Corbosiero Sand	SP-SM	A-2-4-(0)	2.5	NFS	Neg to Med.
Mason Pit Sand	SP-SM	A-3(0)	2.5	NFS	Neg to Med.
Dense Graded Stone	GP-GM	A-1-a (0)	6	S1	Very Low to High
Keating Stone Dust	SM	A-1-b	12	F2	Low to High

cations, that is, very low to high, compared with a low frost susceptibility given by the field performance of Ikalanian silt-sand. This same type of comparison for the other Winchendon soils shows similar results. The Corps of Engineers system provides ranges of frost susceptibility that are too broad to provide accurate predictions of field performance.

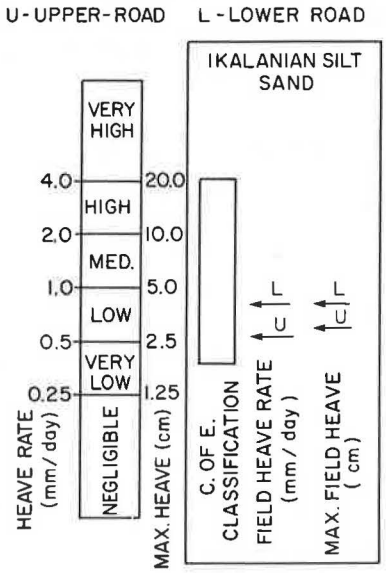

FIGURE 11 Comparison of field performance with Corps of Engineers frost susceptibility classification, Ikalanian silt-sand.

Comparison of Tabulated Freeze Test Data with Field Performance

In this section we compare data from 377 laboratory freeze tests tabulated by the U.S. Army Corps of Engineers with the observed field performance (*12*). The laboratory data base used to develop the Corps of Engineers system (Figure 10) is compared directly with field performance. For each of the 12 Winchendon soils a group of soils that have similar characteristics was selected from the 377 tabulated tests. Emphasis was placed on matching percent finer than 0.075, 0.02, and 0.01 mm; density; and uniformity coefficient when soils were selected. The tabulated laboratory freeze test performance of the selected group of soils was then compared with the field performance of the matching Winchendon soil.

Figure 12 compares the heaves from the tabulated laboratory data (*12*) with measured field heaves for the lower roadway. Overall the tabulated data provide a wide range of frost heave compared with the field heave measured for any one soil. Varying amounts of surcharge and various types of cylinders used in the tabulated freeze tests can have a significant effect on the heave measured during testing. A low value of laboratory heave, say, less than 30 percent in Figure 12, corresponds to a wide range of field observations and does not necessarily correspond to low

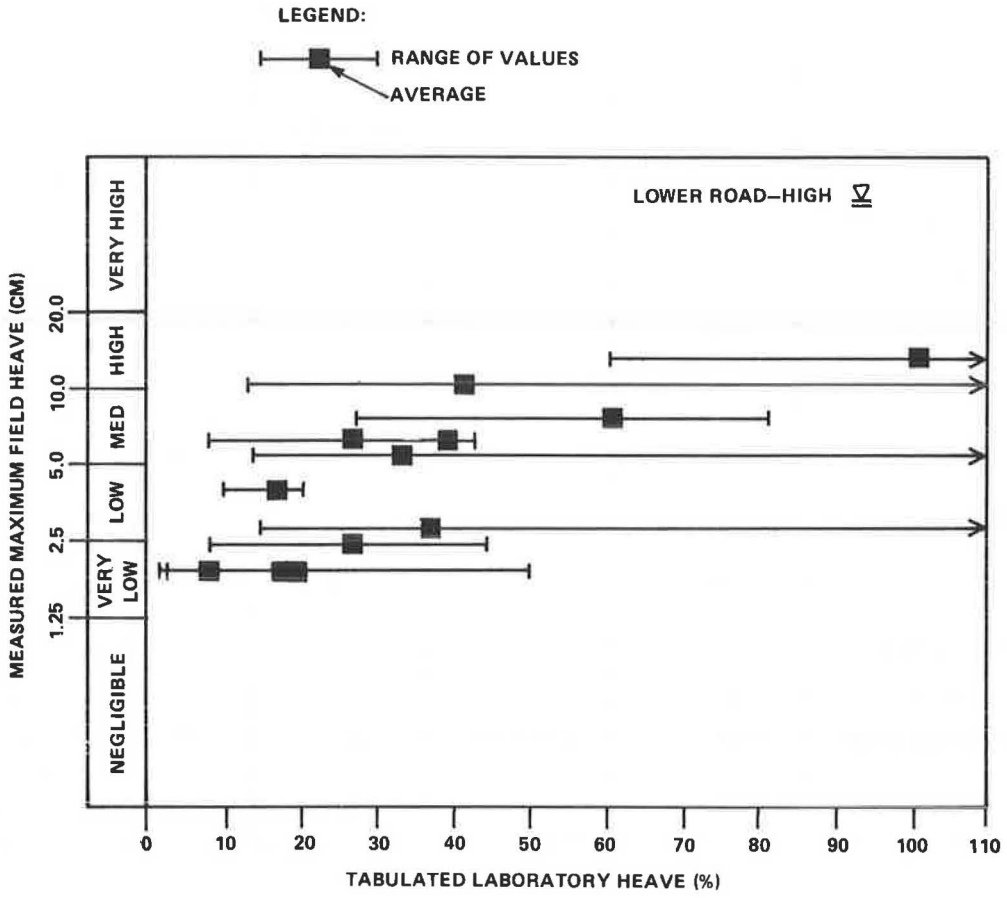

FIGURE 12 Field heave versus laboratory heave of matching soils from Corps of Engineers tabulation, lower roadway.

frost heave in the field. Thus, the method does not identify satisfactory soils. Similar comparisons were made on the basis of laboratory and field heave rates (*2*).

MDPW Heave Stress Test

Figure 13 presents maximum field heave versus the *R*-parameter for the lower roadway. A strong relationship is shown between increasing heave and increasing values of *R* for 10 of the 12 soils. The two soils that do not follow this relationship, Sibley till and Morin clay, contain plastic fines. These soils may have responded more strongly in the laboratory than in the field because of the greater availability of water in the laboratory test. These data suggest that the MDPW heave stress test may be a useful frost susceptibility indicator for nonplastic materials. All soils having an *R*-value less than 18 performed satisfactorily in the field (Table 3).

New CRREL Freeze-Thaw Test

Figure 14 presents the maximum field heave from the lower roadway versus the maximum laboratory heave from the new CRREL freeze-thaw test. The heaves for only the first cycle of the CRREL laboratory test were used because the first cycle was judged to be more representative of Winchendon field conditions (*6*). Figure 14 shows a nonlinear relationship of increasing field heave and increasing laboratory heave. The field heaves are larger than the

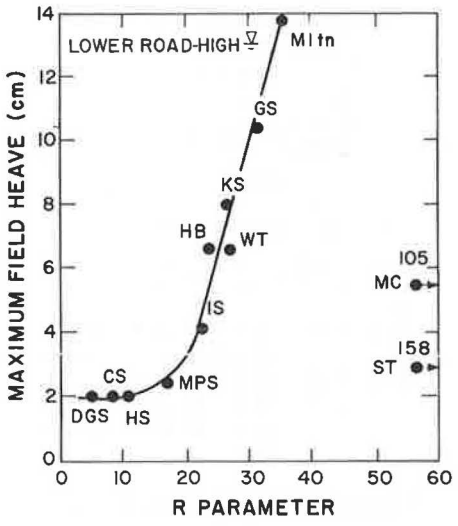

FIGURE 13 Maximum field heave versus *R*-parameter, lower roadway.

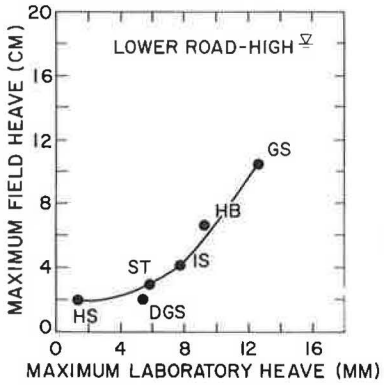

FIGURE 14 Field heave versus laboratory heave measured in new CRREL freeze-thaw test.

laboratory heaves because of the longer duration of freezing in the field. The laboratory heave rates (not shown) are numerically larger than the corresponding field values because of the more severe conditions of moisture availability and temperature in the laboratory test. Nevertheless, these field and laboratory data show strong correlations with little scatter.

Statistical Analyses

Linear regression analyses were performed with the laboratory and field data to provide quantitative measures of the strength of the correlations between them. The best fits through each set of data points and the coefficient of determination (r^2) were calculated. A coefficient of determination equal to 1.0 indicates that the field and laboratory measures are perfectly correlated. A coefficient of determination equal to 0.0 indicates that the values are uncorrelated (*13*). These regression analyses considered both linear relationships and linear transformations.

The coefficients of determination using the 0.075-mm and 0.02-mm grain-size indexes (Table 5) are all significantly less than 0.5 and are of the same order of magnitude. The coefficients for heave rate correlations are all numerically smaller than the corresponding values for maximum heave. This suggests, as discussed earlier, that correlations of heave rates with grain-size criteria provide no statistical advantage over correlations with maximum amounts of heave. Finally, the coefficients of determination for the 0.02-mm correlations are not significantly higher, and in some cases are lower, than the corresponding values for the 0.075-mm correlations. This suggests that the 0.02-mm criterion, which requires the additional expense of a hydrometer test, provides no statistical advantage over the simpler 0.075-mm criterion for predicting field performance.

The regression analyses performed with the tabulated Corps of Engineers laboratory freeze test data show regression coefficients of 0.61 to 0.75 (Table 5). Thus, the method seems to provide better overall statistical fit with the Winchendon field data than do the simple grain-size indexes. However, unlike the simple grain-size indexes, this method does not provide a useful minimum performance requirement, because, as Figure 12 shows, low values of laboratory heave or heave rate from the Corps of Engineers tabulation do not necessarily correspond to excellent performance in the Winchendon field test. Thus, the method cannot identify soils that performed well in the field.

The regression analyses performed with data from the MDPW heave stress test (10 nonplastic soils only) and the new CRREL freeze-thaw test all show high coefficients of determination (except for one value) greater than 0.9. This shows excellent correlations between these test data and the Winchendon field performance data.

THAW-WEAKENING COMPARISONS

Bono (*6*) shows that the percentage of fines serves only as a crude indicator of thaw-weakening behavior during the Winchendon field test. Alternatively, the new CRREL freeze-thaw test is unique among freeze tests in that it

TABLE 5 COEFFICIENTS OF DETERMINATION

Index	Upper Road		Lower Road	
	Max Heave	Heave Rate	Max Heave	Heave Rate
0.075 mm (Figures 7 & 8)	0.45	0.41	0.21	0.17
0.02 mm (Figure 9)	0.44	0.36	0.24	0.15
Tabulated Corps of Engineers Data (Figure 12)	0.67	0.61	0.75	0.63
MDPW Heave Stress Test (Figure 13)	0.96	0.98	0.98	0.91
New CRREL Freeze-Thaw Test (Figure 14)	0.92	0.68	0.98	0.97

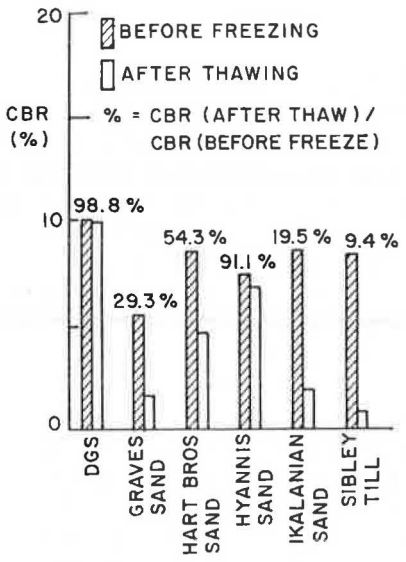

FIGURE 15 CBR before freezing and after thawing in new CRREL freeze-thaw test (*4*).

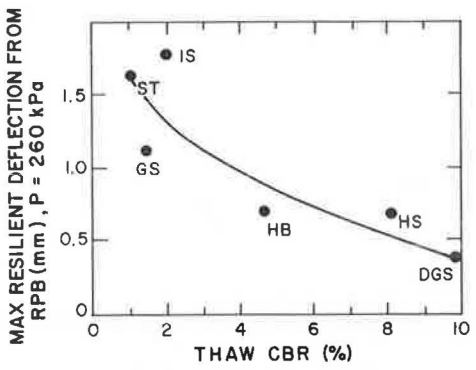

FIGURE 16 Maximum resilient deflection from RPB tests versus thaw CBR.

provides strength data (CBR) on thaw-weakened soil. In this section these CBR data are compared with the maximum vertical resilient displacements measured during the thaw period from the RPB test (Figure 6). Chamberlain (*4*) analyzes these data in more detail than space allows here.

Figure 15 shows a comparison of the CBR values obtained from the new CRREL freeze-thaw test after two freeze-thaw cycles with before-freezing CBRs for the six soils tested. This comparison provides an index measure of the effects of thaw weakening and identifies Sibley till and Ikalanian silt-sand as highly thaw-weakening soils.

Figure 16 is a plot of the maximum pavement deflection from RPB tests versus the thaw CBR for each of the six soils tested. These data show a well-defined relationship between the RPB deflection and thaw CBR, suggesting that the new CRREL freeze-thaw test shows promise of quantifying thaw weakening of soils in the field. Chamberlain (*4*) has recently proposed tentative frost susceptibility criteria for the new CRREL test (Table 6) that include both heave and thaw-weakening behavior.

It is interesting to note that Sibley till showed little to moderate field heave (Table 2) yet very high thaw weakening (Figure 15). The plasticity of this soil may be an indicator of its high thaw weakening. Also, Sibley till developed very high heave stresses in the MDPW heave stress test. Thus, this test may also serve as an indicator of thaw-weakening behavior of plastic soils, although the reasons for this are not understood.

FROST PENETRATION DEPTHS

Table 7 shows the maximum measured frost penetration depth in inches for each of the 12 soils averaged for the three seasons. The 3-year average freeze index (FI) is about 977 °F-days. For eight of the soils the frost penetration values of Table 7 are about 3 to 10 in. deeper for the upper roadway. For the remaining four soils the frost penetration values are slightly deeper (by less than 3 in.) for the lower roadway than for the upper roadway. Thus, frost penetration beneath the lower roadway has been somewhat limited by the higher water-table conditions. This occurs because water has high volumetric heat (62.4 Btu/ft^3/°F), about

TABLE 6 TENTATIVE FROST-SUSCEPTIBILITY CRITERIA FOR NEW FREEZE TEST (*4*)

Frost susceptibility classification	Heave rate (mm/day)	Thaw CBR (%)
Negligible	<1	>20
Very low	1-2	20-15
Low	2-4	15-10
Medium	4-8	10-5
High	8-16	5-2
Very high	>16	<2

TABLE 7 FROST PENETRATION DEPTHS

Soil	Frost Penetration Depth (inches)		
	Measured		Calculated
	Upper Road	Lower Road	
Moulton Pit Silt	15.4	15.9	24.3
Graves Silt Sand	19.7	15.2	25.6
Morin Clay	19.1	21.7	25.9
Ikalanian Silt Sand	28.0	21.8	31.9
Worcester Till	35.0	37.8	38.8
Keating Stone Dust	34.0	27.3	38.8
Hart Brothers Sand	34.3	24.0	35.8
Sibley Till	42.2	32.6	38.8
Mason Pit Sand	32.4	26.9	35.8
Hyannis Sand	30.3	31.3	33.4
Keating Dense Graded Stone	38.6	28.3	40.9
Corbosiero Sand	30.7	27.8	33.4
Average	30.0	25.9	33.6

twice that of soil, relinquishing large amounts of thermal energy as it cools. The measured frost depths are all less than the design frost depth of 52 in. given by MDPW criteria.

The measured frost penetration depths were compared with calculations by the modified Berggren formula:

$$FP = \lambda[(48 * K_s * FI/L)]^{1/2} \quad (1)$$

where

FP = depth of frost penetration,
K_s = thermal conductivity,
FI = surface freezing index,
L = latent heat, and
λ = dimensionless correction coefficient, given as a function of mean annual temperature, mean freezing temperature, volumetric heat (C_s), and L.

The thermal parameters K_s, L, and C_s were calculated from estimated in situ densities and water contents using correlations provided by Aldrich (*14*). The surface freezing index was estimated from the air freezing index, using the Corps of Engineers n-factor approach (*15*). The calculations for a surface FI of 600 °F-days (n = 0.6) are summarized in Table 7. Figure 17 shows a comparison of the frost penetration depths measured for the upper roadway with values computed by Equation 1.

The calculated frost penetration depths agree generally with the measured frost penetration depths. The average calculated frost depth, 33.6 in., is about 10 percent larger than the average frost depth measured beneath the upper roadway and 25 percent larger than the average frost depth measured beneath the lower roadway (Table 7). Aldrich (*14*) points out that Equation 1 may overestimate frost penetration depths because of freezing-point depressions of soil moisture (neglected in these calculations). The freezing-point depression of soil moisture is greatest in fine-grained soils (*16*), and this may account for the particularly large differences between calculated and measured frost penetration depths for Moulton pit silt, Graves

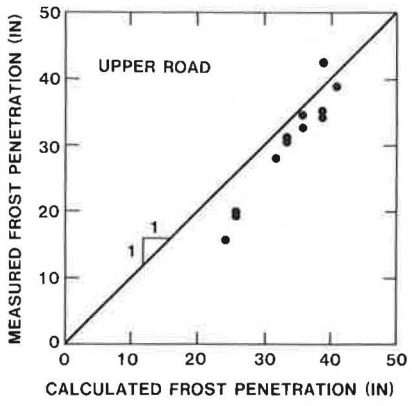

FIGURE 17 Measured frost penetration versus frost penetration calculated by modified Berggren formula; FI = 600 °F-days.

silt sand, and Morin clay. Also, the Winchendon test cells (Figure 1) did not include a base or subbase, did not experience traffic loadings, and were narrower (8 ft) than real highways. Frost penetration depths might have been larger if these features had been modeled in the field test.

SUMMARY AND CONCLUSIONS

This paper presents an analysis of 3 years' worth of field data acquired at the Winchendon field test site to further the understanding of the mechanics of frost action in soils and to improve existing highway frost design criteria. It analyzes and interprets in detail the Winchendon field test data on frost heave, thaw weakening, and frost penetration. A number of frost index tests and classification methods are evaluated. The following conclusions were obtained from these analyses.

Grain-Size Criteria

Simple grain-size criteria such as the percent of particles smaller than 0.075 or 0.02 mm correlate weakly with the Winchendon field performance data. These data show that all soils having few fines (particles smaller than 0.075 mm) performed well in the field test. Of the soils with intermediate and many fines, some performed well and some poorly, with a great deal of scatter. Inevitably these simple criteria reject some soils that heaved small amounts in the field test and hence are not useful for predicting the frost heave susceptibility of soils that fail these criteria.

U.S. Army Corps of Engineers Frost Design Classification System and Tabulated Freeze Test Data

The U.S. Army Corps of Engineers Frost Design Classification System and tabulated freeze test data provided very wide ranges of frost susceptibility compared with the field performance of the 12 test soils. Although most of the field data fall within the ranges of frost susceptibility given by the Corps of Engineers system, the ranges are too broad for accurate predictions of field performance. In addition, a low value of tabulated laboratory heave or heave rate corresponded to a wide range of field observations and not necessarily to negligible to low frost heave in the field. Thus, these methods may reject many satisfactory soils.

Freezing Tests

Comparisons of the field frost heave data with freezing data from the MDPW heave stress test on nonplastic soils and with freezing data from the new CRREL freeze-thaw test show excellent correlations. All soils that developed small heave stresses with time (R less than 18) in the MDPW test performed satisfactorily in the field. Heave stresses for the two plastic soils, Morin clay and Sibley till, were much higher than would be expected from the measured field heaves. However, the large resilient deflections of Sibley till show that the high heave stresses for plastic soils may be a useful indicator of large thaw weakening in the field.

The thaw-weakening CBR data from the CRREL freeze-thaw test correlated well with the resilient deflections from RPB tests in the field. Thus, this test shows promise of quantifying the thaw-weakening behavior of soils in the field. Data from the CRREL test have been used to develop tentative frost susceptibility criteria, which include the factors of both frost heave and thaw weakening (Table 6).

Both the MDPW and CRREL freezing tests require more elaborate test equipment than the simple index measures described earlier. However, they provided the best agreement with the Winchendon field performance data on frost heave and thaw weakening and show great promise.

Frost Penetration Depths

Frost penetration depths calculated by the modified Berggren formula are in general agreement with frost penetrations measured at the Winchendon field test. The average calculated frost penetration is about 10 percent larger than the average frost depth measured beneath the upper roadway and about 25 percent larger than the average frost depth measured beneath the lower roadway. This may possibly be due to the effects of freezing-point depressions of soil moisture, approximations inherent in the n-factor adjustment of air to ground surface temperatures, and other factors not accounted for in the field test. In comparison with the design frost depth for Winchendon of 52 in. given by MDPW design criteria, these data show that it may be possible to achieve savings from the use of reduced base and subbase thicknesses in frost protection of subgrades.

ACKNOWLEDGMENTS

This research was supported by the Department of Public Works (MDPW), Commonwealth of Massachusetts. The authors acknowledge the assistance of numerous MDPW personnel. Richard Berg and Edwin J. Chamberlain of the U.S. Army Corps of Engineers Cold Regions Research and Engineering Laboratory greatly assisted in providing CRREL data on the Winchendon soils.

REFERENCES

1. *Full Depth Testing of Frost Susceptible Soils.* Final Report, HPR Study R-12-9. Massachusetts Department of Public Works, Wellesley, Mass., 1982.
2. L. Edgers and N. Bono. *Highway Design for Frost Susceptible Soils: Laboratory and Field Data—Winchendon Soils.* Department of Civil Engineering, Tufts University, Medford, Mass., 1985.

3. T. C. Johnson, D. L. Bentley, and D. M. Cole. *Resilient Modulus of Freeze-Thaw Affected Granular Soils for Pavement Design and Evaluation.* Part 2: Field Evaluation Tests at Winchendon, Massachusetts, Test Sections. Special Report 86-12. U.S. Army Corps of Engineers, 1986.
4. E. J. Chamberlain. *Evaluation of Selected Frost Susceptibility Test Methods.* CRREL Report 86-14. U.S. Army Corps of Engineers Cold Regions Research and Engineering Laboratory, Hanover, N.H., 1986.
5. E. J. Chamberlain. *Frost Susceptibility of Soils: Review of Index Tests.* CRREL Monograph 81-2. U.S. Army Corps of Engineers Cold Regions Research and Engineering Laboratory, Hanover, N.H., 1981.
6. N. Bono. *Highway Design for Frost Susceptible Soils.* M.S. thesis. Tufts University, Medford, Mass., 1986.
7. A. Casagrande. Discussion of Frost Heaving. *HRB Proc.,* Vol. 11, 1931, pp. 168–172.
8. E. J. Chamberlain, P. N. Gaskin, D. Esch, and R. L. Berg. Survey of Methods for Classifying Frost Susceptibility. In *Frost Action and Its Control,* Technical Council on Cold Regions Engineering Monograph, American Society of Civil Engineers, New York, 1984.
9. *Evaluation of the Heave Stress System in Predicting Frost Susceptibility.* Final Report, HPR Research Study R-122-7. Massachusetts Department of Public Works, Wellesley, Mass., 1982.
10. A. E. Z. Wissa and R. T. Martin. *Behavior of Soils Under Flexible Pavements—Development of Rapid Frost Susceptibility Tests.* R68-77. Department of Civil Engineering, Massachusetts Institute of Technology, Cambridge, 1968.
11. D. C. Esch, R. L. McHattie, and B. Connor. Frost-Susceptibility Ratings and Pavement Structure Performance. In *Transportation Research Record 809,* TRB, National Research Council, Washington, D.C., 1981, pp. 27–34.
12. R. L. Berg and T. C. Johnson. *Revised Procedure for Pavement Design Under Seasonal Frost Conditions.* Special Report 83-27. U.S. Army Corps of Engineers Cold Regions Research and Engineering Laboratory, Hanover, N.H., 1983.
13. J. R. Benjamin and C.A. Cornell. *Probability, Statistics, and Decision for Civil Engineers.* McGraw-Hill, New York, 1977.
14. H. P. Aldrich. Frost Penetration Below Highway and Airfield Pavements. *HRB Bulletin 135.* HRB, National Research Council, Washington, D.C., 1956.
15. R. L. Berg. *Design of Civil Airfield Pavements for Seasonal Frost and Permafrost Condition.* FAA Report FAA-RD-74-30. FAA, U.S. Department of Transportation, 1974.
16. J. F. Haley. Cold-Room Studies of Frost Action in Soils: A Progress Report. *HRB Bulletin 71.* HRB, National Research Council, Washington, D.C., 1953.

Publication of this paper sponsored by Committee on Frost Action.